NACA

RESEARCH MEMORANDUM

for the

Bureau of Aeronautics, Navy Department

TANK TESTS OF 1/5.5-SCALE POWERED DYNAMIC MODEL OF THE COLUMBIA XJL-1 AMPHIBIAN - LANGLEY TANK MODEL 208

TED NO. NACA 2336

By

Robert F. Havens

Langley Memorial Aeronautical Laboratory
Langley Field, Va.

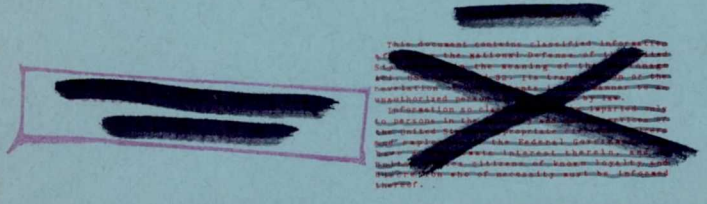

NATIONAL ADVISORY COMMITTEE
FOR AERONAUTICS

WASHINGTON

NATIONAL ADVISORY COMMITTEE FOR AERONAUTICS

RESEARCH MEMORANDUM

for the

Bureau of Aeronautics, Navy Department

TANK TESTS OF 1/5.5-SCALE POWERED DYNAMIC MODEL OF THE COLUMBIA XJL-1 AMPHIBIAN - LANGLEY TANK MODEL 208

TED NO. NACA 2336

By Robert F. Havens

SUMMARY

Tests of a powered dynamic model of the Columbia XJL-1 amphibian were made in Langley tank no. 1 to determine the hydrodynamic stability and spray characteristics of the basic hull and to investigate the effects of modifications on these characteristics. Modifications to the forebody chine flare, the step, and the afterbody, and an increase in the angle of incidence of the wing were included in the test program.

The seaworthiness and spray characteristics were studied from simulated taxi runs in smooth and rough water. The trim limits of stability, the range of stable positions of the center of gravity for take-off, and the landing stability were determined in smooth water. The aerodynamic lift, pitching moment, and thrust were determined at speeds up to take-off speed.

INTRODUCTION

Tests of a 1/5.5-scale powered dynamic model of the Columbia XJL-1 amphibian were made in Langley tank no. 1 to determine the hydrodynamic stability and spray characteristics of the basic hull, and to investigate modifications that might improve its performance on the water.

The investigation included tests of the final design submitted by Columbia Aircraft Corporation and tests of the model with modified

chine flare on the forebody, with steps of different depth and plan form, with several types of afterbodies, and with the angle of incidence of the wing increased. The seaworthiness and spray characteristics of the model in rough water were observed during simulated taxi-runs at speeds below hump speed. Tests were made in smooth water to determine the spray characteristics, the trim limits of stability, the range of stable positions of the center of gravity for take-off, and the landing stability. The aerodynamic lift, pitching moment, and thrust were determined at speeds up to take-off speed.

These tests were requested by the Bureau of Aeronautics, Navy Department, in a letter to the Committee dated June 9, 1944, Aer-E-23-FAL, C 15444.

A part of the tests was observed by Messrs. G. D. Evans and M. Lauridsen of Columbia Aircraft Corporation. The tests were made from December 1944, through May 1945.

DESCRIPTION OF MODEL

The basic model, furnished by the Columbia Aircraft Corporation, was designated Langley tank model 208. The general arrangement of the basic model and the body plan of the hull are shown in figures 1 and 2, respectively. A photograph of the model is given in figure 3. The principal dimensions of the basic model and of the full-size airplane are presented in table 1. The angles of the forebody and afterbody keels, the angles of incidence of the wing and the stabilizer are measured relative to the base line which is parallel to the thrust line. Trim was measured between the straight portion of the forebody keel and the free-water surface.

In order to facilitate changes in the form of hull and in the position and depth of step, the hull was constructed in four sections as shown in figure 2. Five principal forebodies and nine principal afterbodies were tested. All forebodies had a keel angle of -5°. The plating which projects from the forebody chines of the full-size airplane was simulated from the bow to the step on forebodies I and II. On forebodies III, IV, and V, it extended from the bow to station 210. For convenience, this simulated plating is neglected in most of the sketches of the configurations other than the basic model. The principal forebodies are described as follows:

Forebody I: The basic forebody had a dead rise at the step of 20° excluding chine flare, and 13.5° including chine

flare. The chine flare had a constant down angle of 20° from the bow to the step (fig. 2).

Forebody II: This forebody was identical to forebody I from the bow to station 160. From station 160 to the step, the angle of chine flare and the line of tangency of the flare with the planing bottom was varied as shown in figure 4. The dead rise at the step was 20° excluding chine flare, and 17.5° including chine flare.

Forebody III: This forebody was identical with forebody I from the bow to station 210. From station 210 to the step, the angle of flare had a constant angle of 0° with the same line of tangency as forebody I. This change in flare produced a discontinuity in the chine at station 210 (fig. 5). The dead rise at the step was 20° excluding chine flare, and 17.25° including chine flare.

Forebody IV: This forebody was the same as forebody III, except that the bottom had no chine flare from station 210 to the step (fig. 5).

Forebody V: This forebody was the same as forebody I forward of station 185. From station 185 to station 210, the flare gradually decreased from down 20° to down 6°. From station 210 to the step, a constant down-flare of 6° was maintained as shown in figure 6. The dead rise at the step was 20° excluding chine flare and 16.5°, including chine flare.

Afterbody I: The basic afterbody (fig. 2) had a warped bottom with a maximum angle of dead rise of 29.5° at approximately station 315. The variation of the angle of dead rise with station location for afterbody I and five other afterbodies is plotted in figure 7. The keel angle of afterbody I was 12.5° and the sternpost was at station 442.

Afterbody II: This afterbody was the same as afterbody I, except that the keel angle was 13.5°. To form afterbody II, afterbody I was rotated about a horizontal axis through the point of the step and the sternpost was raised 0.57 inches (fig. 5).

Afterbody III: Forward of station 300 the dead rise of afterbody III was maintained at a constant angle of 29° (figs. 5 and 7). The keel angle, the position of the sternpost, and the shape of the hull aft of station 300 were the same as those of afterbody II.

Afterbody IV: Forward of station 315 the angle of dead rise of afterbody IV was maintained at a constant angle of 29.5° (figs. 7 and 8). The keel angle, the position of the sternpost, and the shape aft of station 315 were the same as those of afterbody I.

Afterbody V: This afterbody was the same as afterbody IV, except that the keel angle was 11.5°. To form afterbody V, afterbody IV was rotated about a horizontal axis through the intersection of the keel and the sternpost.

Afterbody VI: This afterbody had a keel angle of 10.5° and a constant dead rise of 25°. The keel at the sternpost was 0.9 inches lower for afterbody VI than for afterbody I (fig. 4).

Afterbody VII: From station 300 forward to station 233 (step at chine), the bottom of afterbody VII was warped by decreasing the dead rise linearly from 29° to 18° (fig. 7). All other dimensions were the same as those of afterbody I.

Afterbody VIII: This afterbody had a keel angle of 11.3° and a constant dead rise of 20°. The position of the sternpost was the same as that of afterbody I (fig. 6).

Afterbody IX: This afterbody was the same as afterbody VIII except that the length was increased 5 inches by adding a section aft of the original sternpost. The chines of the added section were straight lines tangent to the chines of afterbody VIII (fig. 10).

The model numbers and descriptions of modifications using these principal forebody and afterbody forms are given in table II. Sketches of the various modifications are given in figures 1 through 18, as indicated in table II. The angle of incidence of the wing was 4° (relative to the thrust line) for models 208M, 208N, and 208P. For all other models including the basic model, the angle of wing incidence was 0°. The stabilizer was set at an angle of -2° (relative to the thrust line). Early in the tests, the area of the stabilizer was increased 27.5 percent by adding panels to the tips of the original tail, as shown in figure 1. The added surface had the same airfoil section as the original tail. Slats were attached to the leading edge of the wing to delay the stall and increase the maximum lift coefficient.

The power plant consisted of two 2-horsepower alternating current induction motors mounted in tandem with the shafts joined

by a flexible coupling. This power plant turned a three-blade propeller having a diameter of 1.94 feet and a blade angle of 14° at 0.75 radius.

The pitching moment of inertia of the ballasted model was determined by swinging the model as a compound pendulum. The results are as follows:

Center of gravity (percent M.A.C.)	Moment of inertia (slug-ft^2)
20	4.57
40	3.94

APPARATUS AND PROCEDURE

Apparatus

The towing carriage and tank are described in reference 1. The test apparatus was essentially the same as that described in reference 2, except that the model was towed under the main carriage. For the tests in rough water, fore-and-aft freedom relative to the towing carriage was obtained by the use of the apparatus described in reference 3.

Aerodynamic Tests

The effective thrust of the model was determined with flaps at 0° and the thrust line parallel to, and 21 inches above, the surface of the water. During the tests to determine thrust, the lowest point of the forebody keel was approximately 1 inch above the water. For the tests to determine lift and pitching moment, the model was raised so that the sternpost just cleared the water at a trim of 16°. The aerodynamic lift and pitching moment were determined for the following conditions:

Angle of wing incidence (deg)	Stabilizer area (percent basic)	Flaps (deg)	Propeller (rpm)	Center of moment (percent M.A.C.)
0	100	0, 30, 60	0	24
0	100	30	5500	24
0	127.5	60	2750	36
0	127.5	30	5500	36
4	127.5	30	5500	Moments not measured

Brief tests were made with the model free to trim in the air to investigate the aerodynamic longitudinal stability.

Spray Characteristics

Observation of the spray characteristics of several of the modifications in smooth water were supplemented by still photographs and motion pictures. For the tests in rough water, model 208M was accelerated slowly through waves, to simulate taxiing at speeds below hump speed. The propeller thrust approximated that required for self-propulsion. Tests were made in waves (length-to-height ratio of 20) of three sizes:

Height, model size (in.)	Height, full size (ft)
13	6
$6\frac{1}{2}$	3
$2\frac{1}{4}$	1

Hydrodynamic Stability Tests

The trim limits of stability were determined for the greater part of the tests with a flap deflection of 30°, take-off power (5500 rpm), and a gross load of 77.4 pounds (13,000 pounds full size).

The variation of trim with speed with determined by towing the model with fixed-elevator settings at an acceleration of approximately 1 foot per second per second to take-off. Data were obtained with elevator deflections from 0° to -30° and with the center of gravity at positions from 22 to 44 percent of the mean aerodynamic chord. The effects of load, power, and flap setting were also investigated. From these data, the maximum amplitude of porpoising, the hump trim, and take-off characteristics of the model were obtained.

Landings were made by trimming the model in the air to the desired landing trim and decelerating the towing carriage at about 2 feet per second per second. Landings of all modifications having a wing incidence of 0° were made with the flaps deflected 60° and the propeller turning at 2750 rpm. Landings of model 208M, 208N, and 208P, with a wing incidence of 4°, were made with the

flaps deflected 45° and a propeller speed of 2750 rpm. The effect of position of the center of gravity and gross load was determined for the basic model only.

RESULTS AND DISCUSSION

Aerodynamic Tests

The variation of effective thrust and air drag with speed is plotted in figure 19. The results show that the thrust of model 208, with a propeller speed of 5500 rpm, was in close agreement with the required scale thrust (Columbia Aircraft Corporation, Report E-20) at speeds from 16 to 60 feet per second. The power absorbed by the propeller when turning at 5500 rpm was designated as take-off power.

The variation of aerodynamic lift and pitching moment with speed for the basic model is shown in figure 20. The aerodynamic lift and pitching-moment coefficients of the model with the basic and the increased tail area are given in figures 21 through 23. The aerodynamic lift coefficients with the increased angle of wing incidence is plotted in figure 24. The coefficients are of the standard NACA form, based however, on carriage speed which is about 95 percent of true air speed, Results of the force tests and the tests made free to trim in the air showed that:

1. Less lift was developed with flaps set at 60° than at 30°.

2. The effect of applying take-off power was to increase the lift coefficient by about 20 percent at a trim of 10° and a speed of 50 feet per second.

3. The basic model was longitudinally unstable at speeds near 50 feet per second, with the center of gravity at 36 percent mean aerodynamic chord, flaps set at 60°, and the propeller turning at 2750 rpm. Under the same conditions, the model with the increased stabilizer area was stable. At trims above 12° and below 4°, however, small changes in elevator deflection caused appreciable changes in attitude and resulted in a tendency to over control the model.

4. The increase in wing incidence from 0° to 4° (model 208M) increased the lift at all trims investigated.

Spray Characteristics

Photographs showing the spray characteristics of the basic model at a gross load of 77.4 pounds (13,000 lb, full size) with take-off power and the center of gravity at 26-percent mean aerodynamic chord are given in figures 25 and 26. No spray broke over the bow at low speeds, and only light spray entered the propeller at speeds near 8 feet per second (11 knots full size). Spray wet the flaps moderately within the range of speeds from 13.5 to 22.5 feet per second (19 to 31.5 knot, full size). Before striking the flaps, the water which emerged from the bottom of the forebody was broken up into large drops by the combined action of the chine flare and the slipstream. With the elevators deflected -30°, some spray hit the tips of the horizontal tail at speeds from 17 to 25 feet per second and the outboard ends of the flaps at speeds from 28 to 34 feet per second.

Motion pictures and observations of the taxiing tests of model 208M in rough water showed that the bow did not submerge in any of the waves. Some water from the 6.5-inch waves broke over the bow at speeds near 5 feet per second. When the model contacted the crests of the 6½-inch and 13-inch waves at speeds near 8 feet per second, a moderate amount of water was forced from under the chines into the propeller. The chine flare was effective in dispersing the water to each side of the hull when contact was made with wave crests at speeds higher than 10 feet per second.

The spray characteristics of most of the modifications were not appreciably different from those of the basic model. Modifications having hump trims higher than the hump trim of the basic model generally had inferior spray characteristics. Increasing the angle of incidence of the wing (model 208M) lowered the trailing edge 0.93 inch (5.1 inches, full size) and increased slightly the amount of spray which wet the flaps. The flaps of model 208N were wet within a range of speeds from 13.5 to 18.5 feet per second. This range was less extensive than the range for the basic model, inasmuch as the method of reducing the chine flare at the step produced a lower spray blister at speeds higher than 18.5 feet per second. This effect was also noted during tests of models 208-5 and 208A-1. The spray on the flaps of both model 208H (with the chine flare faded out just ahead of the step) and model 208-7 (without chine flare at the step) was heavier than that of the basic model.

Hydrodynamic Stability Tests

Representative data, obtained furing investigation of the take-off stability, are given in figures 27 through 46. The model number, gross load, flap deflection, amount of power, and position of the center of gravity are indicated on the figures. Tests of the model with and without the increased stabilizer area showed no effects on the hydrodynamic characteristics. No distinction is made, therefore, between modifications with different sizes of the stabilizer.

Trim limits of stability.- The trim limits of the basic model are shown in figures 27 and 28. In addition to the lower and upper trim limits of stability there was a region of instability extending from the upper limit at intermediate planing speeds to the lower limit at higher planing speeds. Porposising in this intermediate region was erratic (sometimes requiring a disturbance for activation) and was characterized by rapid changes in trim with little change in rise. The amplitude of intermediate porpoising generally increased as the intermediate region approached the upper limit. The upper limits were difficult to define at the juncture with the intermediate region of porpoising. The model frequently commenced upper limit porpoising at this juncture when the amplitude of intermediate porpoising was sufficient to trim the model above the upper limit. The position of the lower limit was indefinite at speeds above 32.5 feet per second. If the model was disturbed, lower limit porpoising occurred 1° to 1.5° above the lower limit obtained without disturbance. During lower limit porpoising at low trims, the forebody chines were wet as far forward as the plane of the propeller. The flow of water from under the forebody appeared to be disturbed irregularly by the chine flare.

Porpoising in the intermediate region of instability occurred in varying degrees for all configurations tested, except models 208D, 208F, and 208K. This type of porpoising occurred while the afterbody was wet heavily by jets of water which emerged from the step as shown in figure 29.

The wetting of the afterbody was accentuated by the slipstream, increases in the load on the water, and decreases in the clearance of the afterbody from the wake of the forebody. The effects of load and the application of power can be seen by comparing the curves given in figures 27 and 28. In general, the extent of the intermediate region was increased by increasing the load on the water and by applying power. The effect of increasing the wing incidence was similar to the effect of a decrease in gross load, as shown in figure 30. The extent of the region of intermediate porpoising was reduced by progressively changing the plan form

of the step from 45° - vee to 30° - vee, 20° - vee, and transverse, while the depth of step at the keel was held constant (models 208, 208A, 208B, and 208C; figs. 27 and 31). It should be noted that the greatest reduction was obtained with the transverse step, model 208C. Inasmuch as the afterbody of model 208C was raised 0.54 inch above the position of the afterbodies of models 208, 208A, 208B to permit installation of the transverse step, the effects of both plan form and afterbody clearance were included in results of tests of model 208C. Results of tests of other configurations that had an afterbody clearance (above the wake from the forebody) greater than that of the basic model showed that afterbody clearance was the most significant hull parameter affecting the region of intermediate porpoising. The effect of different amounts of afterbody clearance on the trim limits and the intermediate type of porpoising is shown by a comparison of figures 27, 32, and 33 (models 208, 208G, and 208F) and by figure 34 (models 208H and 208H - 13).

The results of tests of model 208-8 showed that with the angle of dead rise of the basic afterbody increased behind the step, the region of intermediate porpoising was diminished slightly. Decreasing the dead rise behind the step to form a shallow vee step (model 208L) lowered the upper limit, decreasing trim, nearly to the lower limit, but did not affect the other limits or the intermediate region of instability.

The addition of chine flare to the afterbody increased the amplitude of the intermediate type of porpoising as shown by a comparison of figure 27 (model 208) and figure 35 (model 208-2). An increase of 5 inches (27.5 inches, full size) in the length of the afterbody of model 208N lowered the upper trim limit but had no significant effect on the intermediate region of instability.

Take-off stability.- The variation of trim of the basic model with speed is shown in figures 36 and 37 for gross loads of 60.5 pounds (10, 164 pounds, full size) and 77.4 pounds (13,000 pounds, full size). From figure 36 it can be seen that with take-off power, the model trimmed down after the true hump (at a speed of about 15 fps) and then suddenly trimmed up to a second hump. At the light load, the second hump was generally higher than the true hump. Motion pictures of the basic model and of the model with the wing removed (model 208F-3) show that the rapid increase in trim to the second hump was accompanied by the elevation of the forebody chines above the surface of the water and a sudden wetting of the chines and bottom of the afterbody. Without power, the model showed only a slight tendency to trim to a second hump. Comparison of figure 36 with figure 37 shows that the effectiveness of the elevators in trimming the model was greater with power than without power.

The relation between the free-to-trim curves and the trim limits of stability is shown in figure 38. The model porpoised when the free-to-trim curves entered either the intermediate region of instability or the regions outside the trim limits of stability.

The maximum amplitude of porpoising that occurred during take-off of the basic model is plotted in figure 39. The effect of gross load on the maximum amplitude of lower-limit porpoising is shown to be small. Figure 39 shows that take-offs with an amplitude of lower-limit porpoising of less than 2° (which are assumed stable) were possible when the center of gravity was at 24-percent mean aerodynamic chord and the elevator was set at -10°. The amplitude of porpoising in the intermediate region of instability was increased when the gross load was increased from 60.5 pounds to 77.4 pounds. At a gross load of 77.4 pounds, the model porpoised 2° in the intermediate region of instability with the center of gravity at 26-percent mean aerodynamic chord and the elevator set at -10°. True upper-limit porpoising was first encountered with full up-elevators (-30°) and the center of gravity at 32-percent mean aerodynamic chord. The manufacturer expected that positions of the center of gravity required for operation of the full-size airplane would be from 23.5- to 35-percent mean aerodynamic chord.

The abrupt change in trim after the true hump was eliminated when the chine flare forward of the step was decreased according to the lines of model 208G. The effect of decreasing the chine flare is shown in figure 40 (models 208G and 208G-12). It can be seen that the trim at either of the two humps was unaffected by the chine flare, but that the trim between the humps was raised when the chine flare was reduced.

A constant chine flare of down 6° (model 208N) did not eliminate the change in trim after the hump, but did produce an appreciable decrease in the amplitude and rapidity of the trim change compared with that of the basic model.

The effect of changing the plan form and the effective position and depth of the step on the maximum amplitude of porpoising is shown in figure 41 (models 208, 208A, 208B, and 208C). The shift in the range of stable positions for the center of gravity was nearly the same as the change in position of the centroid of the step. Due to the small amount of intermediate porpoising obtained with the transverse step (model 208C), stable take-offs could be made with an elevator setting of -10° with the center of gravity as far aft as 35-percent mean aerodynamic chord. The range of stable positions for the center of gravity was greater than that of the basic model. Similarly, with a deep transverse step

(model 208F) stable take-offs could be made with the center of gravity in a greater range of positions than for the basic model.

Although the results of tests without an afterbody (model 208D, fig. 42) showed conclusively that increased afterbody clearance was desirable for the elimination of intermediate porpoising, models having afterbodies with a clearance greater than that of the basic model (such as models 208C, 208E, 208F, 208H-13, and 208K) gave extremely high hump trims and spray characteristics inferior to those of the basic model. Several modifications which incorporated means of changing the flow of water and air over the afterbody without changing the position of the forebody or afterbody were not satisfactory as a substitute for raising the afterbody. The addition of hydrodynamic spoilers at the aft end of the afterbody (model 208-9) increased the amplitude of intermediate porpoising. The same spoilers behind the step (model 208-10) had no effect on the variation of trim during take-off. Longitudinal steps on the forebody (model 208G-11) raised the hump trim and increased the hump speed but had no appreciable effect on the intermediate porpoising. Longitudinal strips on the afterbody (model 208H-14) had no effect on the hydrodynamic stability. The addition of a hook on the forebody of model 208H at the step (model 208H-15) lowered the trim tracks at speeds beyond the hump and eliminated the intermediate porpoising at trims from 8° to 9°, as shown in figure 43. Use of a hook of this type would require that the step be moved forward to avoid porpoising at forward positions of the center of gravity.

Results of tests with an angle of afterbody keel of 11.5° (models 208I and 208J) are given in figure 44. The results show that some intermediate porpoising was encountered at trims above 7°. Similar results were obtained from tests of models 208N and 208P.

A comparison of the results of the take-off tests of the model with an increased angle of wing incidence (model 208M) with the results obtained from the basic model showed that increasing the wing incidence by 4° decreased the extent of the region of intermediate porpoising, lowered the get-away speed, and had no appreciable effect on the change in trim to a second hump. The results of typical take-offs of model 208M are given in figure 45. The maximum amplitude of porpoising obtained during take-offs of model 208M with flap deflection of 0°, 30°, and 45° is shown in figure 46. Comparison of figure 46 (model 208M) with figure 39 (model 208) shows that increasing the angle of incidence shifted aft the range of stable positions for the center of gravity. Increasing the angle of flap setting from 0° to 45° decreased slightly the extent of the region of intermediate porpoising and shifted aft the range of stable positions of the center of gravity.

Landing stability.- Results of landing tests of the basic model showed that, at a gross load of 60.5 pounds (10, 164 pounds, full size) and with the center of gravity at 24-percent mean aerodynamic chord, stable landings could be made at trims from 4° to 12°. At a gross load of 77.4 pounds (13,000 pounds, full size), landings made with the center of gravity at 24- and 32-percent mean aerodynamic chord were stable at trims from 4° to 7°. At trims from 7° to 10°, the model heaved slightly. Above 10°, the number of skips increased with trim until as many as 5 skips were observed at a trim of 14°. Control of the basic model in the air was extremely difficult with the center of gravity at the aft positions; a satisfactory landing technique could not be obtained until the area of the stabilizer was increased.

In general, the landing characteristics of the modifications which had vee steps of greater depth than the step of the basic model were superior to the landing characteristics of the basic model. Model 208N, with an afterbody having a constant dead-rise angle of 20°, skipped lightly throughout the range of trims investigated from 2.5° to 15°. Models 208E, 208G, 208H, 208I, 208J, and 208K landed stably at all trims investigated from 4°, to 13° with the center of gravity at 28-percent mean aerodynamic chord.

The landings made with model 208C were generally similar to the landings obtained with the basic model. Model 208F landed stably at trims from 4° to 15° with the center of gravity at 24-percent mean aerodynamic chord, but skipped once at all trims investigated from 4° to 13° with the center of gravity at 36-percent mean aerodynamic chord.

Model 208L, with the dead rise of the afterbody decreased just behind the step to give a very shallow step, skipped violently at trims above 7° but landed stably at trims of 5° and 6°. Model Model 208-15, with the hook on the step, landed stably at trims of 4°, 7.5°, and 12.5°, but trimmed down rapidly immediately after contact. A comparison of the results of landing tests of models 208N and 208P showed that lengthening the afterbody increased the number of skips after landing at trims above 6°, but had no effect at trims below 6°.

Model 208M, with the angle of incidence of the wing increased, had about the same landing characteristics as the basic model.

CONCLUSIONS

The investigation of the hydrodynamic stability and spray characteristics of the basic model showed that:

1. The spray characteristics were satisfactory in both smooth and rough water at a gross load of 77.4 pounds (13,000 pounds, full size). The bow showed no tendency to submerge while taxiing in rough water.

2. In addition to the upper and lower trim limits of stability, there was a region of intermediate porpoising which extended from the upper limit at intermediate planing speeds to the lower limit at high planing speeds. The extent of this intermediate region of instability was decreased by decreasing the gross load and decreasing the amount of power. The lower trim limit of stability was difficult to define at high planing speeds due to the disturbance in flow caused by the forebody chine flare.

3. The variation of trim with speed was characterized by the formation of a second hump after the true hump, and by porpoising which occurred when the trim crossed the intermediate region of instability. At a gross load of 77.4 pounds, some porpoising occurred for all elevator settings from 0° to -30° and center-of-gravity positions from 22- to 32-percent of the mean aerodynamic chord. At gross loads of either 60.5 pounds or 77.4 pounds (10,164 pounds or 13,000 pounds, full size), take-offs could be made with an amplitude of lower-limit porpoising of less than 2°, with the center of gravity at 24-percent mean aerodynamic chord and the elevator at -10°. Upper limit porpoising was not encountered with an elevator setting less than -30° and the center of gravity forward of 32-percent mean aerodynamic chord.

4. At a gross load of 77.4 pounds, the model landed stably at trims from 4° to 7°, heaved during landing at trims from 7° to 10° and skipped during landing at trims above 10°. At a gross load of 60.5 pounds, the model landed stably at trims from 4° to 12°.

Results of tests of several modifications showed that:

1. The amount of spray wetting the flaps was decreased by reducing the chine flare just ahead of the step from down 20° to down 6°. With the elimination of all chine flare, however, the spray on the flaps was much heavier than with a flare of down 20°.

2. Configurations which had higher hump trims also had less satisfactory spray characteristics than the basic model.

3. The change in trim to a second hump was eliminated by fading out the chine flare just forward of the step.

4. The extent of the intermediate region of instability was decreased by changing the plan form of the step from 45° - vee to transverse while maintaining a constant depth of step at the keel and by increasing the clearance of the afterbody above the wake from the forebody.

5. Configurations with less extensive regions of intermediate porpoising than the basic model also had wider ranges of stable positions of the center of gravity for take-off.

6. An increase in the angle of wing incidence decreased slightly the extent of the region of intermediate instability and shifted aft the range of stable positions of the center of gravity.

7. The landing characteristics of modifications having vee-steps of greater depth than the step of the basic model were superior to the landing characteristics of the basic model.

8. The additions of chine flare and transverse spoiler steps on the afterbody aggravated the porpoising in the intermediate region.

9. Longitudinal steps on the forebody, longitudinal strips on the afterbody, a hook on the step, aerodynamic spoilers on the sides of the afterbody, and an increase in the length of the afterbody were ineffective means of improving the hydrodynamic stability.

Langley Memorial Aeronautical Laboratory
National Advisory Committee for Aeronautics,
Langley Field, Va.

Robert F. Havens
Robert F. Havens
Aeronautical Engineer

Approved: John B. Parkinson
John B. Parkinson
Chief of Hydrodynamics Research Division

ORB

REFERENCES

1. Truscott, Starr: The Enlarged N.A.C.A. Tank, and Some of Its Work. NACA TM No. 918, 1939.

2. Olson, Roland E., and Land, Norman S.: The Longitudinal Stability of Flying Boats as Determined by Tests of Models in the NACA Tank. I - Methods Used for the Investigation of Longitudinal-Stability Characteristics. NACA ARR, Nov. 1942.

3. Parkinson, John B., and Olson, Roland E.: Tank Tests of a 1/5 Full Size Dynamically Similar Model of the Army OA-9 Amphibian with Motor-Driven Propellers - NACA Model 117. NACA ARR, Dec. 1941.

TABLE I

COMPARISON OF PRINCIPAL DIMENSIONS OF 1/5.5-SCALE DYNAMIC MODEL AND FULL-SIZE COLUMBIA XJL-1 AIRPLANE

	Model	Full size
Hull:		
Beam, including plating projecting from chines, in.	13.84	76.0
Lengths parallel to straight portion of forebody keel, in.		
Forebody, bow to centroid of step	41.69	229.3
Afterbody, centroid of step to sternpost	36.27	199.5
Tail extension, sternpost to trailing edge of rudder	18.18	100.0
Over all, bow to trailing edge of rudder	96.14	528.8
Depth of step (plan form 45° vee) in.		
At keel	1.14	6.27
At centroid	0.93	5.11
At chine	1.44	7.98
Angle of forebody keel relative to base line, deg	-5.0	-5.0
Angle of afterbody keel relative to base line, deg	12.5	12.5
Angle between keels, deg	7.5	7.5
Angle of dead rise of forebody at step, deg		
Excluding chine flare	20.0	20.0
Including chine flare	13.5	13.5
Angle of dead rise of afterbody, deg		
Step at station 233	24.0	24.0
Maximum, at station 315	29.5	29.5
At sternpost	20.0	20.0
Center line of pivot holes below thrust line, in.	4.37	----
Wing:		
Area, sq ft	13.65	413.0
Span, ft	9.1	50.0
Root chord (section NACA 4418)in.	20.0	110.0
Tip chord (section NACA 4412) in.	12.0	66.0
Angle of wing setting, deg		
Reference to base line	0	0
Reference to forebody keel	5.0	5.0
Mean aerodynamic chord, M.A.C., in.	18.39	101.17
Leading edge M.A.C. parallel to base line		
Aft of bow, in.	32.0	176.0
Below thrust line, in.	3.27	18.0

TABLE I - Concluded

COMPARISON OF PRINCIPAL DIMENSIONS OF 1/5.5-SCALE DYNAMIC MODEL AND FULL SIZE COLUMBIA XJL-1 AIRPLANE - Concluded

	Model	Full size
Wing (continued):		
Flap setting, deg		
Take off	30	
Landing	45	
Horizontal tail:		
Span, ft	3.64	20.0
Chord (section NACA 0012), ft	0.91	5.0
Area, stabilizer, sq ft	2.03	61.3
Area, elevator, sq ft	1.27	38.7
Total Area, sq ft	3.3	100.0
Angle of stabilizer to base line, deg	-2.0	-2.0
Vertical tail:		
Total area (section NACA 0012), sq ft	1.25	38.2
Propeller:		
Blades	3	3
Diameter, ft	[a]1.94	10.5
Blade angle, deg	14	
Take-off power, rpm	[a]5500	1800
Landing power, rpm	[a]2750	
Angle of thrust line to base line, deg	0	0
Thrust line above keel at centroid of step perpendicular to base line, in.	17.4	208.8
Static thrust, lb.	27.5	4410
Loading conditions:		
Normal gross load, lb.	60.5	10,164
Maximum design load, lb.	77.4	13,000
Center of gravity (28-percent M.A.C.)		
Forward of centroid of step parallel to straight portion of forebody keel, in.	3.94	21.7
Above forebody keel perpendicular to straight portion of forebody keel, in.	13.44	74.0
Average pitching moment of inertia, slug-ft^2	[a]4.25	19,400

[a]These values not to scale.

TABLE II.- DESCRIPTION OF MODIFICATIONS

Model	Forebody	Afterbody	Figure	Remarks
208	I	I	1,2,3	Basic model; 45° -vee step, 0.93 in. deep at centroid.
208-2	I	I	11	Chine flare on basic afterbody.
208-5	III	II	5	45°-vee step in basic position, 0.93 in. deep at centroid.
208-6	III	III		45°-vee step in basic position, 1.28 in. deep at centroid.
208-7	IV	III	5	45°-vee step in basic position, 1.28 in. deep at centroid.
208-8	I	IV		45°-vee step in basic position, 1.32 in. deep at centroid.
208-9	I	IV	12	Hydrodynamic spoiler on afterbody at station 365.
208-10	I	IV	12	Hydrodynamic spoiler on afterbody at station 300.
208 A	I	I	13	30°-vee step, 1.23 in. deep at centroid. Centroid 1.91 in. aft of centroid of basic step.
208A-1	I	I		Chine flare of basic model filled with moulding clay (plastilene) to give 0° angle of flare.
208B	I	I	13	20°-vee step, 1.39 in. deep at centroi . Centroid 2.87 in. aft of centroid of basic step.
208C	I	I	13	Transverse step, 1.42 in. deep at distance of 1/3 beam from keel. Formed by lowering the forebody 0.54 in. perpendicular to baseline. Location, 0.14 in. forward of centroid of basic step.
208C-4	I	I	15	Aerodynamic spoilers on sides of afterbody of model 208C.
208D	I	-----		Afterbody removed. 45°-vee, approximately 9 in. deep at centroid. Model sealed aft of step along parting line (waterline 95).
208E	I	I	14	20°-vee step, 1.42 in. deep at centroid. Formed by lowering the forebody 0.54 in. perpendicular to baseline. Centroid 0.14 in. forward of centrois of basic step.
208F	I	I	14	Transverse step, 2.00 in. deep at distance of 1/3 beam from keel. Formed by lowering forebody 0.54 in. and raising afterbody 0.52 in. perpendicular to baseline. Location at centroid of basic step.
208F-3	I	I		Wing removed from model 208F.

TABLE II.- DESCRIPTION OF MODIFICATIONS - Concluded

Model	Forebody	Afterbody	Figure	Remarks
208G	II	VI	4	45°-vee step, 1.48 in. deep at centroid. Position of centroid, same as basic step.
208G-11	II	VI	16	Longitudinal steps on forebody of model 208G.
208G-12	I	VI		Basic chine flare restored on forebody of model 208G.
208H	II	IV	8	45°-vee step, 1.4 in. deep at centroid. Position of centroid, same as basic step.
208H-13	II	IV	17	Afterbody aft of station 300 raised $\frac{3}{4}$ in.
208H-14	II	IV		Three $\frac{1}{4}$ in. by $\frac{1}{4}$ in. square strips each side of keel and parallel to keel. Spaced at 2 in. intervals from keel, extending from station 280 back to intersection with afterbody chine.
208H-15	II	IV	17	Hook on forebody of model 208H at the step.
208I	II	V	9	45°-vee step, 1.9 in. deep at centroid. Position of centroid same as basic step.
208J	II	V	9	30°-vee step, 1.9 in. deep at centroid. Position of centroid same as basic model.
208K	II	IV	18	30°-vee step, 2.34 in. deep at centroid. Position of centroid same as basic model.
208L	I	VII		45°-vee step, 0.5 in. deep at centroid, 0.84 in. deep at chine. Position of centroid same as basic model.
208M	I	I		Basic model with angle of incidence of wing changed to 4° relative to baseline. Rotated about point midway between upper and lower surface at 35-percent root chord.
208N	V	VIII	6	30°-vee step, 1.23 in. deep at centroid. Position of centroid same as basic model.
208P	V	IX	10	Length of afterbody of model 208N increased 5 in.

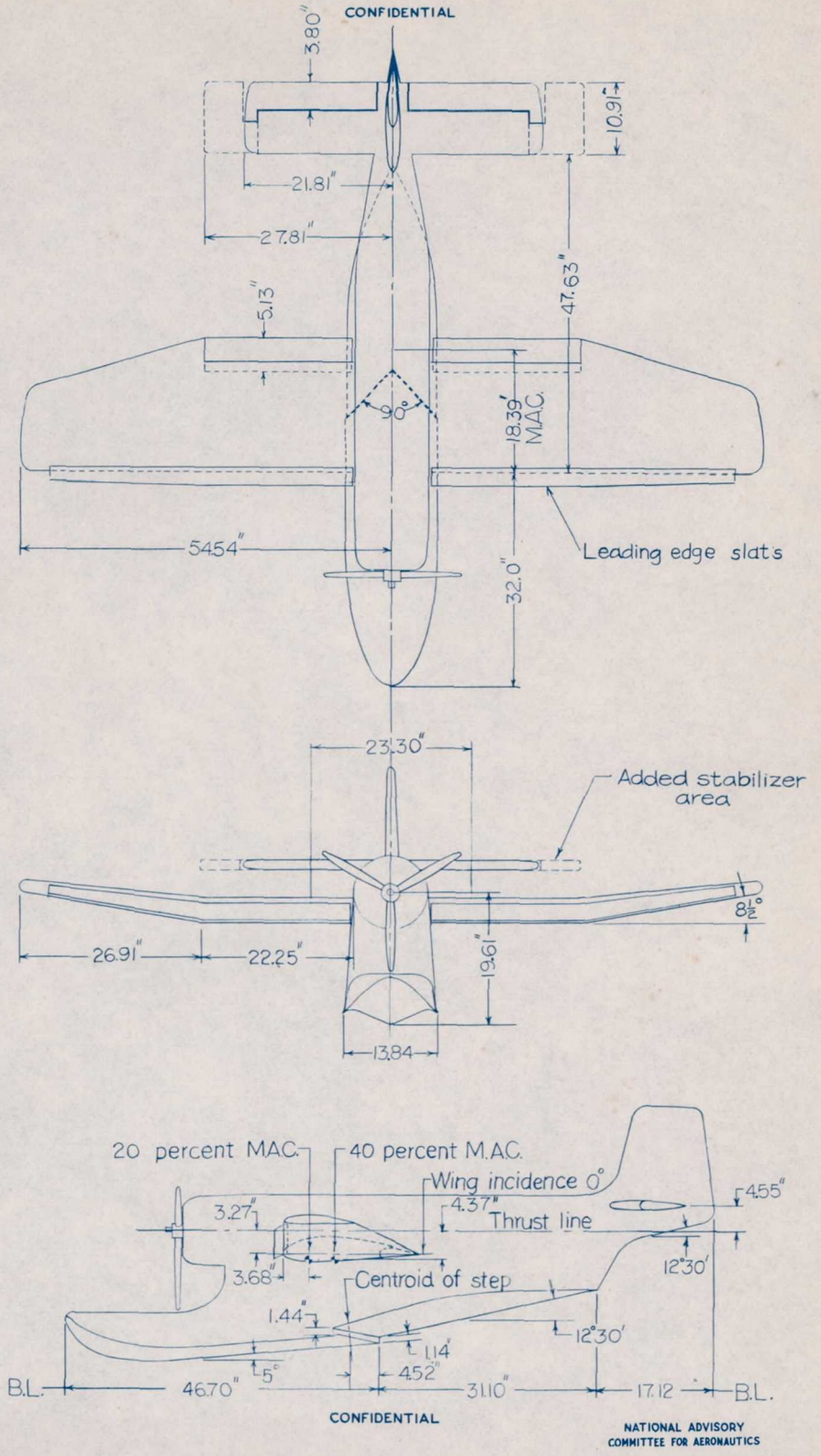

Figure 1.- Model 208. General Arrangement.

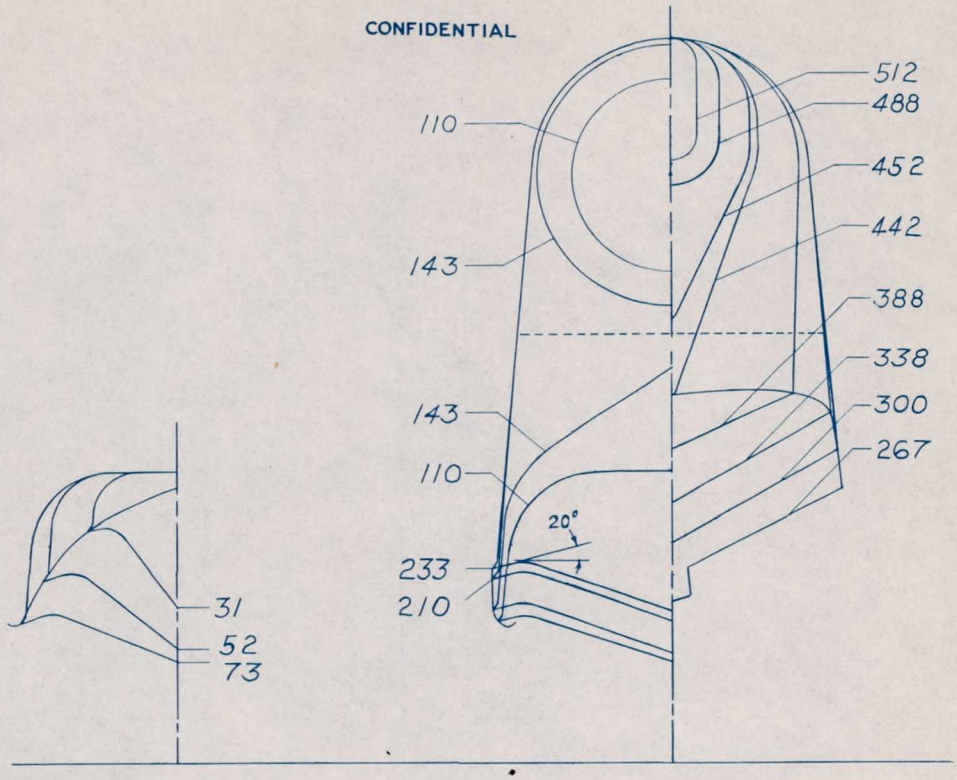

--------- PARTING LINES ON MODEL

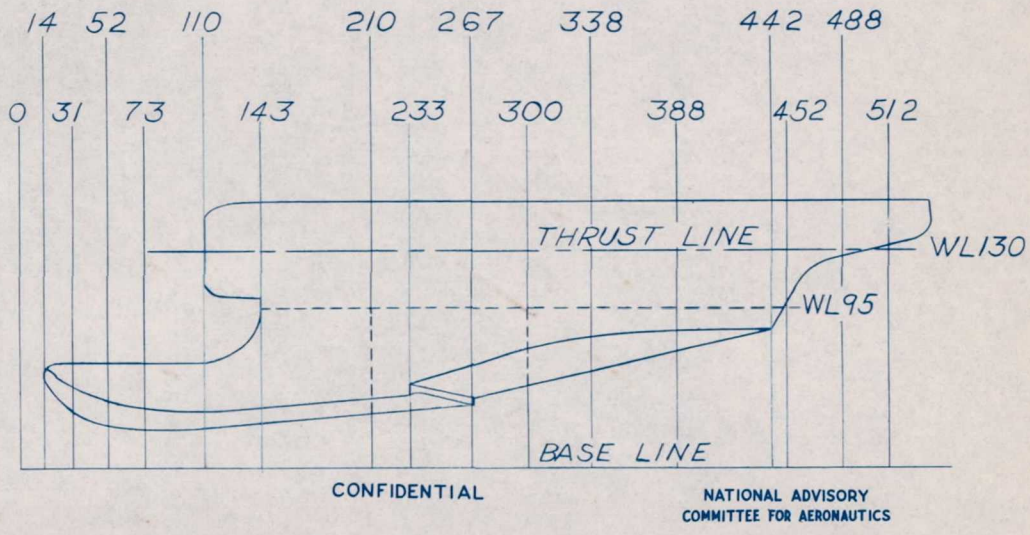

FIGURE 2.-MODEL 208. BODY PLAN

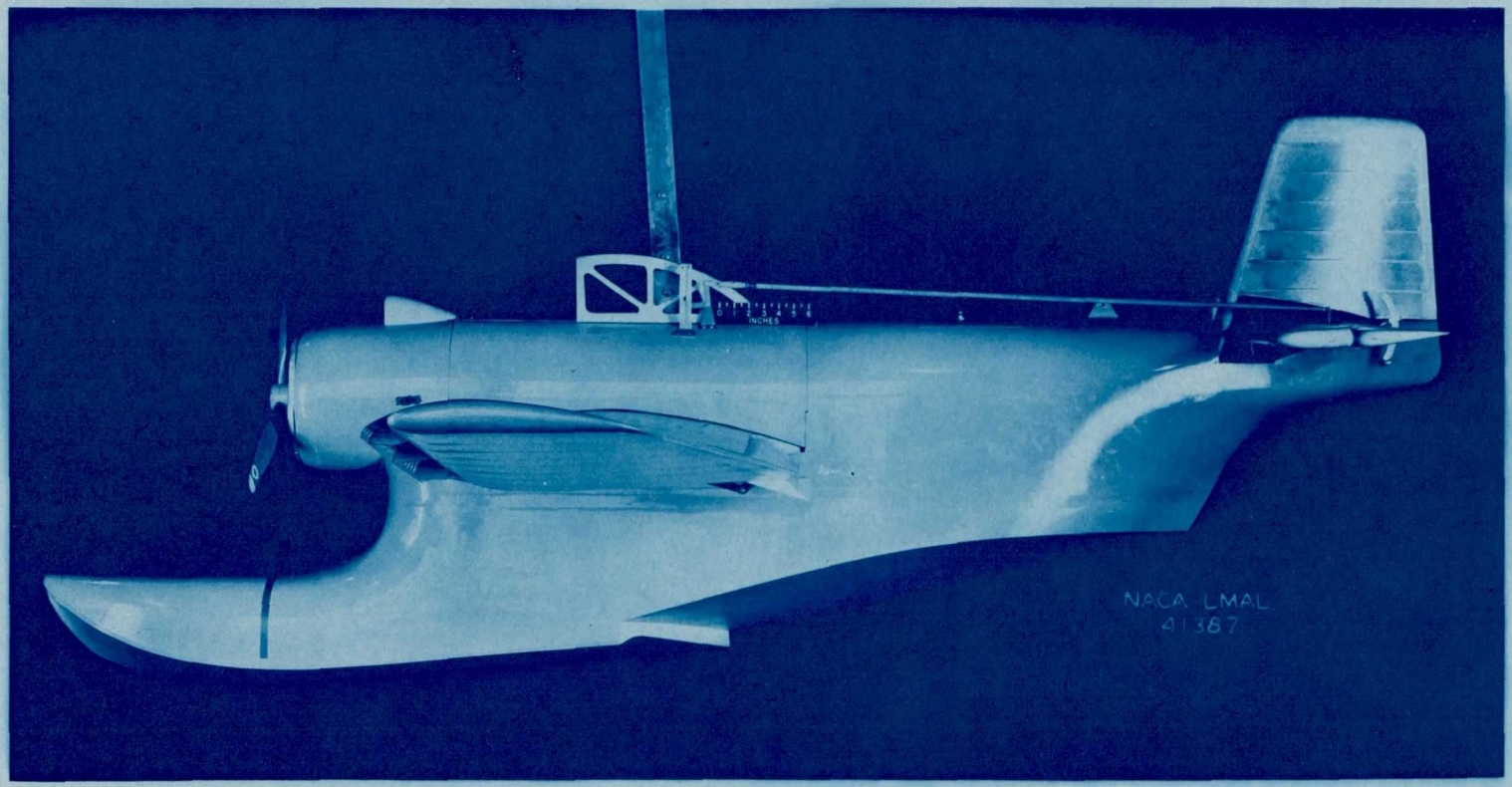

Figure 3.- Side view of Model 208.

NATIONAL ADVISORY COMMITTEE FOR AERONAUTICS
LANGLEY MEMORIAL AERONAUTICAL LABORATORY - LANGLEY FIELD, VA.

NACA RM No. L6I20

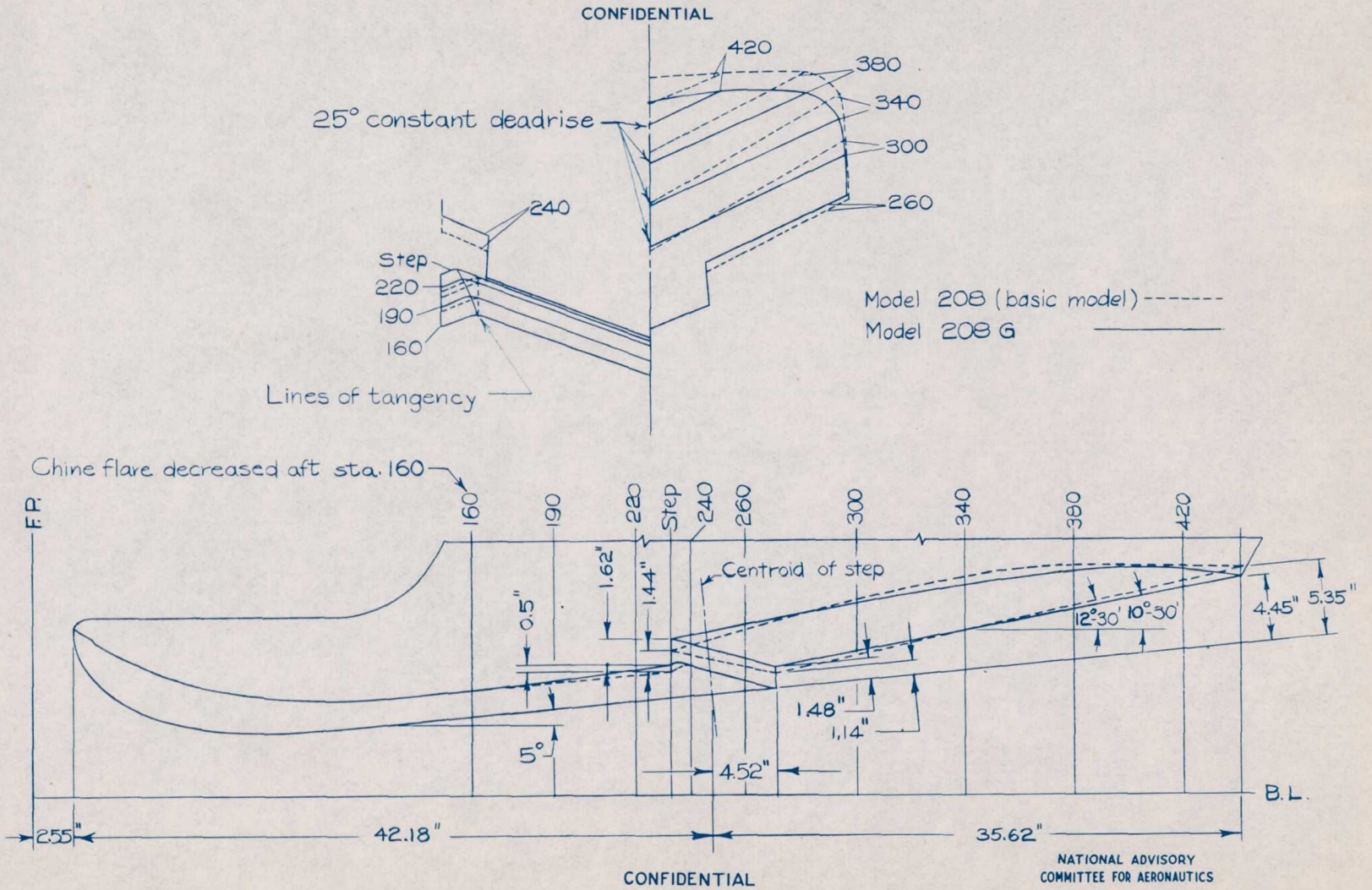

Figure 4. — Comparison of model 208 G with basic model. Forebody II and afterbody VI.

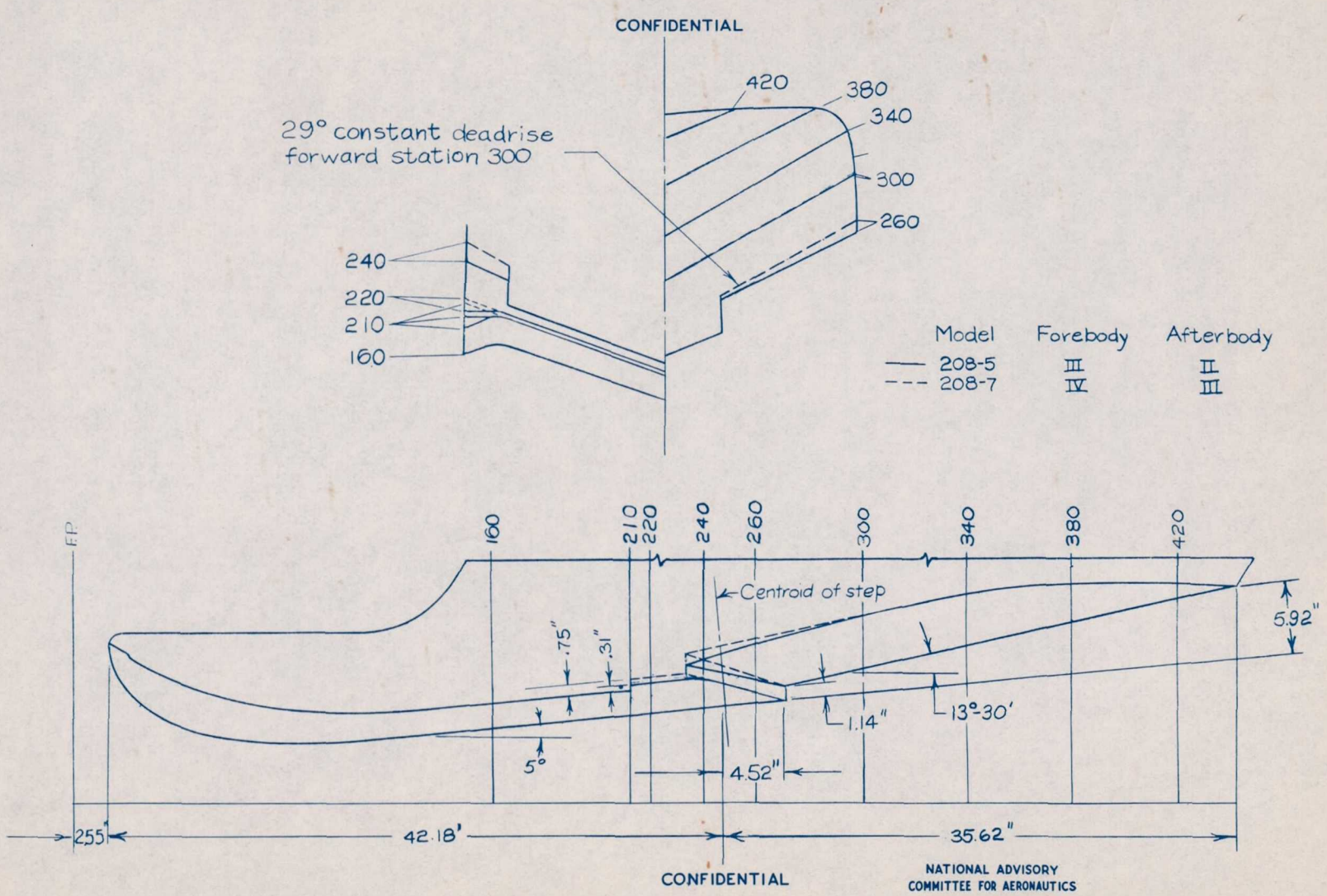

Figure 5.- Models 208-5 and 208-7. Forebodies III, IV and afterbodies II, III.

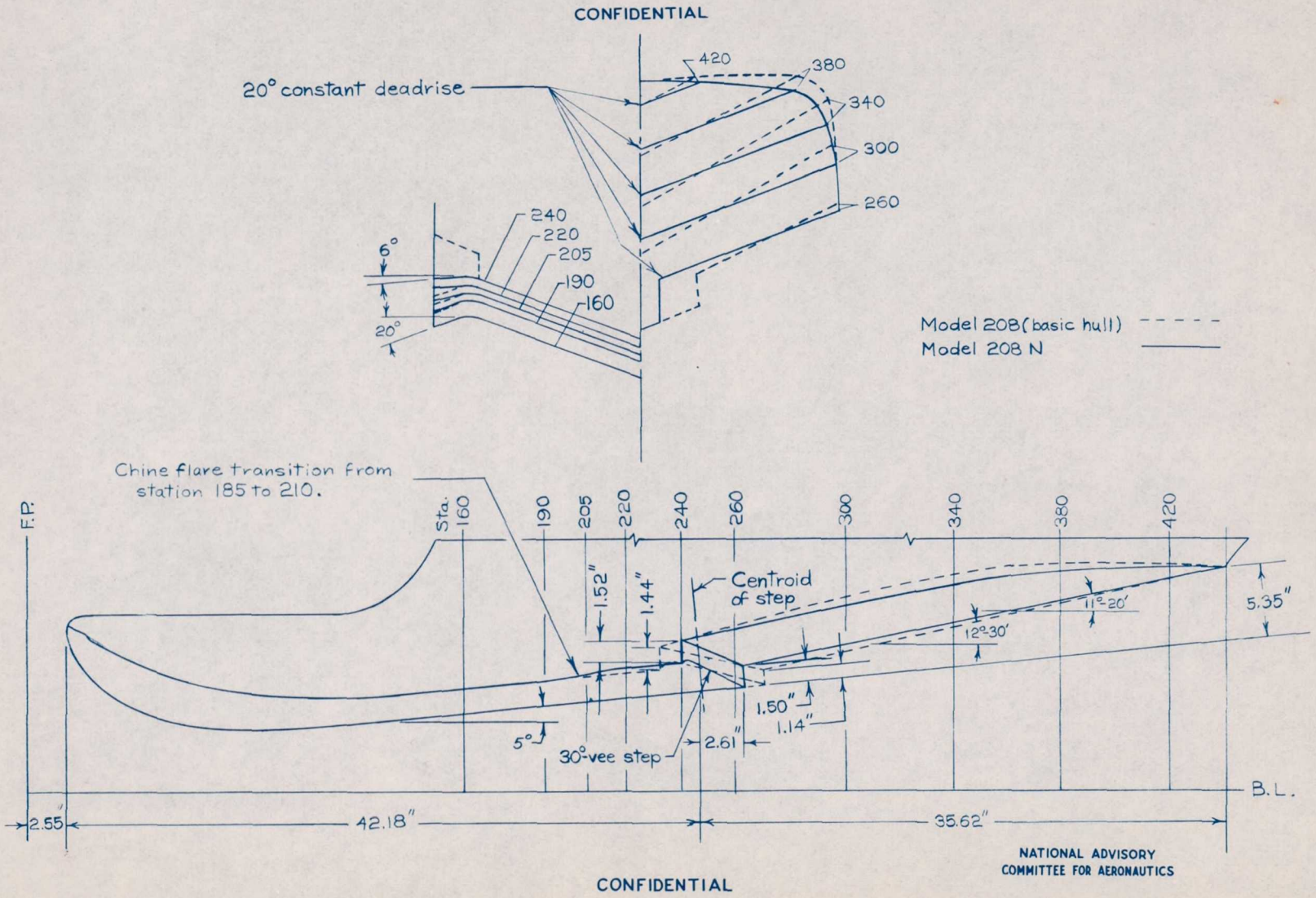

Figure 6. – Comparison of model 208N with basic model. Forebody V and afterbody VIII.

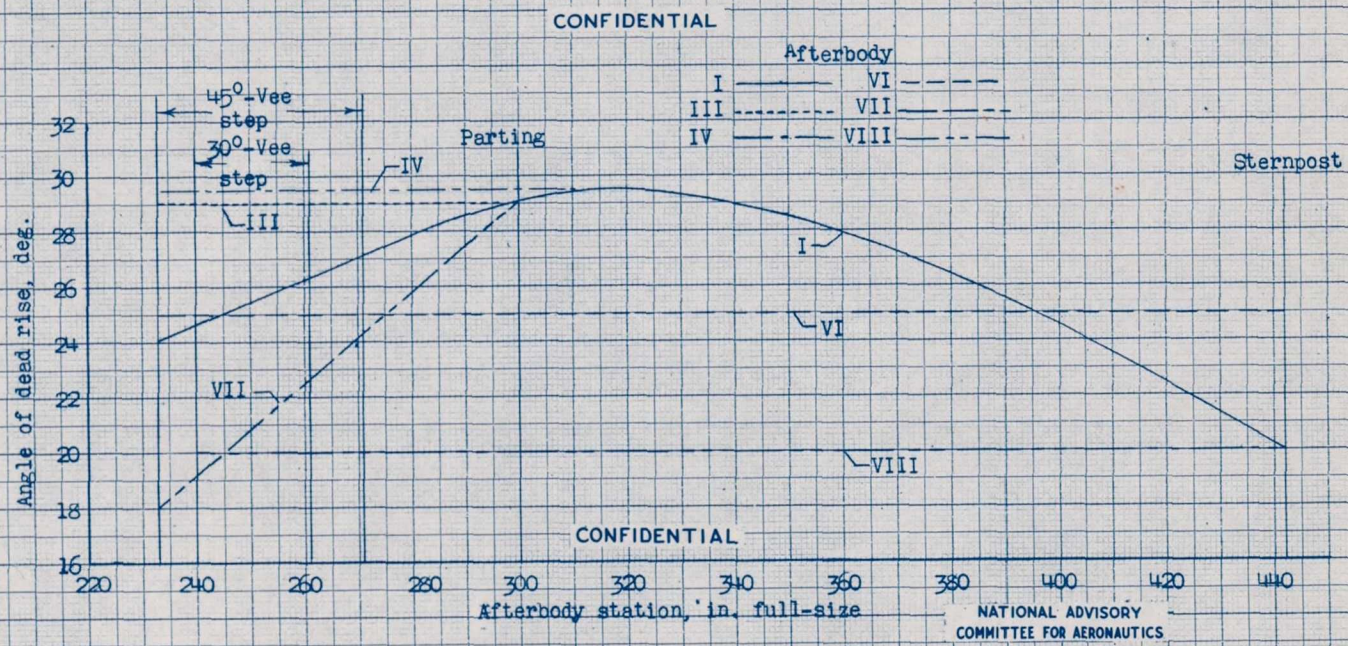

Figure 7.- Variation of angle of dead rise with afterbody-station location. Dead rise taken from model templates.

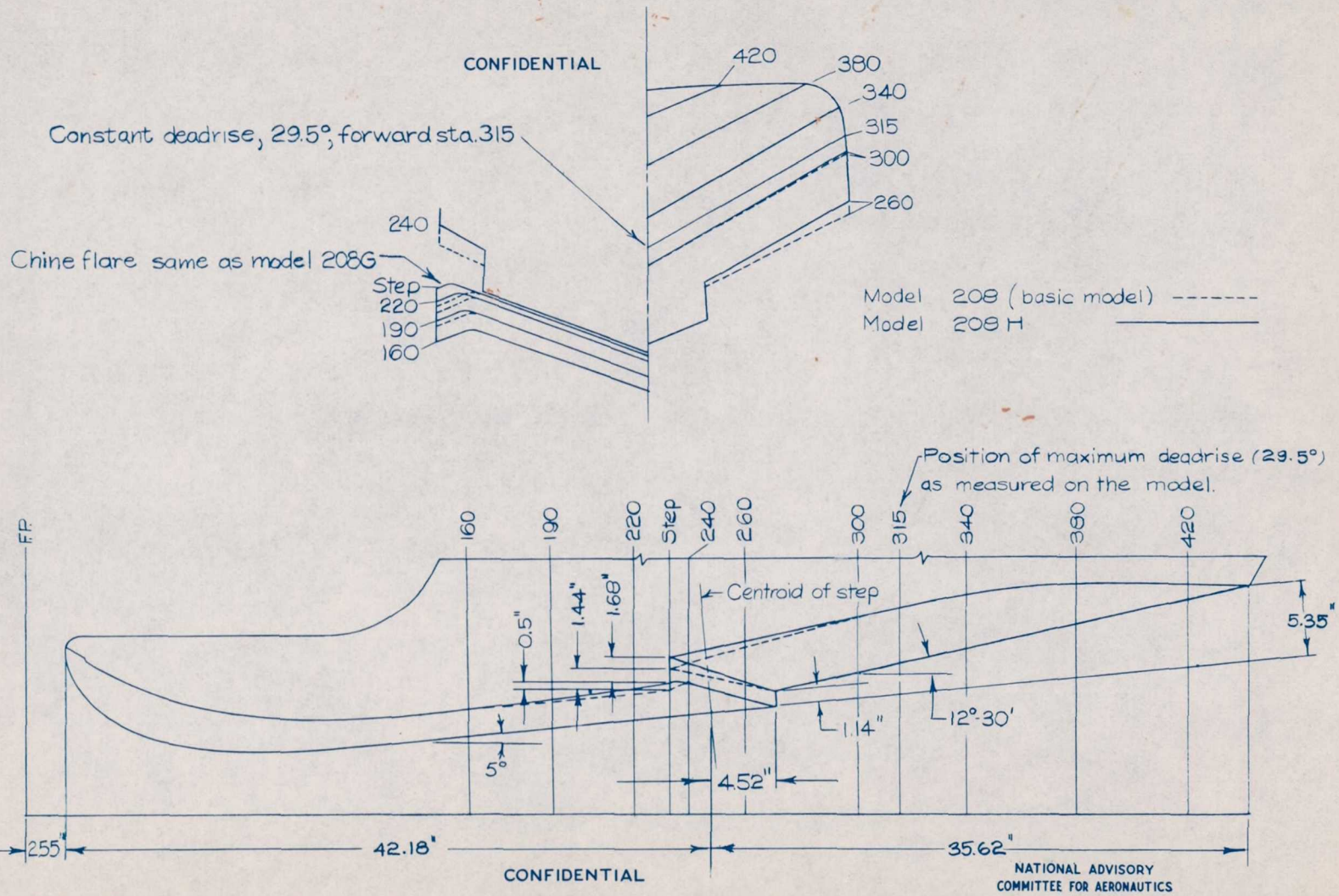

Figure 8 .- Comparison of model 208 H with basic model. Forebody II and afterbody IV.

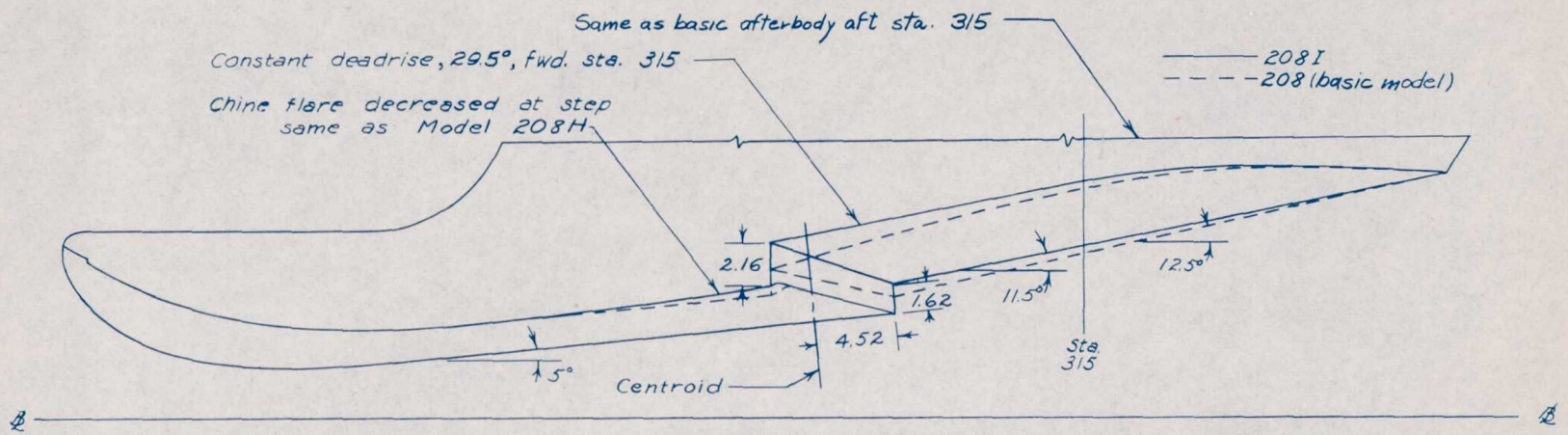

(a) Model 208I (same as Model 208H, with afterbody rotated at sternpost to increase depth of step)

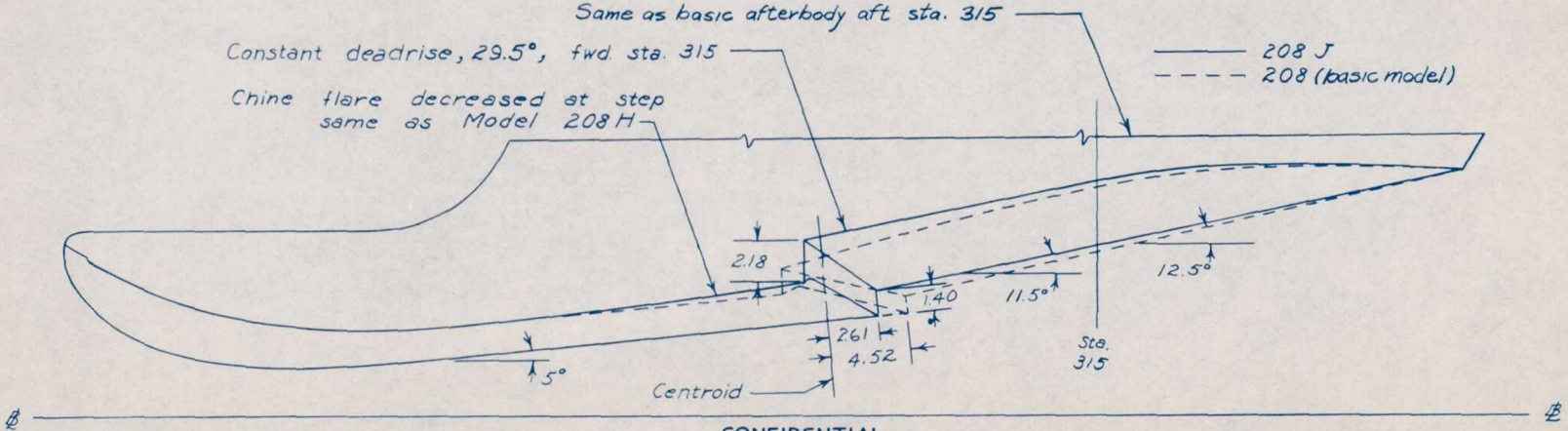

(b) Model 208J (same as Model 208I, with 30°-Vee step)

NATIONAL ADVISORY COMMITTEE FOR AERONAUTICS

Figure 9 .- Comparison of models 208I and 208J with basic model. Forebody II and afterbody V.

NACA RM No. L6I20

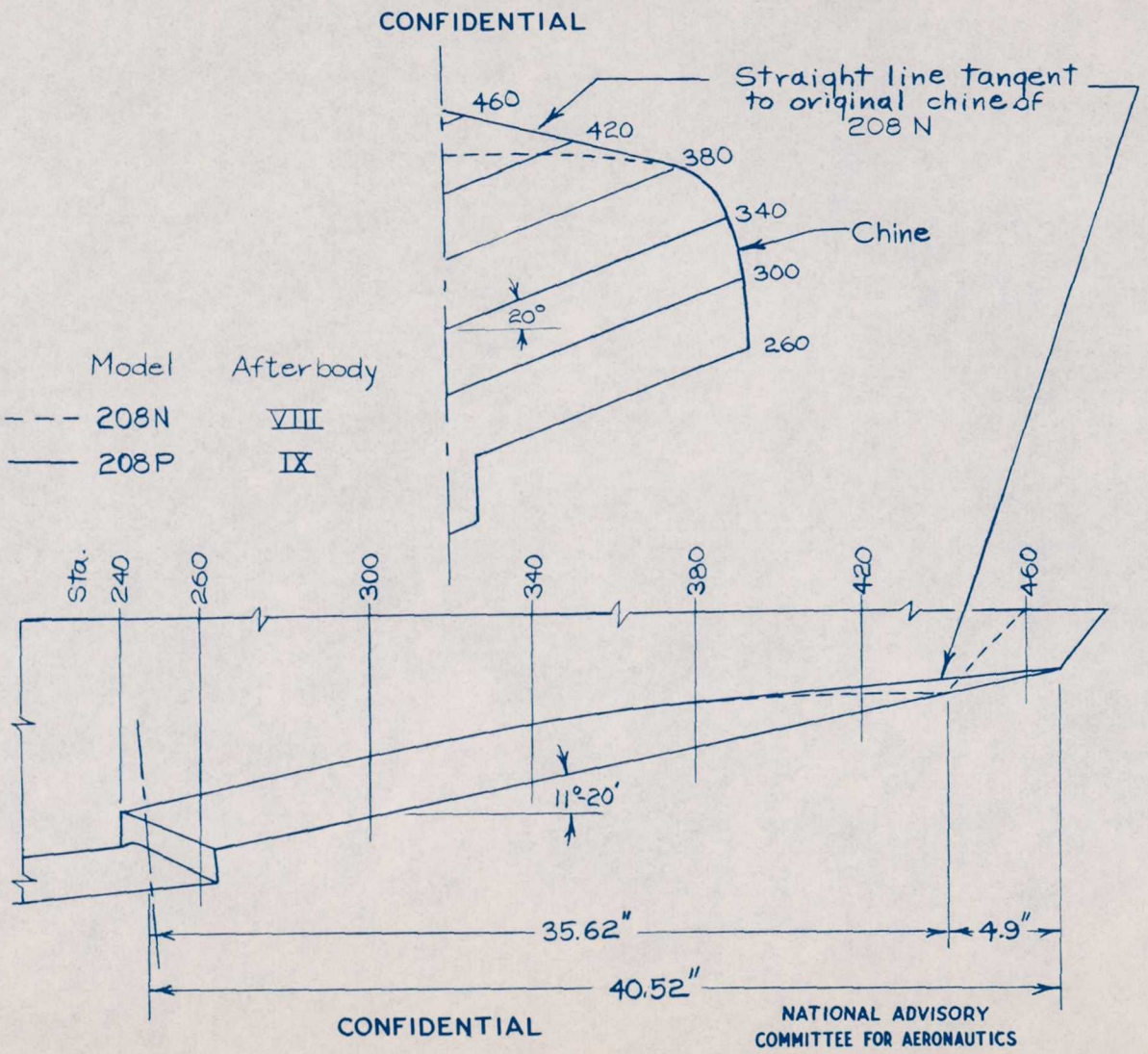

Figure 10. Comparison of afterbodies of models 208N and 208P. Afterbodies VIII and IX.

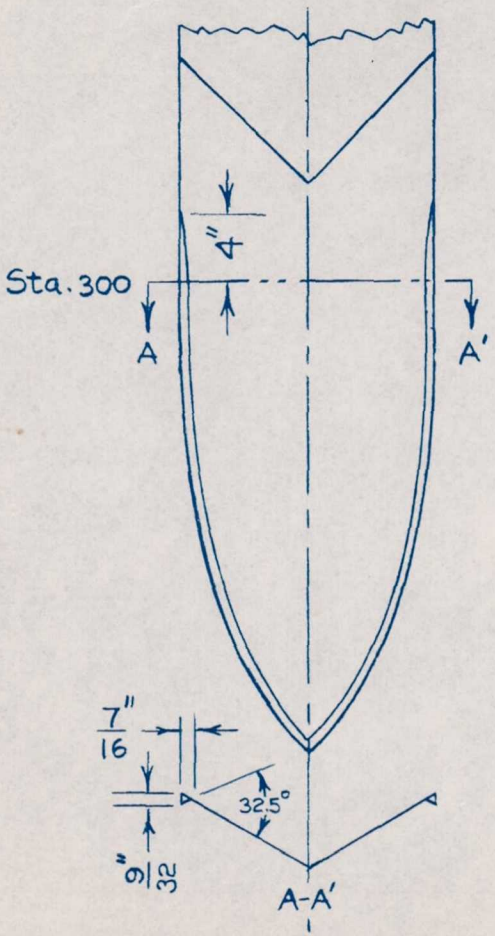

Figure 11.- Model 208-2. Afterbody chine flare.

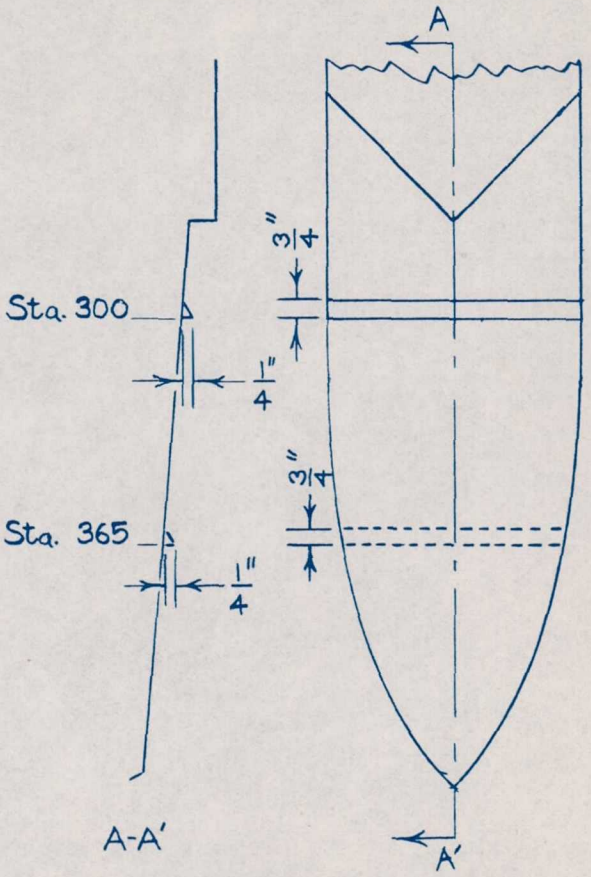

Model	Location
--- 208-9	Sta. 365
—— 208-10	Sta. 300

NATIONAL ADVISORY COMMITTEE FOR AERONAUTICS

Figure 12.- Models 208-9 and 208-10. Hydrodynamic spoilers on afterbody.

NACA RM No. L6I20

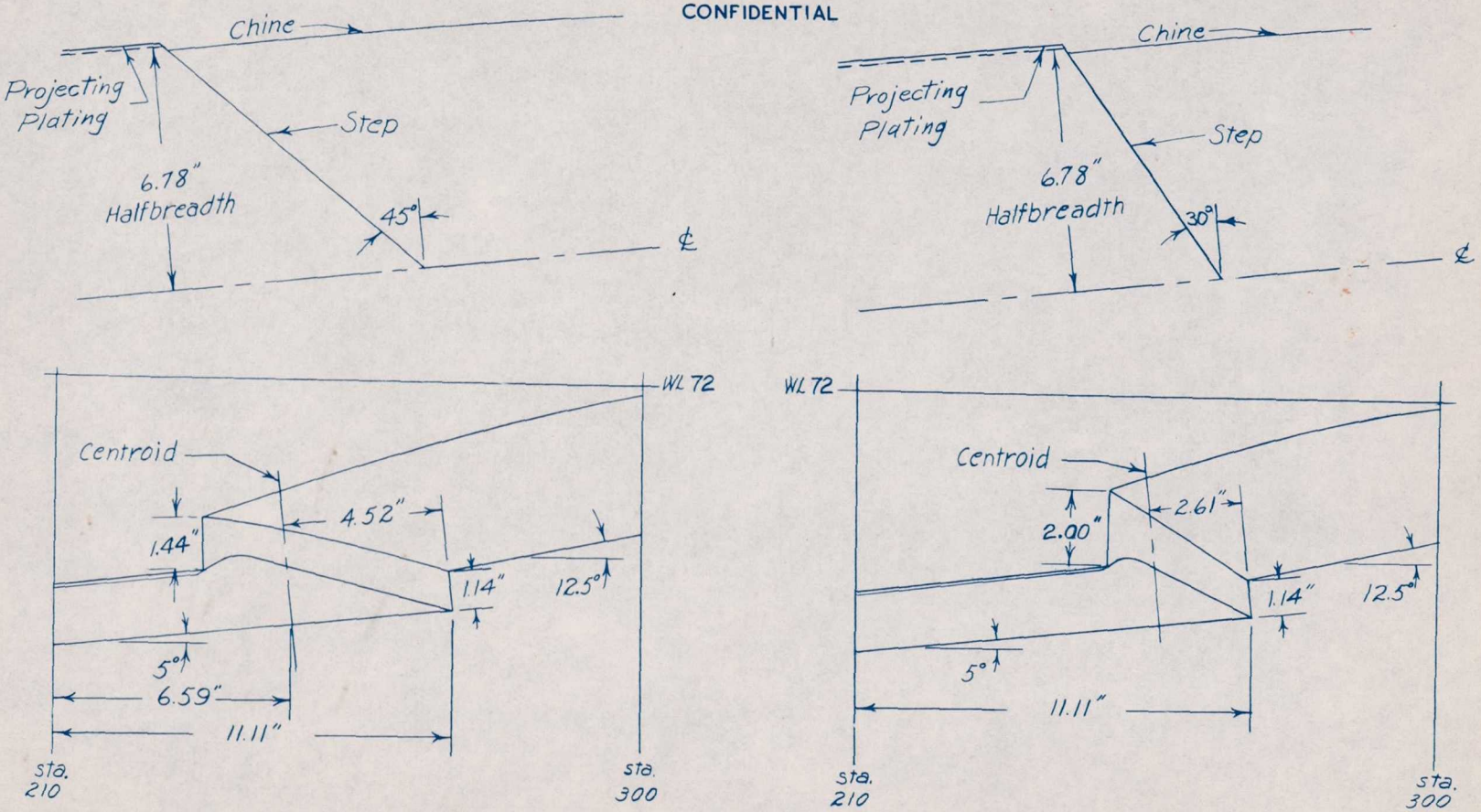

NATIONAL ADVISORY COMMITTEE FOR AERONAUTICS

Figure 13.- Model 208. Details of step modifications. Dimensions as measured on model.

NACA RM No. L6I20

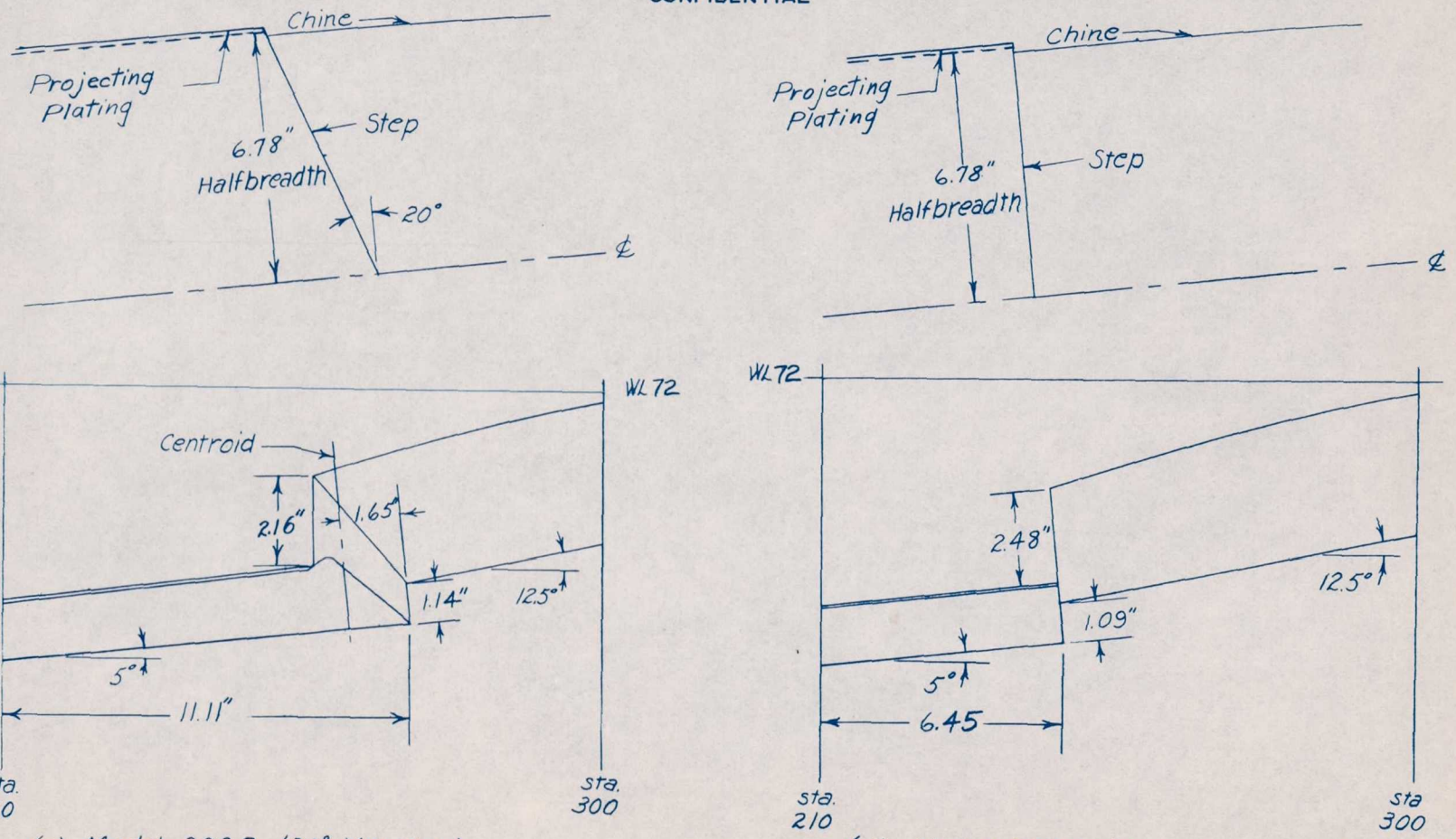

Figure 13.- Concluded.

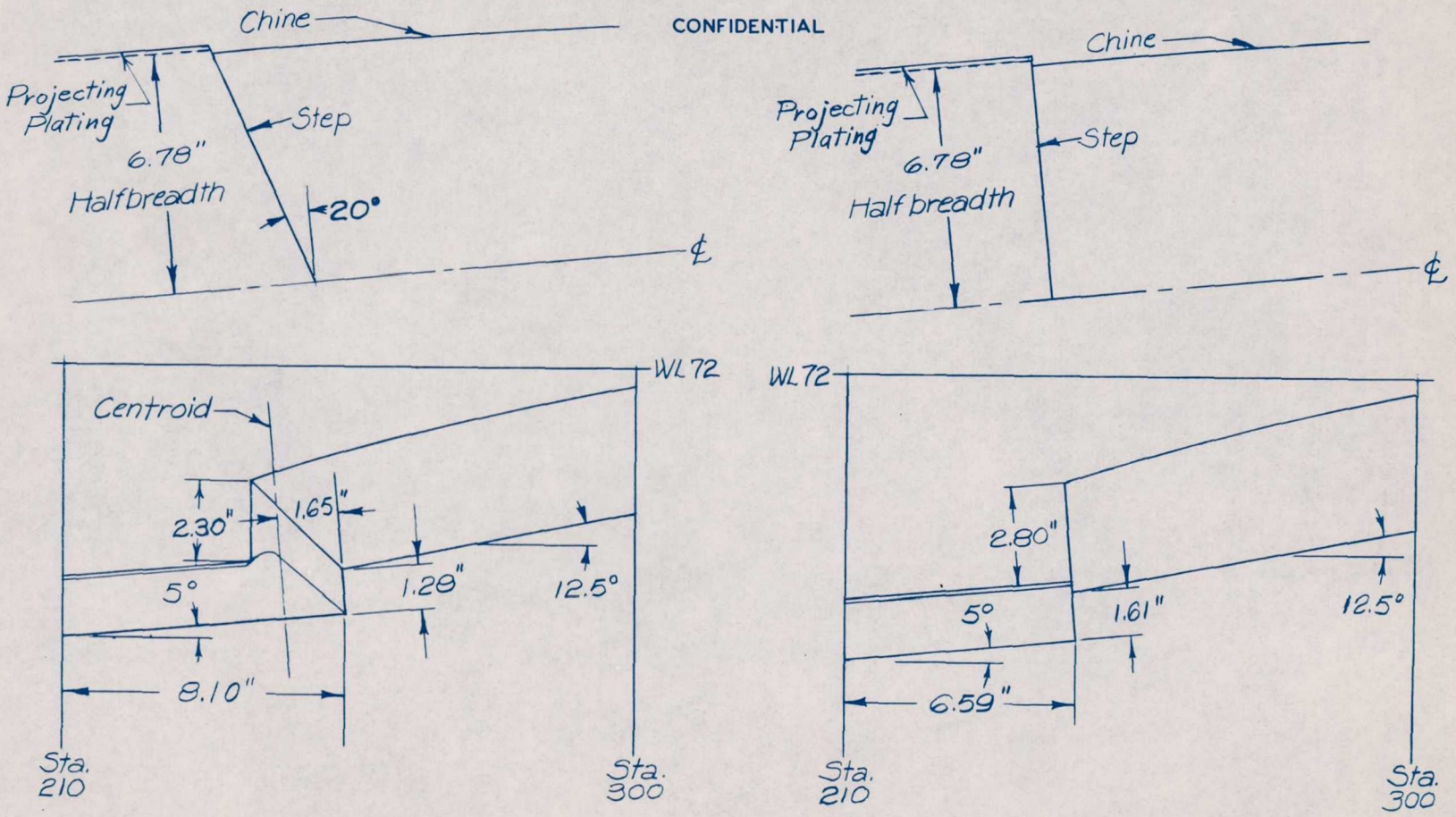

(a) Model 208 E (deep 20°-Vee step)

(b) Model 208F (deep transverse step)

NATIONAL ADVISORY COMMITTEE FOR AERONAUTICS

Figure 14. - Model 208. Details of step modifications. Dimensions as measured on model.

NACA RM No. L6I20

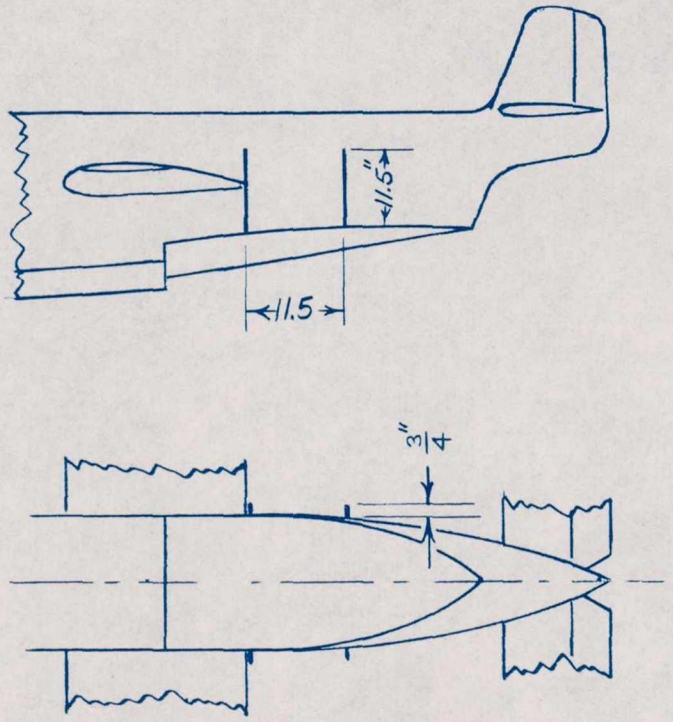

Figure 15.- Model 208C-4. Aerodynamic spoilers on sides of afterbody.

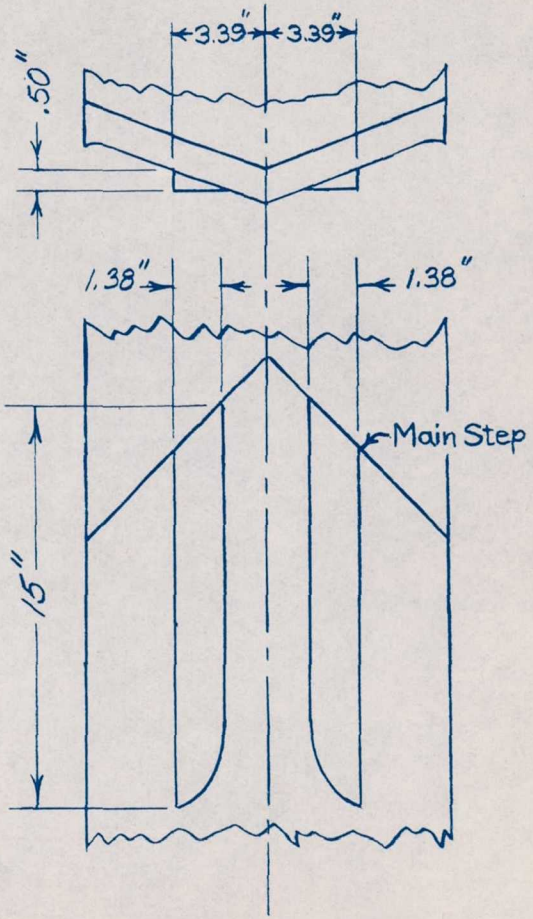

Figure 16.- Model 208G-11. Longitudinal steps on forebody.

NATIONAL ADVISORY
COMMITTEE FOR AERONAUTICS

NACA RM No. L6I20

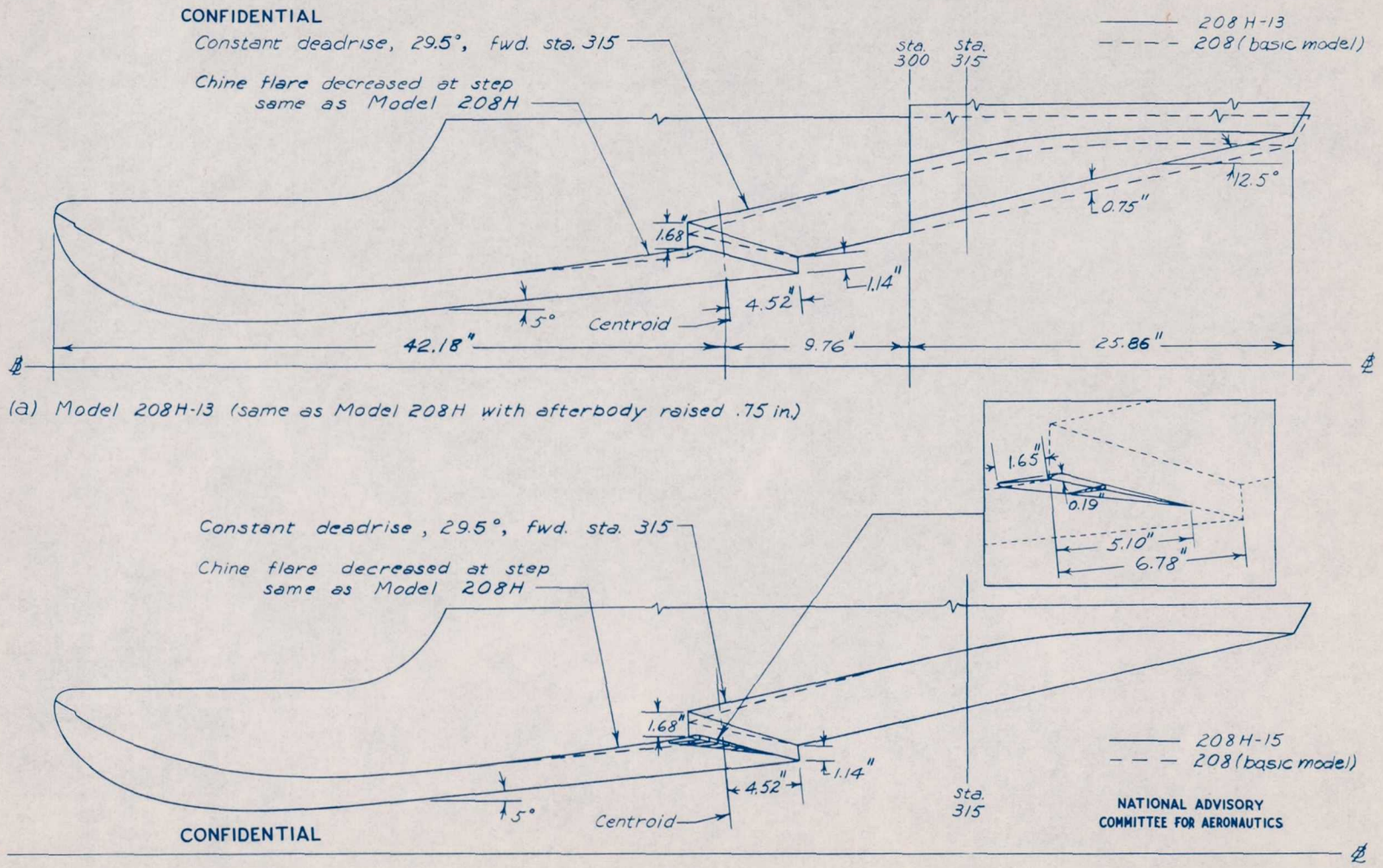

(a) Model 208H-13 (same as Model 208H with afterbody raised .75 in.)

(b) Model 208H-15 (same as Model 208H, with hook on step)

Figure 17 .- Models 208H-13 and 208H-15. Modifications of hull.

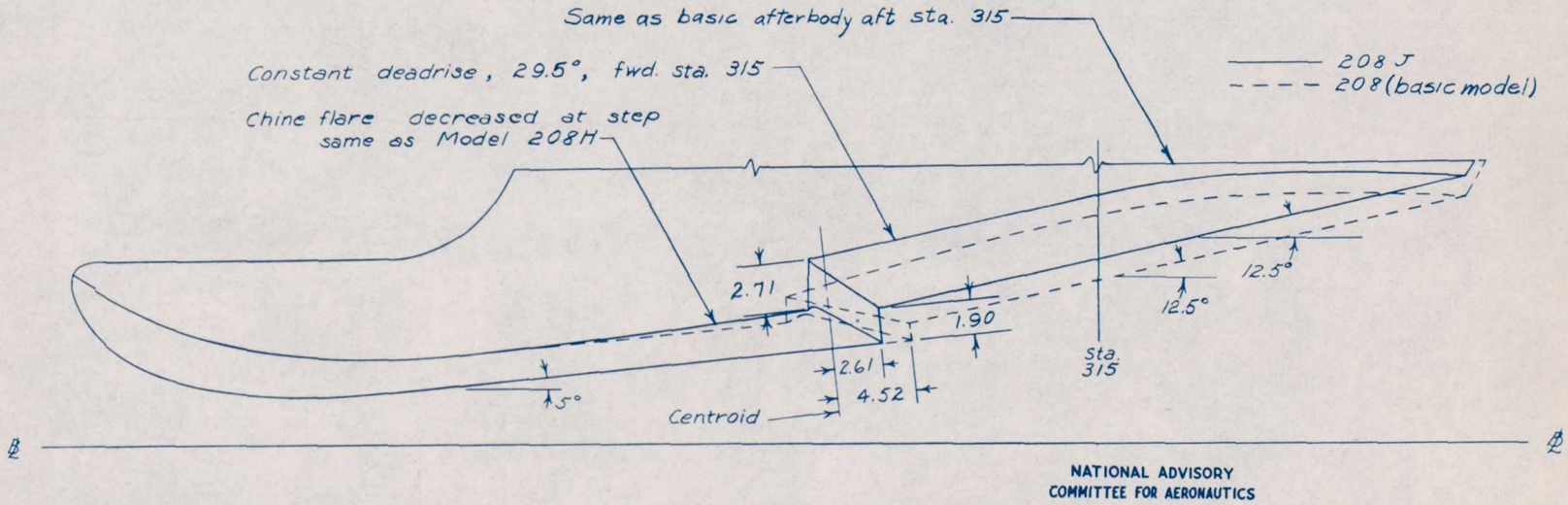

Figure 18.- Model 208 K (deep 30°-Vee step) Forebody II and afterbody IV.

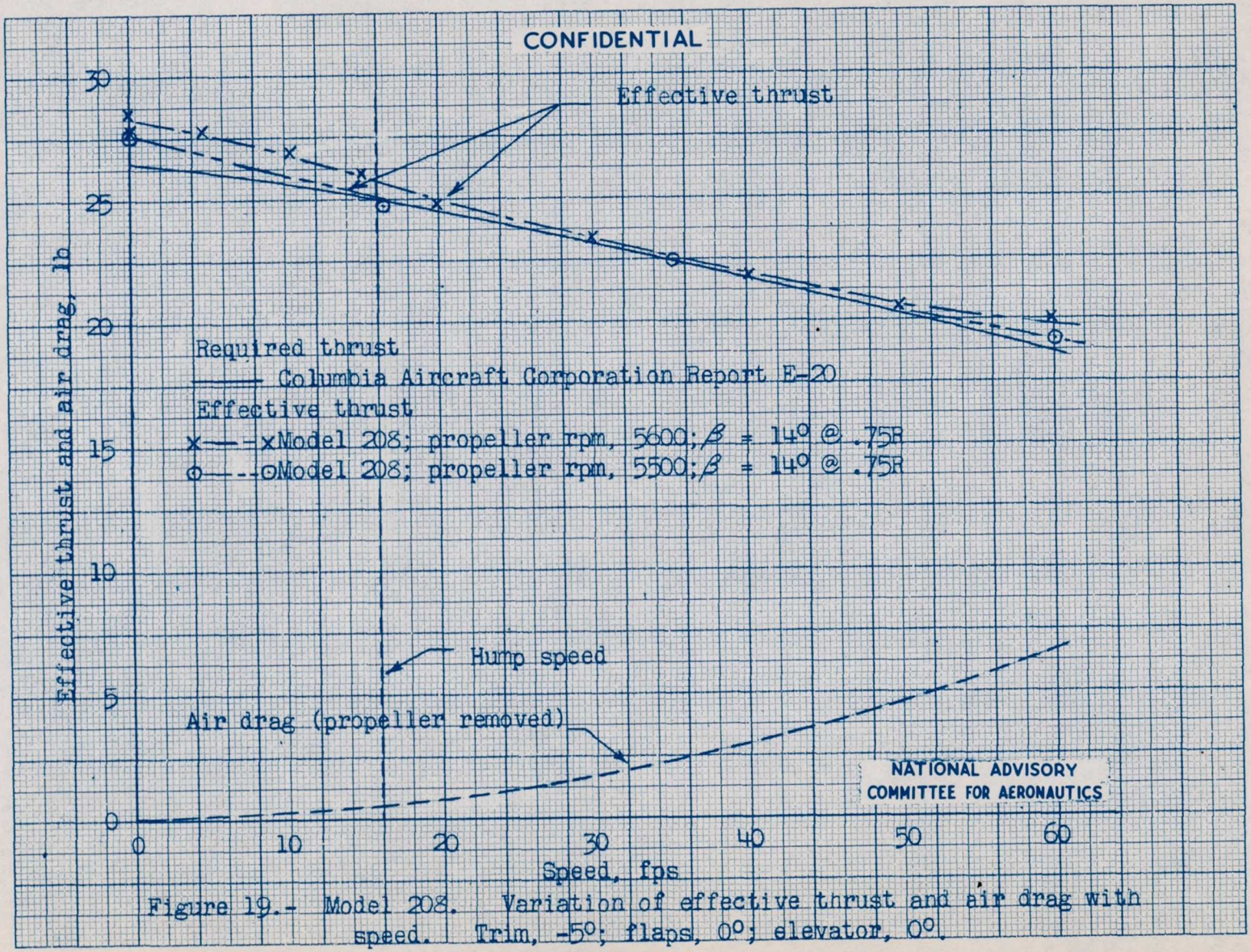

Figure 19.- Model 208. Variation of effective thrust and air drag with speed. Trim, -5°; flaps, 0°; elevator, 0°.

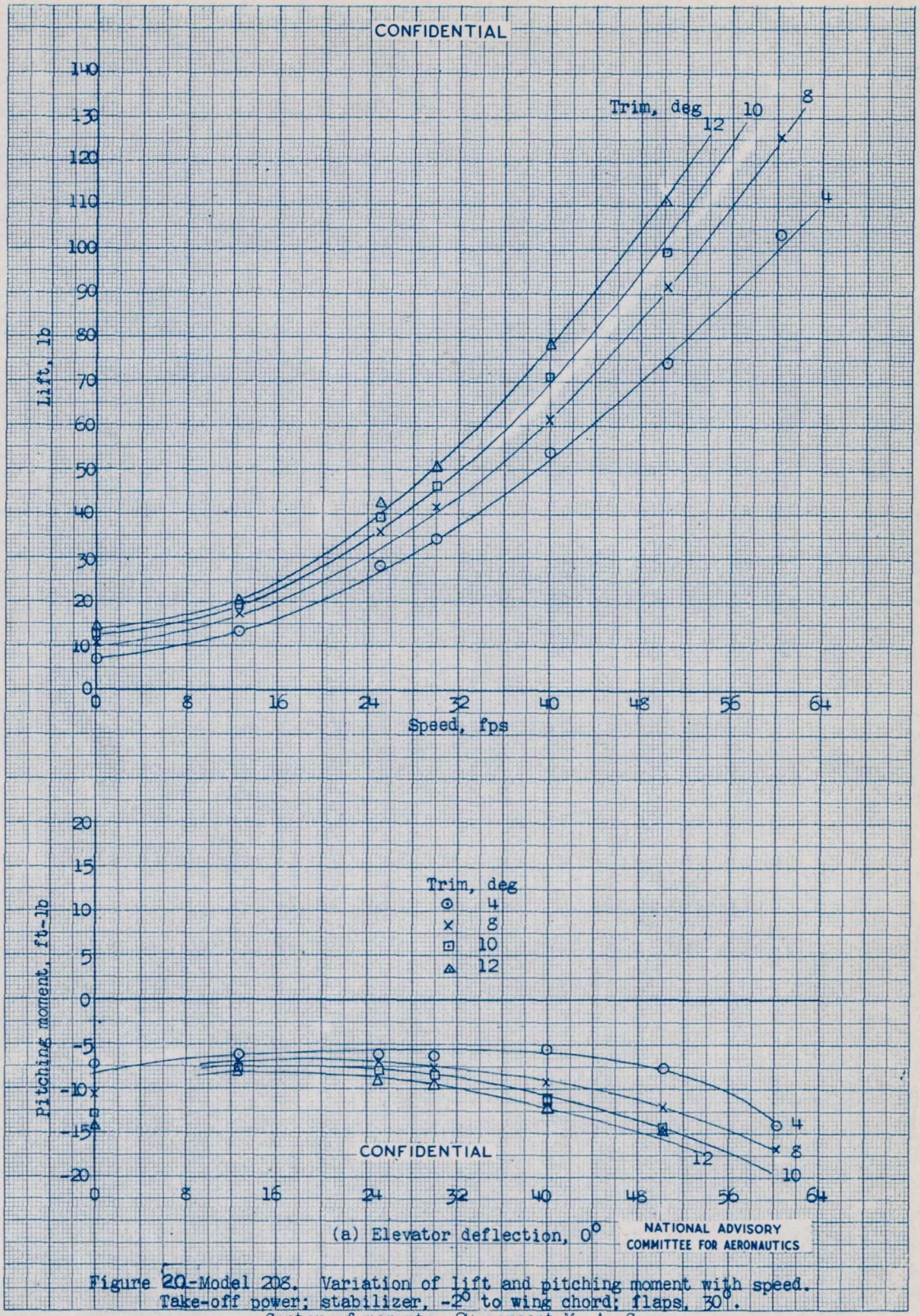

Figure 20.-Model 208. Variation of lift and pitching moment with speed. Take-off power; stabilizer, -2° to wing chord; flaps, 30°. Center of moments, 24 percent M. A. C.

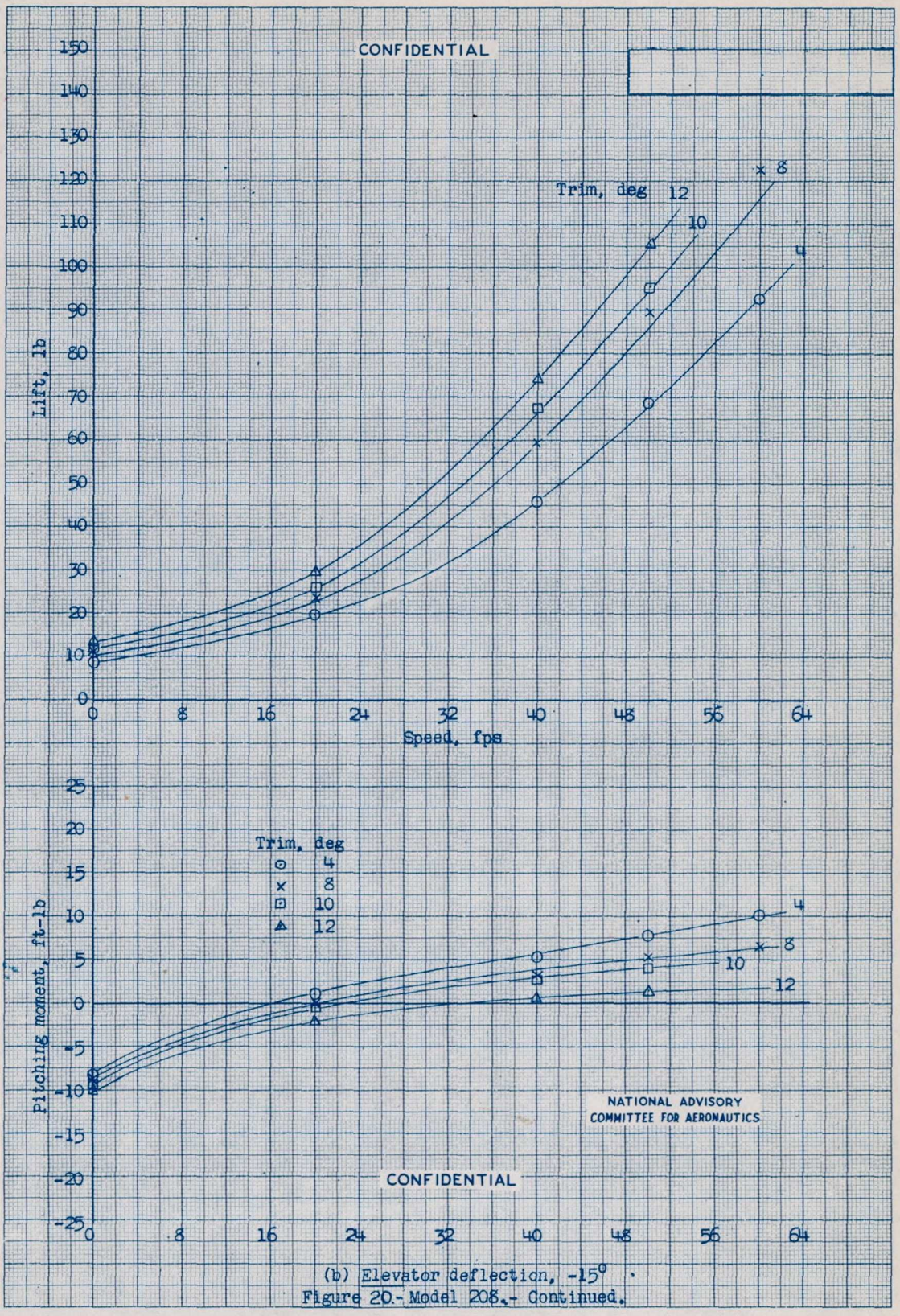

(b) Elevator deflection, -15°

Figure 20.- Model 208.- Continued.

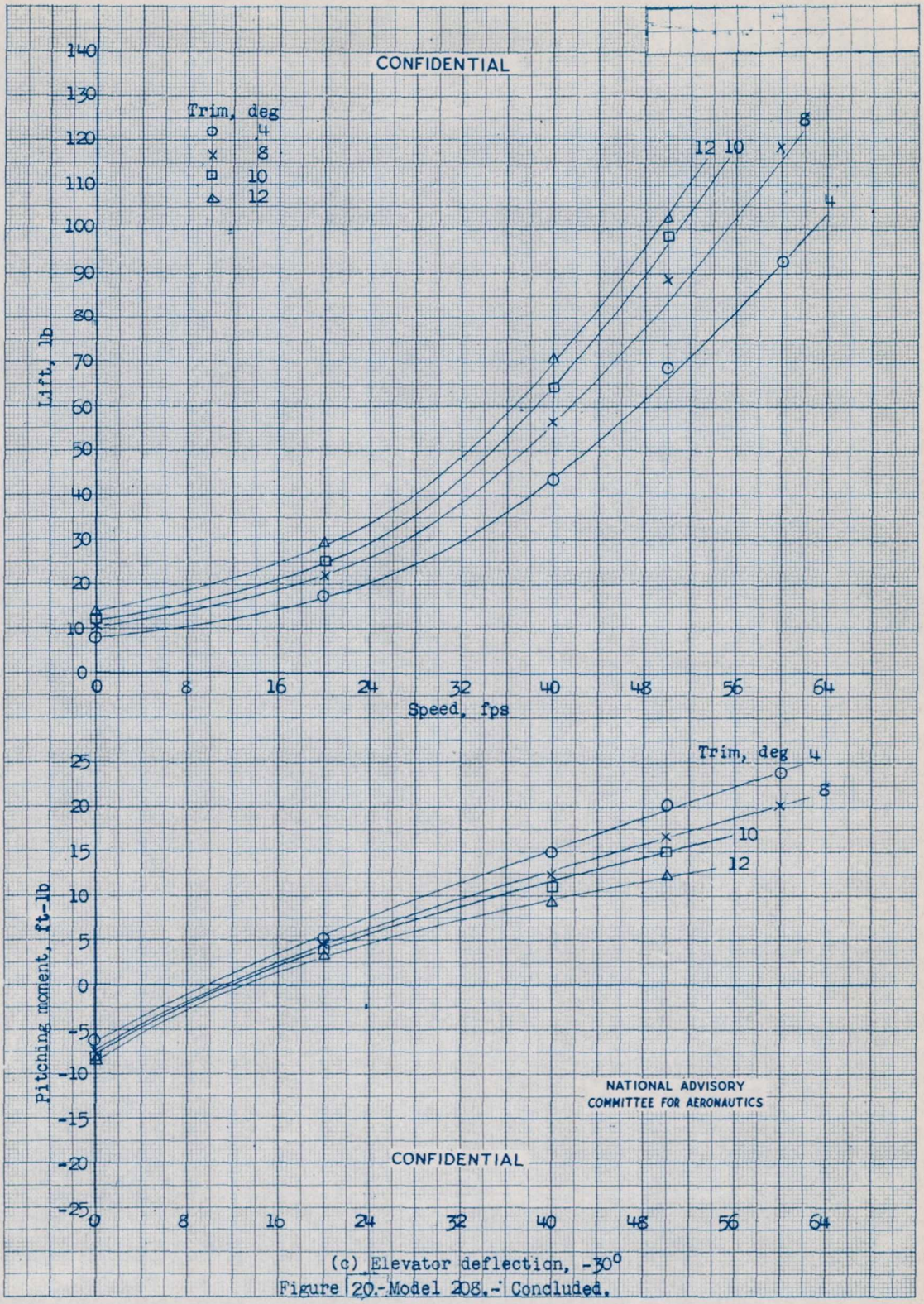

(c) Elevator deflection, -30°

Figure 20.- Model 208.- Concluded.

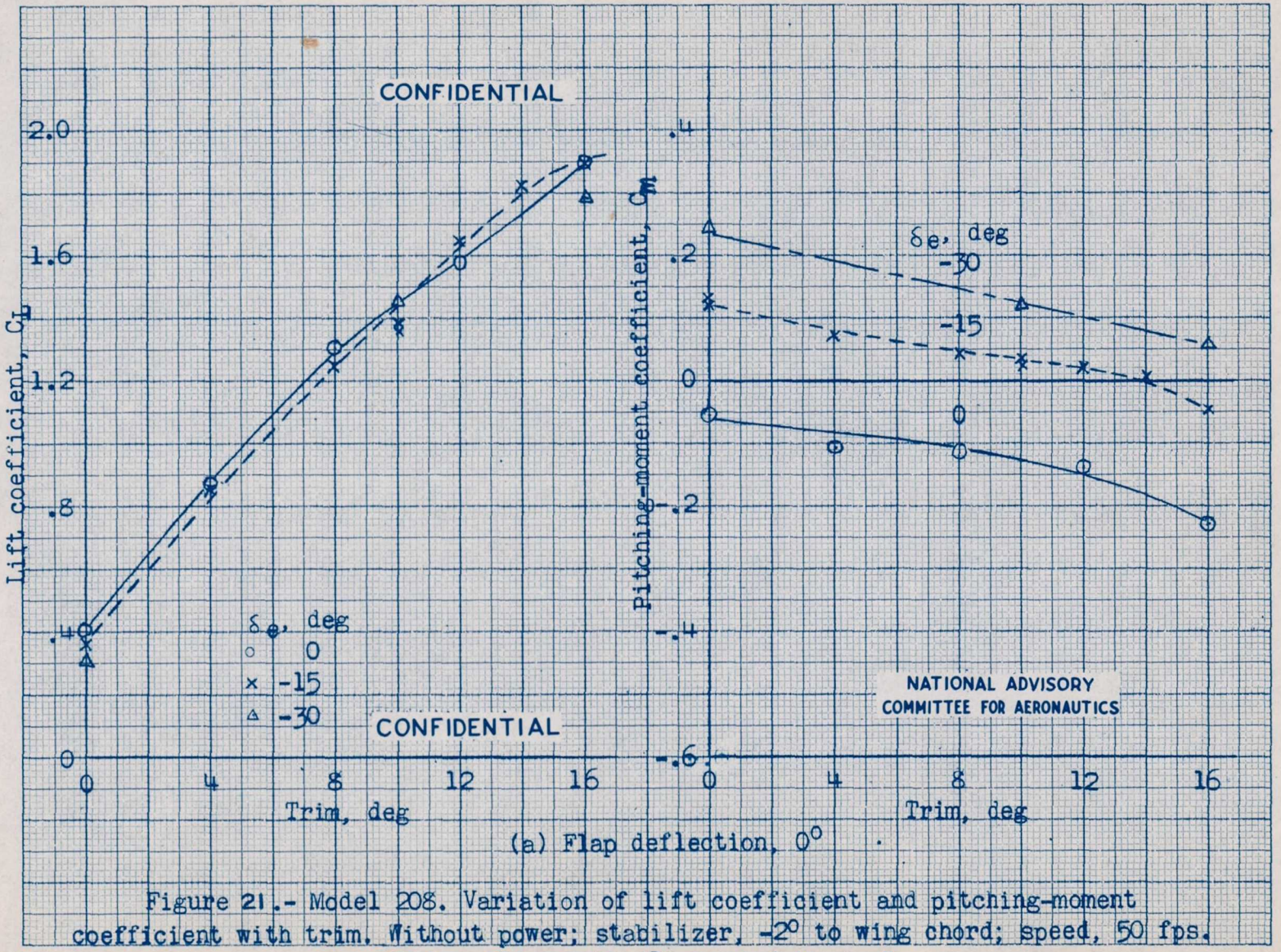

(a) Flap deflection, 0°

Figure 21.- Model 208. Variation of lift coefficient and pitching-moment coefficient with trim. Without power; stabilizer, -2° to wing chord; speed, 50 fps. Center of moments, 24 percent M. A. C.

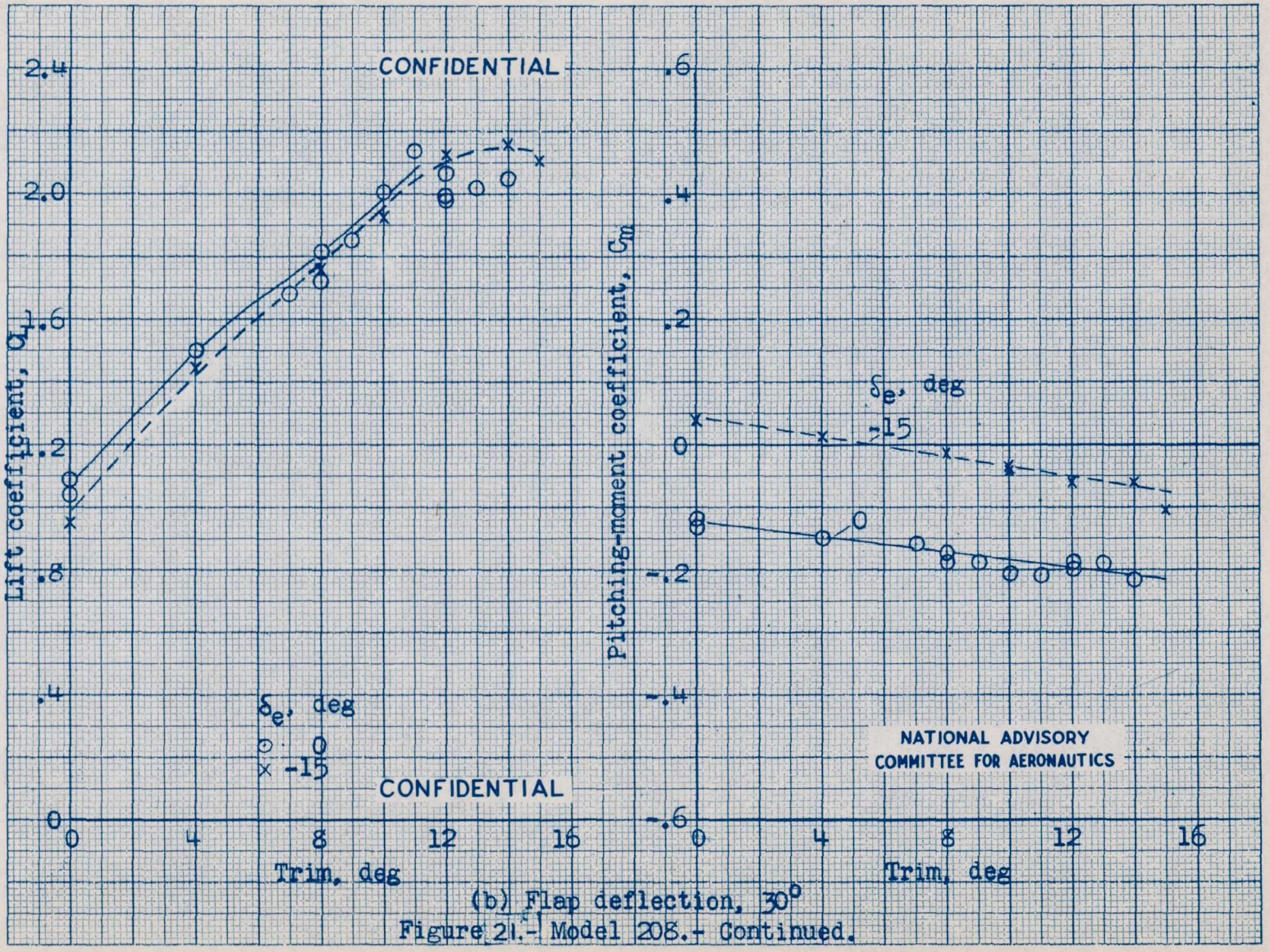

(b) Flap deflection, 30°

Figure 21.- Model 208.- Continued.

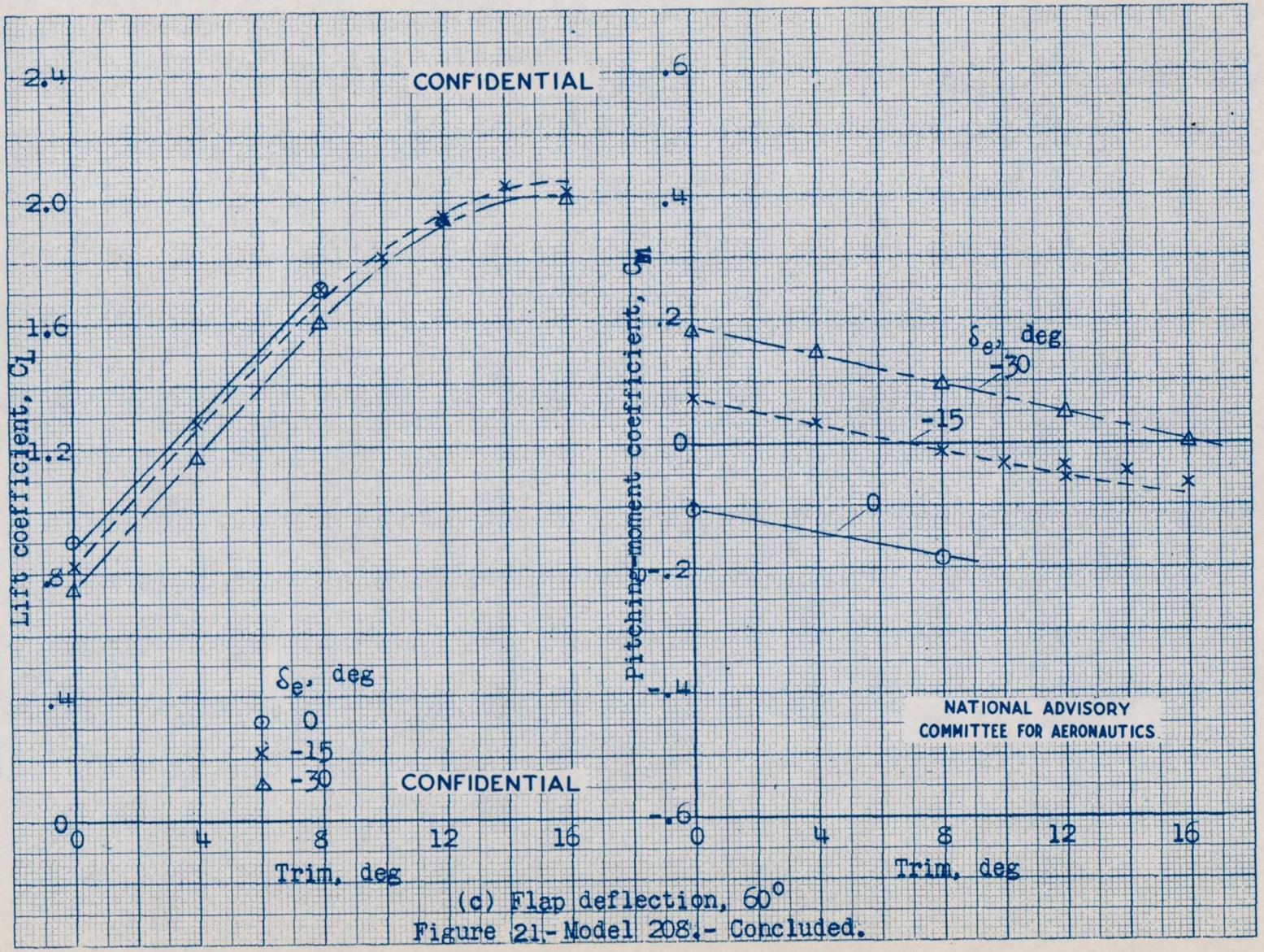

(c) Flap deflection, 60°

Figure 21.- Model 208.- Concluded.

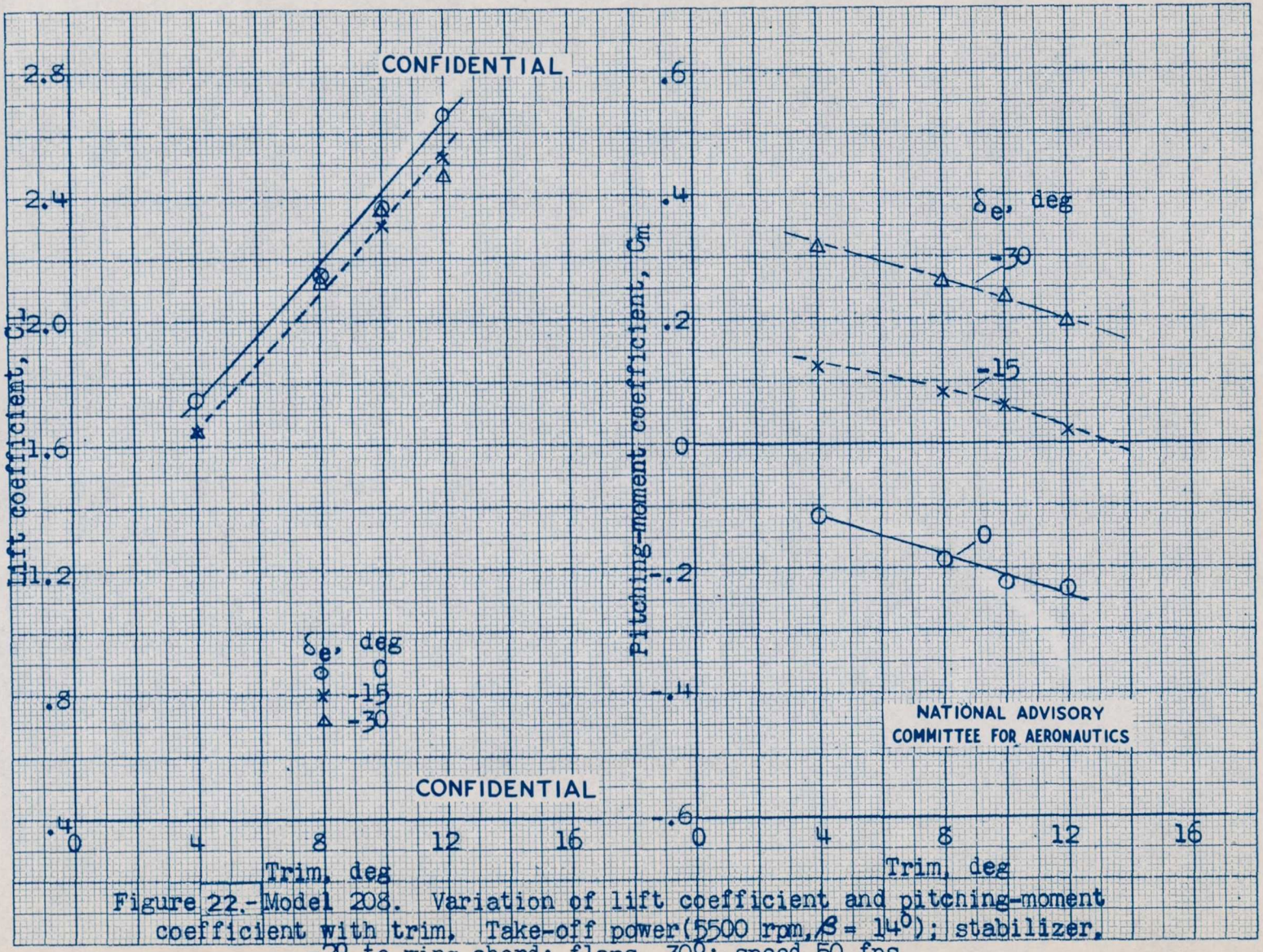

Figure 22.- Model 208. Variation of lift coefficient and pitching-moment coefficient with trim. Take-off power (5500 rpm, $\beta = 14^\circ$); stabilizer, -2° to wing chord; flaps, 30°; speed, 50 fps. Center of moments, 24 percent M. A. C.

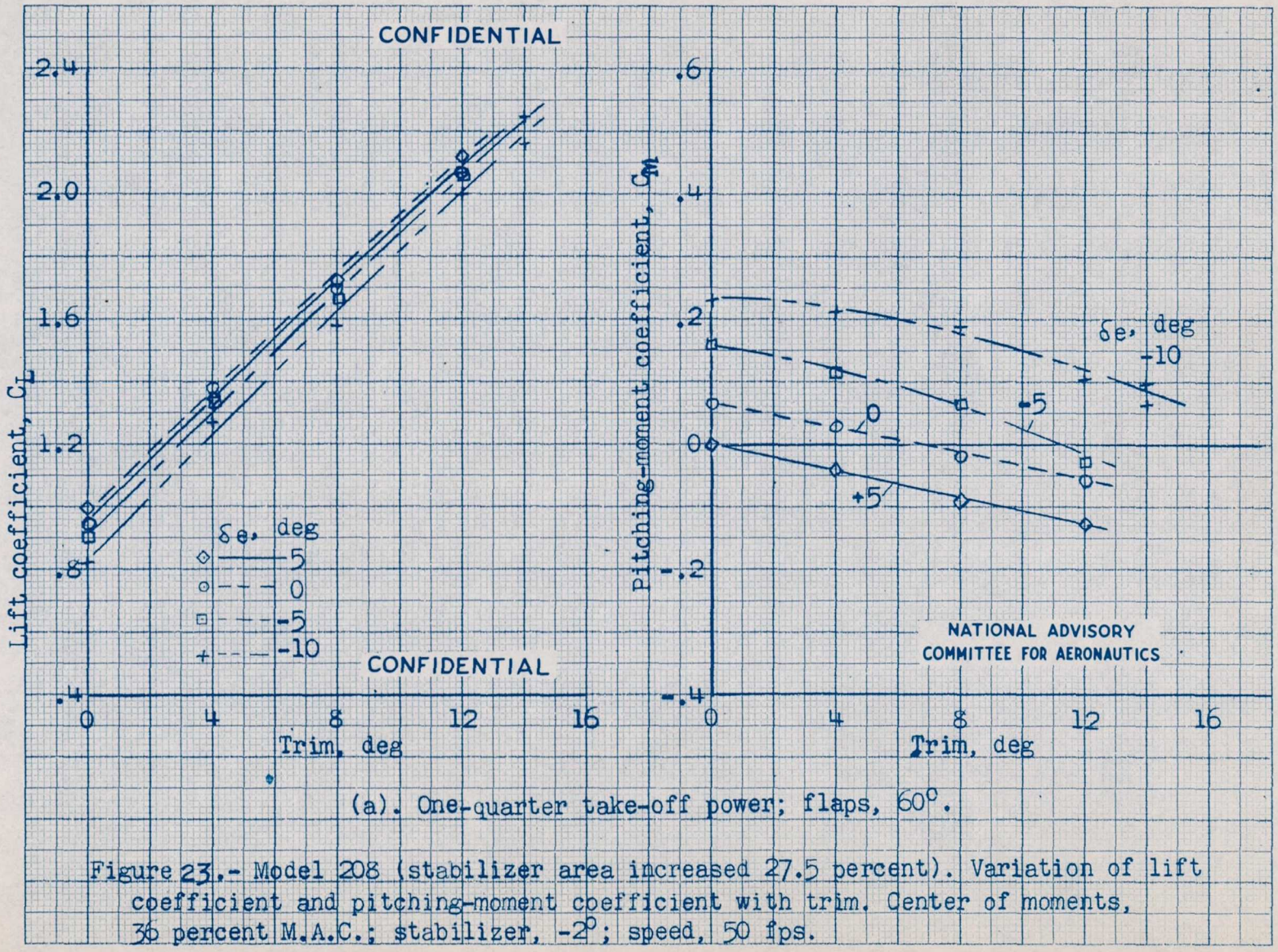

(a). One-quarter take-off power; flaps, 60°.

Figure 23.- Model 208 (stabilizer area increased 27.5 percent). Variation of lift coefficient and pitching-moment coefficient with trim. Center of moments, 36 percent M.A.C.; stabilizer, -2°; speed, 50 fps.

NACA RM No. L6I20

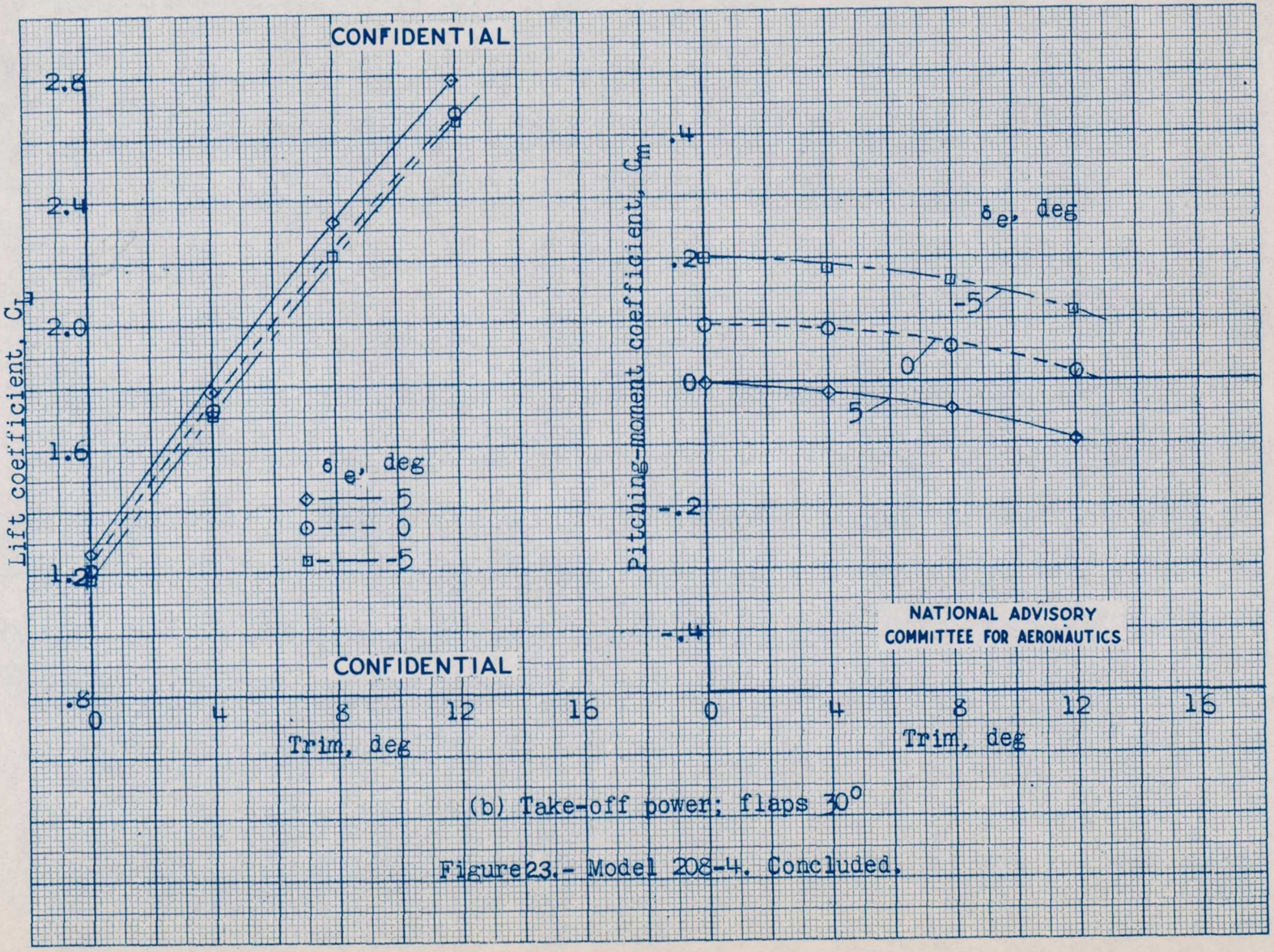

(b) Take-off power; flaps 30°

Figure 23.- Model 208-4. Concluded.

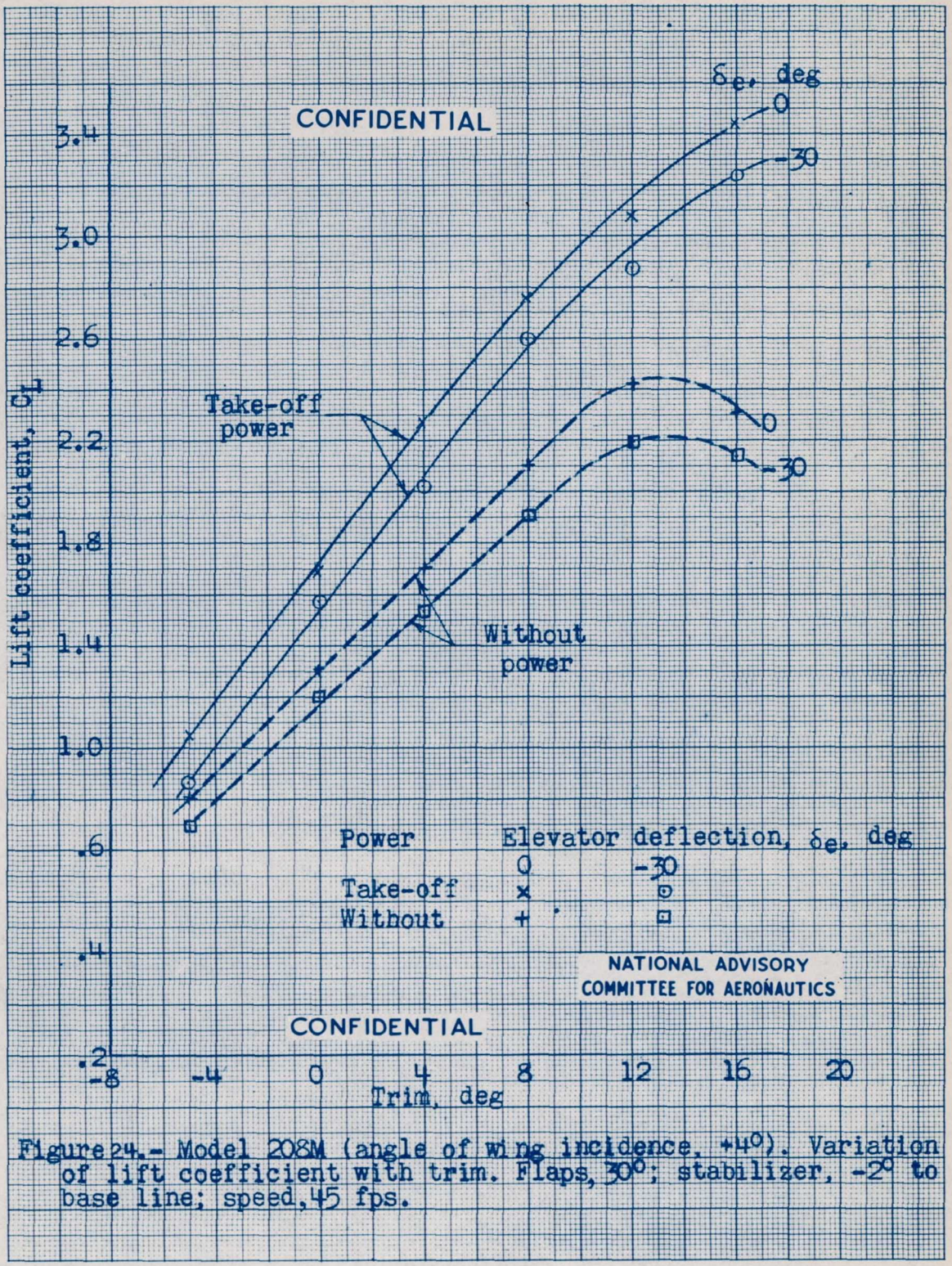

Figure 24.- Model 208M (angle of wing incidence, +4°). Variation of lift coefficient with trim. Flaps, 30°; stabilizer, -2° to base line; speed, 45 fps.

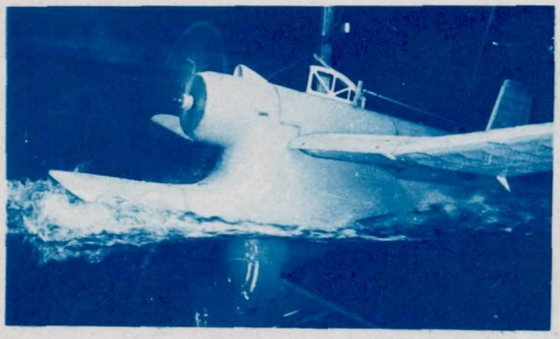

τ, 1.8 V, 5.9

τ, 4.1 V, 7.2

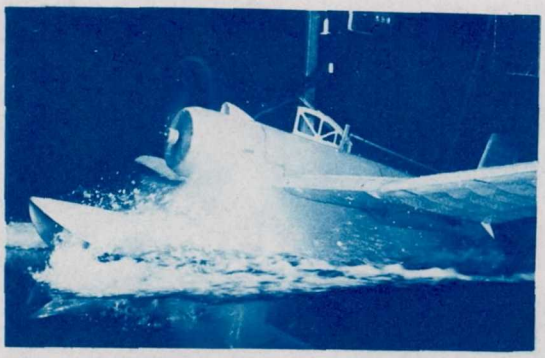

τ, 5.1 V, 8.1

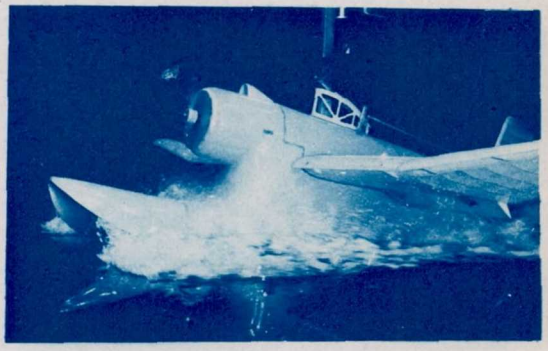

τ, 5.9 V, 9.1

Figure 25.- Model 208. Spray characteristics in speed range where spray wets propeller. Take-off power; flaps, 30°; gross load, 77.4 lb. (13,000 lb. full-size); elevator, 0°. τ, trim, deg; V, speed, fps.

NATIONAL ADVISORY COMMITTEE FOR AERONAUTICS
LANGLEY MEMORIAL AERONAUTICAL LABORATORY - LANGLEY FIELD, VA.

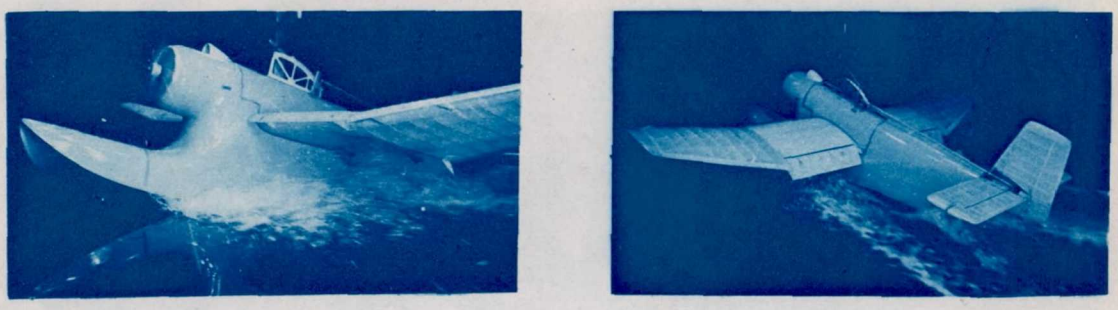

τ,8.0 V,13.0 δ_e,0

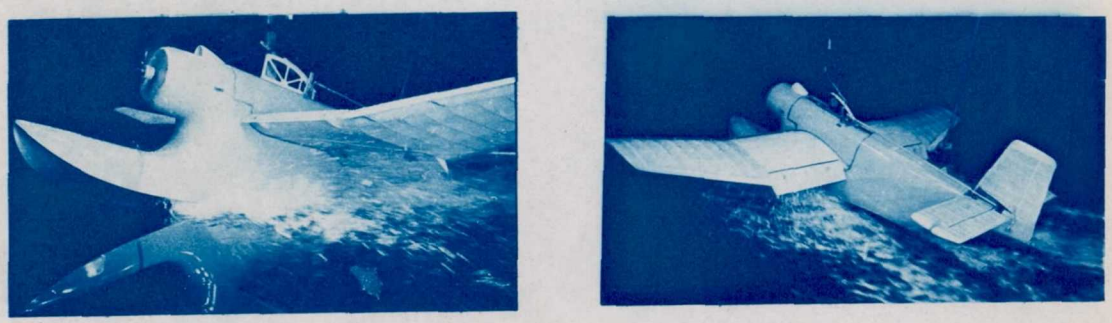

τ,9.2 V,14.1 δ_e,0

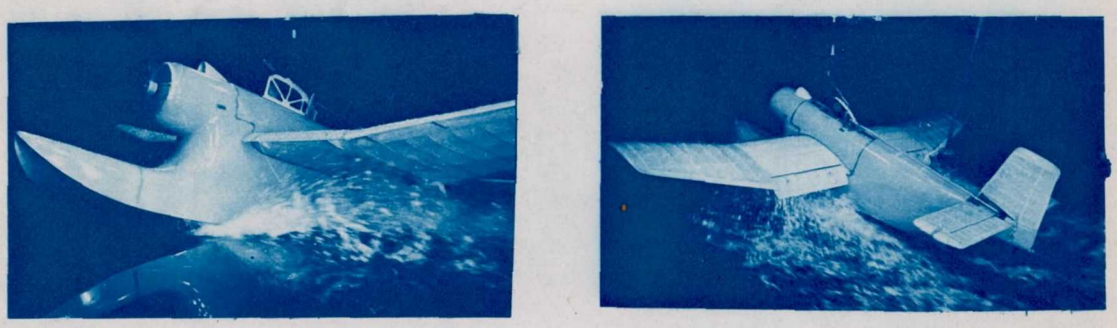

τ,10.0 V,15.9 δ_e,0

Figure 26.- Model 208. Spray characteristics in speed range where spray wets flaps. Take-off power; flaps, 30°; gross load, 77.4 lb. (13,000 lb. full-size). τ, trim, deg; V, speed, fps; δ_e, elevator deflection, deg.

NATIONAL ADVISORY COMMITTEE FOR AERONAUTICS
LANGLEY MEMORIAL AERONAUTICAL LABORATORY - LANGLEY FIELD, VA.

τ, 10.5 V, 18.1 δ_e, 20

τ, 9.8 V, 19.1 δ_e, 20

τ, 9.1 V, 20.1 δ_e, 20

τ, 8.5 V, 21.2 δ_e, 20

Figure 26.- Model 208. Concluded.

NATIONAL ADVISORY COMMITTEE FOR AERONAUTICS
LANGLEY MEMORIAL AERONAUTICAL LABORATORY - LANGLEY FIELD, VA.

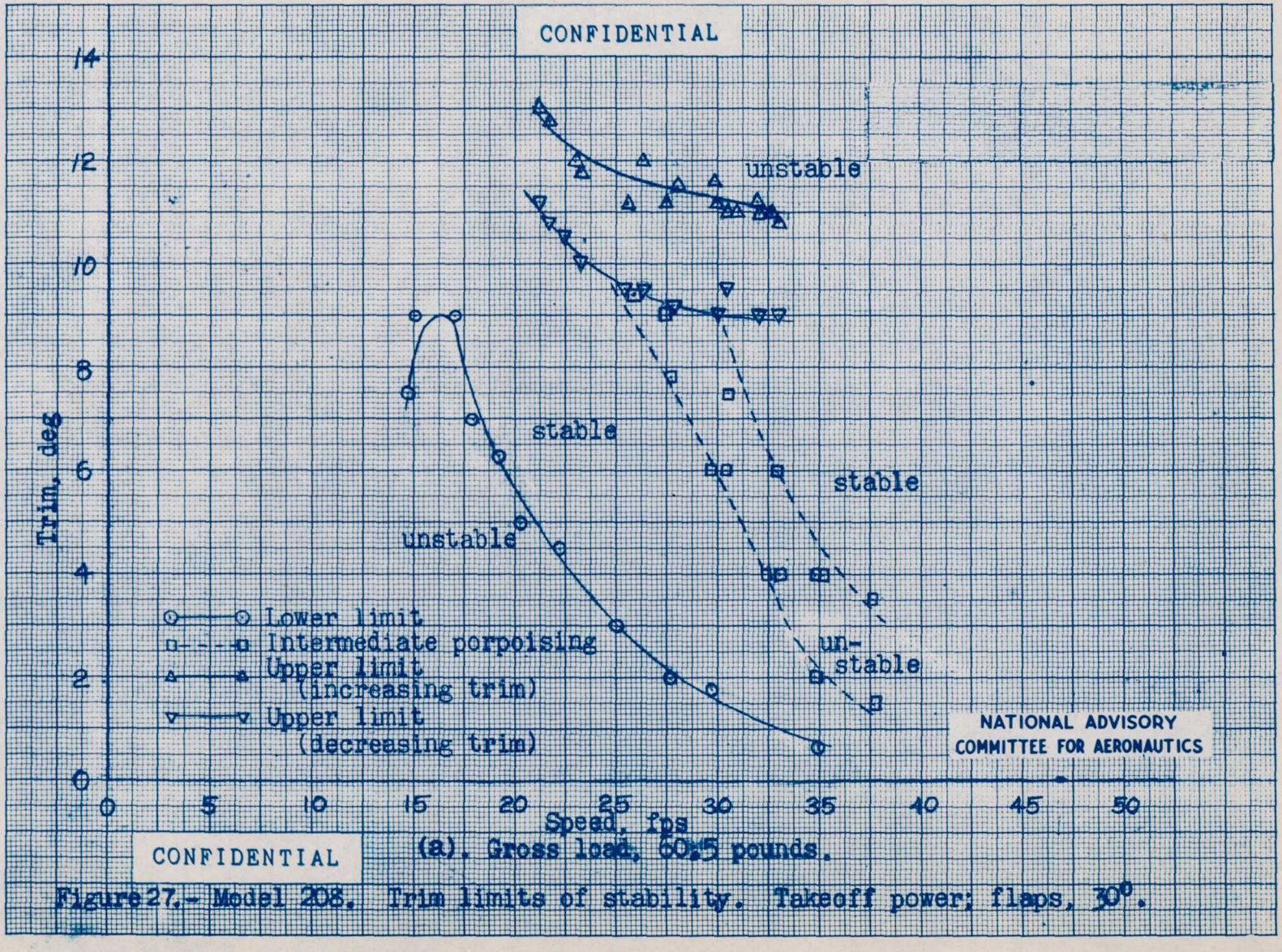

(a). Gross load, 60.5 pounds.

Figure 27.- Model 208. Trim limits of stability. Takeoff power; flaps, 30°.

NACA RM No. L6I20

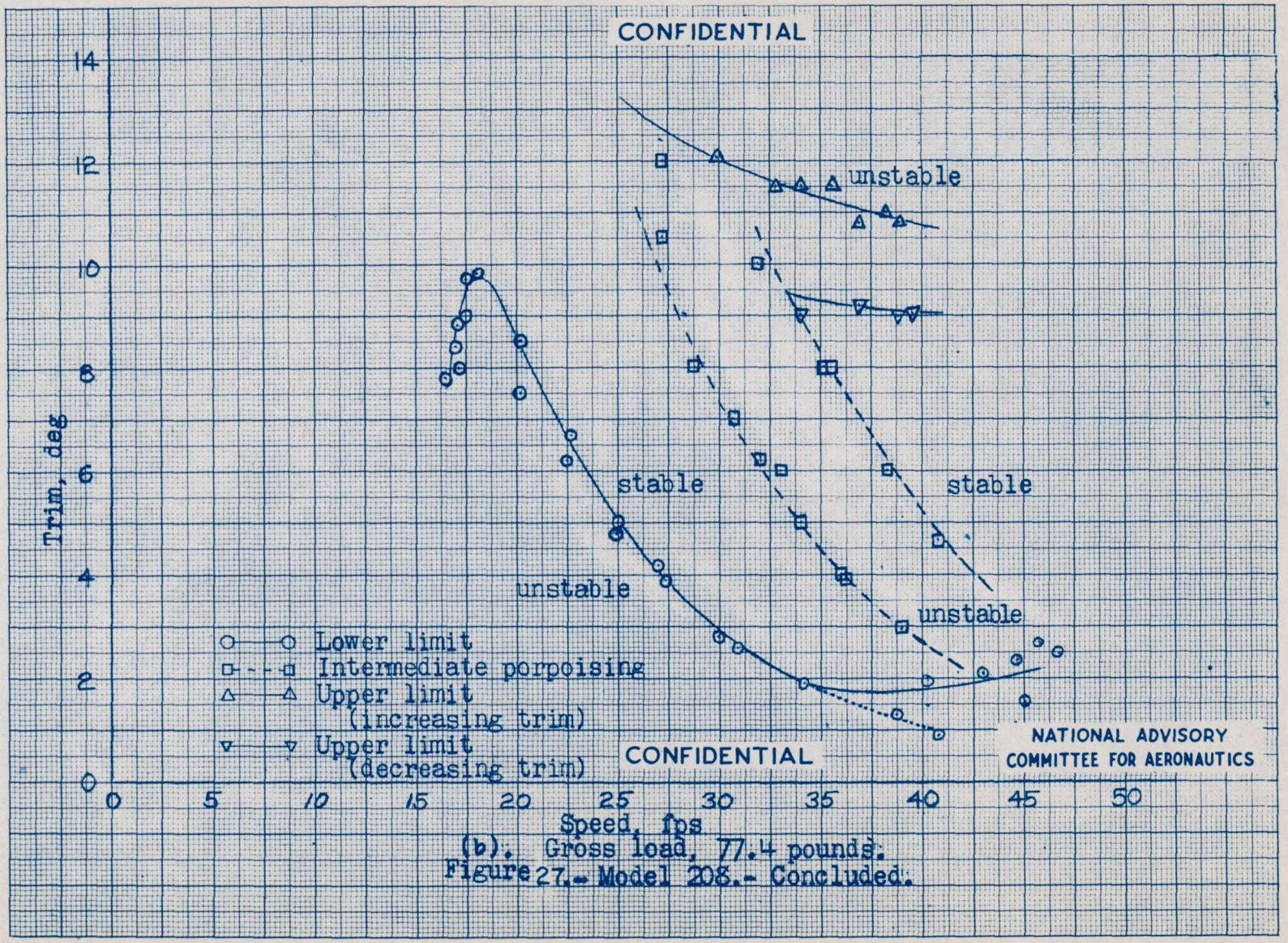

(b). Gross load, 77.4 pounds.

Figure 27.- Model 208.- Concluded.

NACA RM No. L6I20

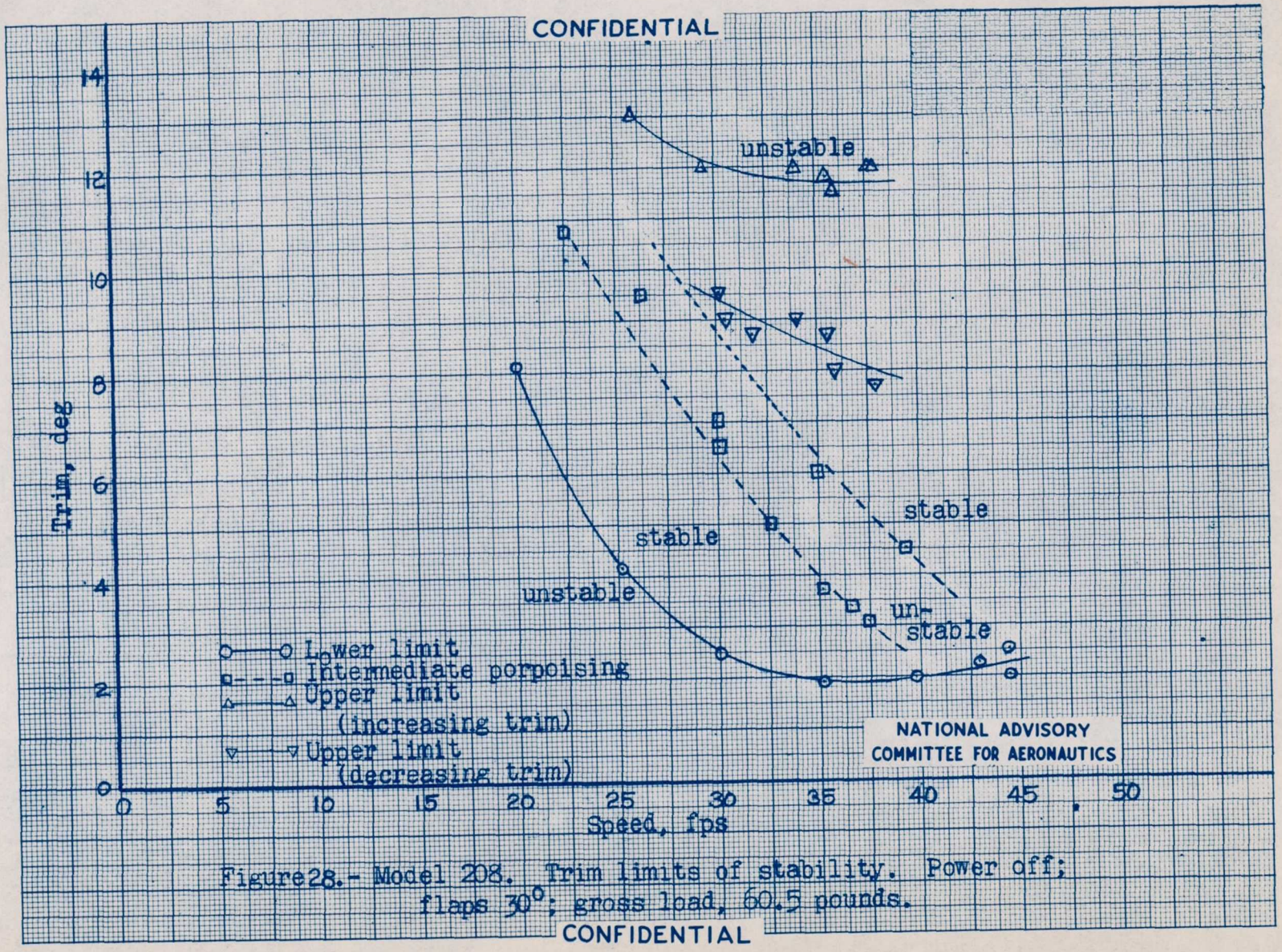

Figure 28.- Model 208. Trim limits of stability. Power off; flaps 30°; gross load, 60.5 pounds.

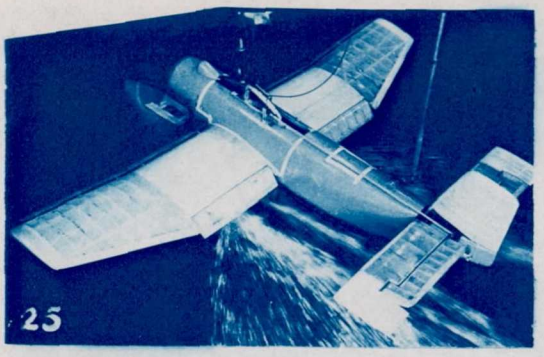

T, 8.0 V, 25.0

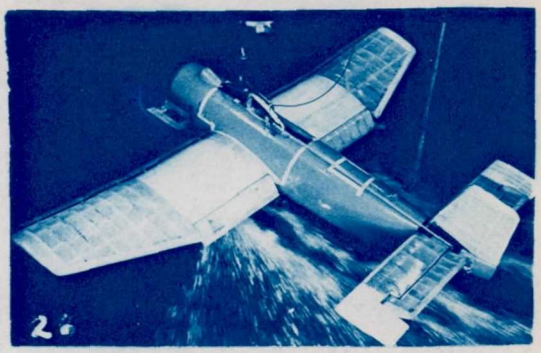

T, 9.0 V, 25.0

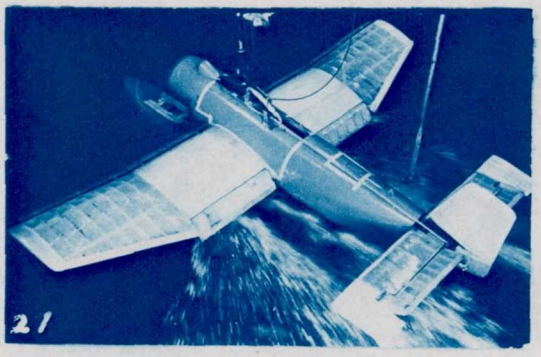

T, 10.0 V, 25.0

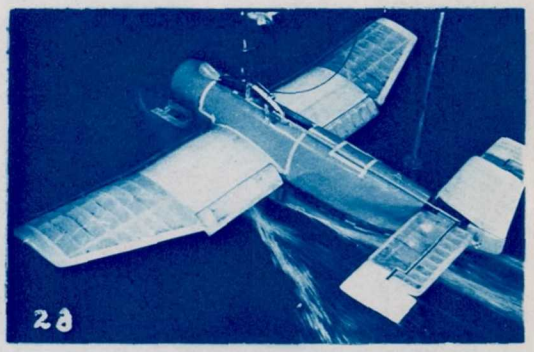

T, 5.0 V, 35.0

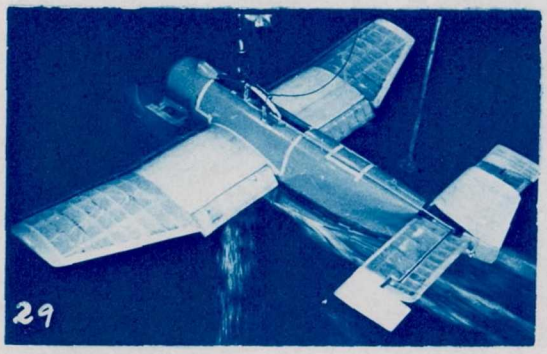

T, 7.0 V, 35.0

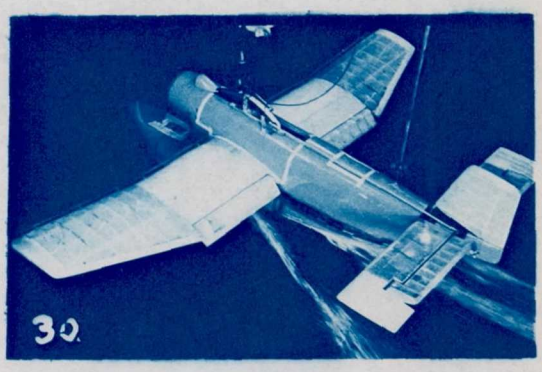

T, 4.0 V, 40.0

Figure 29.- Model 208H-14. Flow around afterbody. Take-off power; gross load, 77.4 lb (13,000 lb, full-size); flaps, 30°; stabilizer, -2°; V, speed, fps; τ, trim, deg.

NATIONAL ADVISORY COMMITTEE FOR AERONAUTICS
LANGLEY MEMORIAL AERONAUTICAL LABORATORY - LANGLEY FIELD, VA.

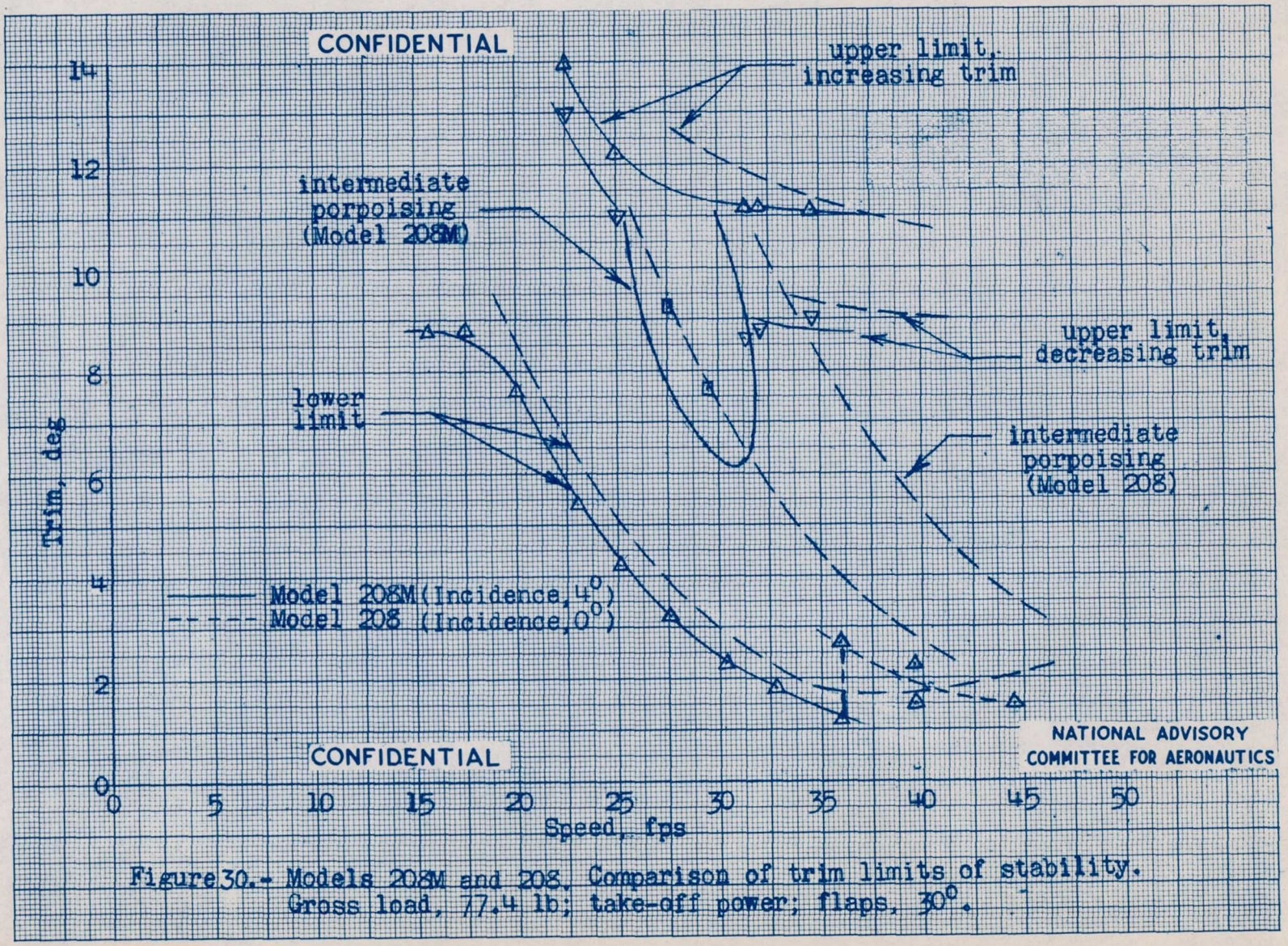

Figure 30.- Models 208M and 208. Comparison of trim limits of stability. Gross load, 77.4 lb; take-off power; flaps, 30°.

NACA RM No. L6I20

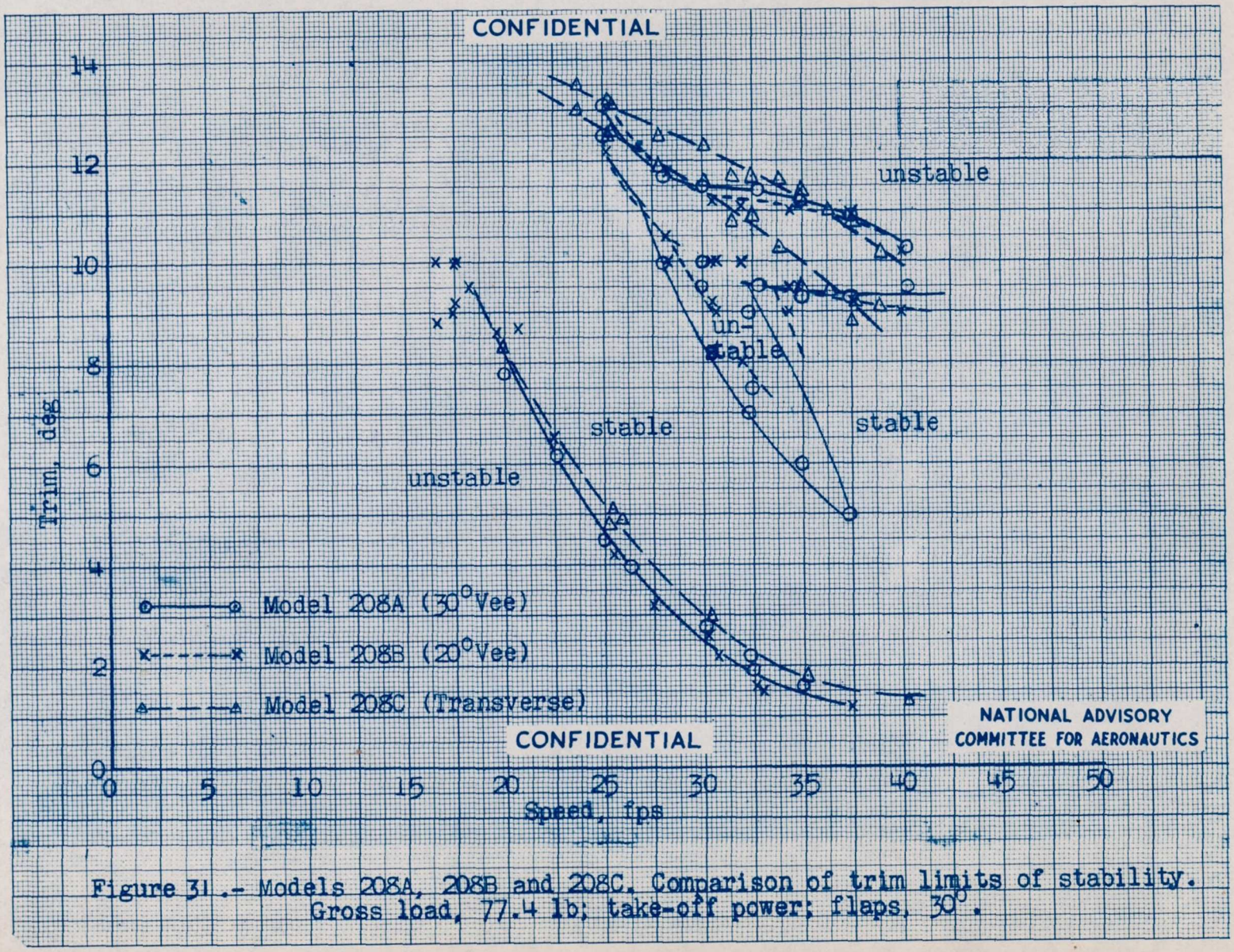

Figure 31.- Models 208A, 208B and 208C. Comparison of trim limits of stability. Gross load, 77.4 lb; take-off power; flaps, 30°.

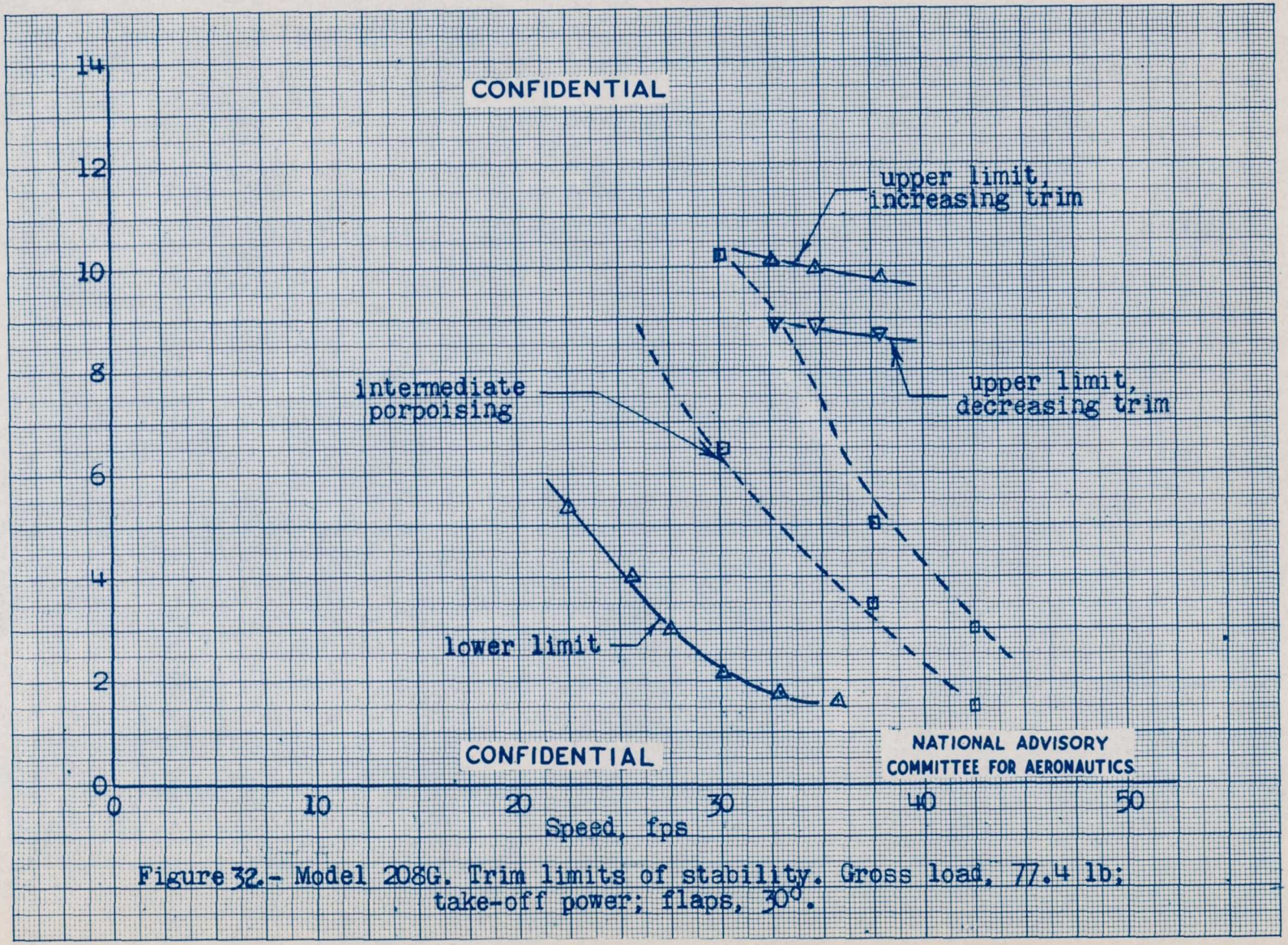

Figure 32.- Model 208G. Trim limits of stability. Gross load, 77.4 lb; take-off power; flaps, 30°.

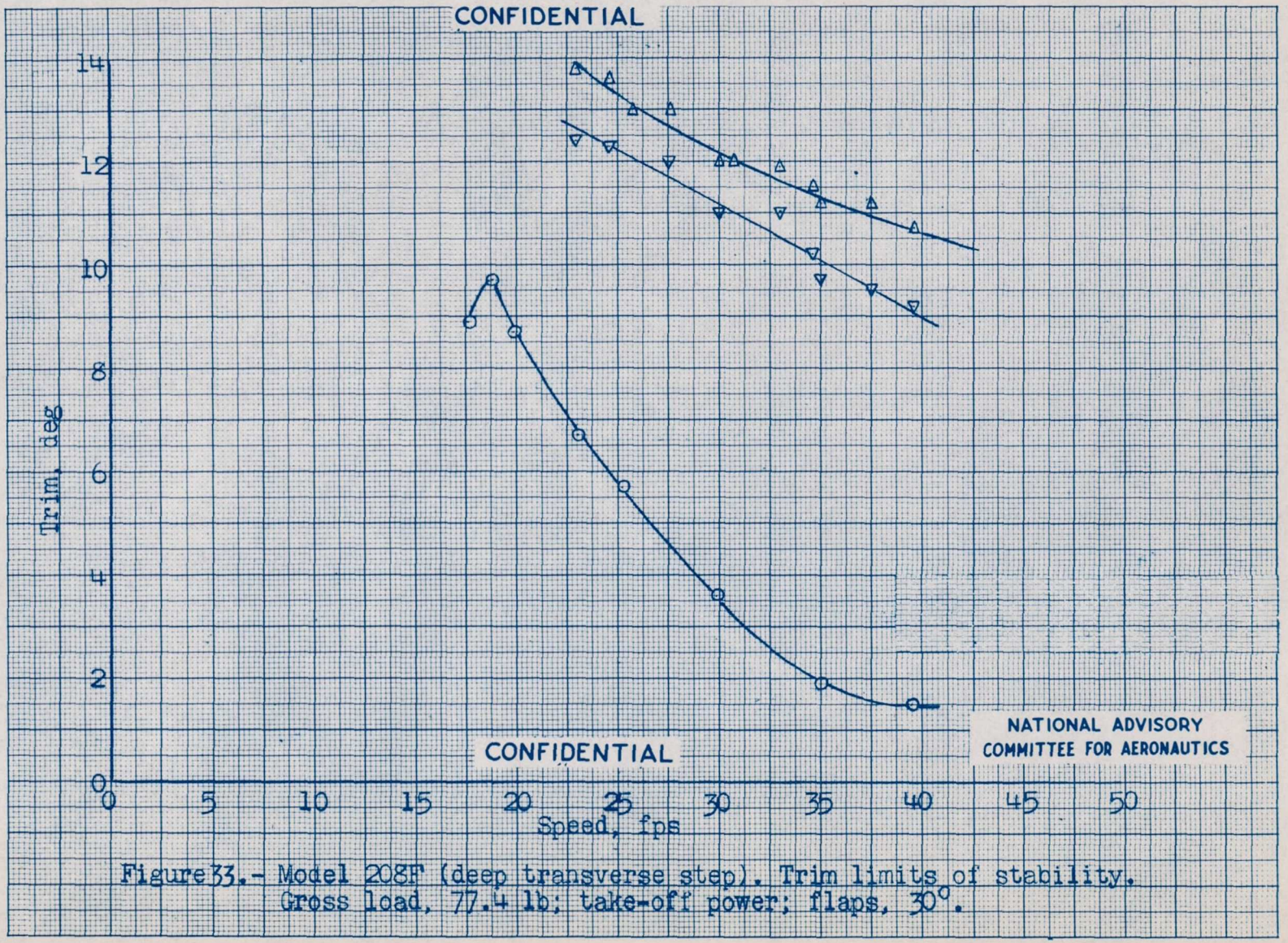

Figure 33.- Model 208F (deep transverse step). Trim limits of stability. Gross load, 77.4 lb; take-off power; flaps, 30°.

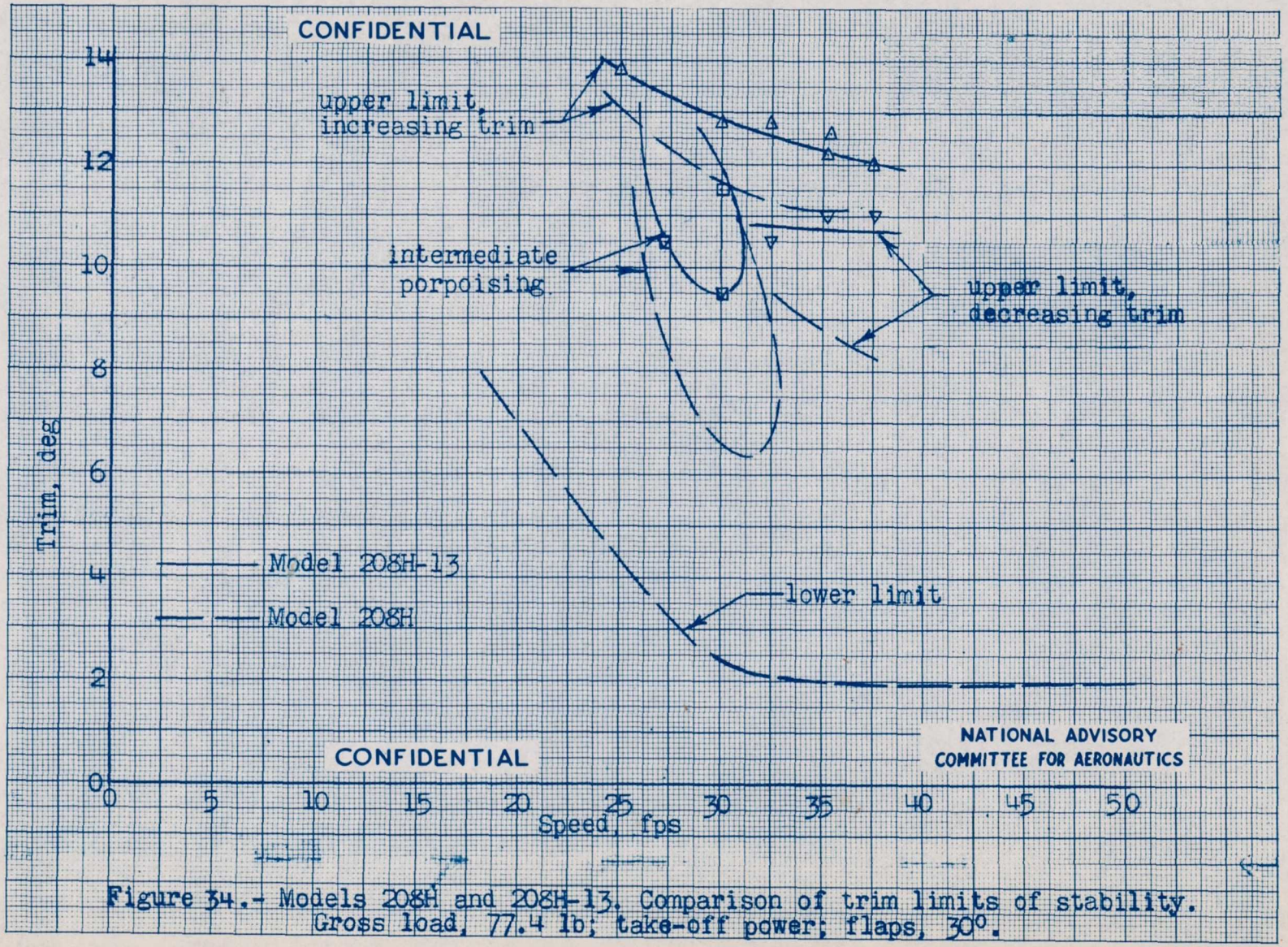

Figure 34.- Models 208H and 208H-13. Comparison of trim limits of stability. Gross load, 77.4 lb; take-off power; flaps, 30°.

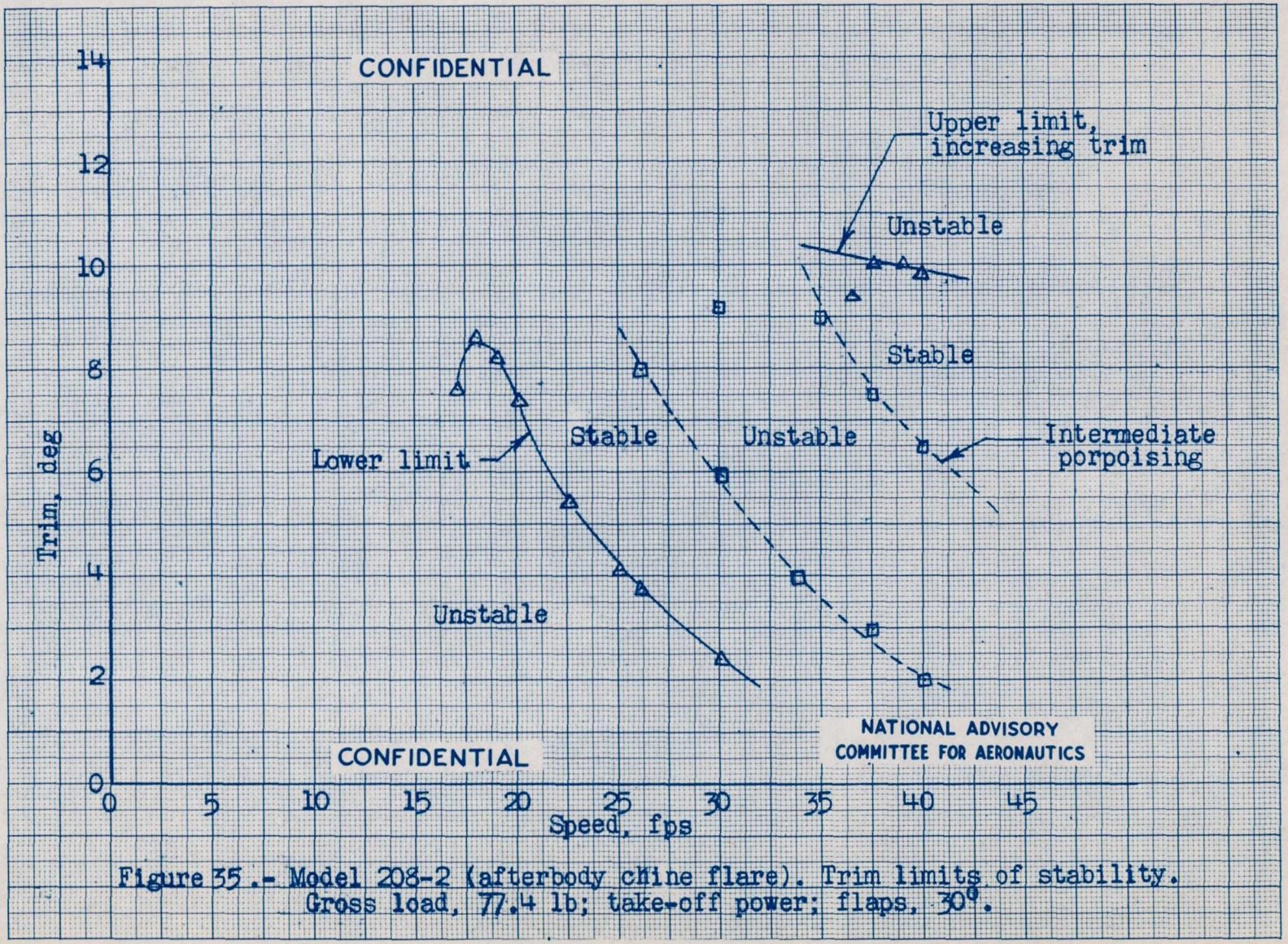

Figure 35.- Model 208-2 (afterbody chine flare). Trim limits of stability. Gross load, 77.4 lb; take-off power; flaps, 30°.

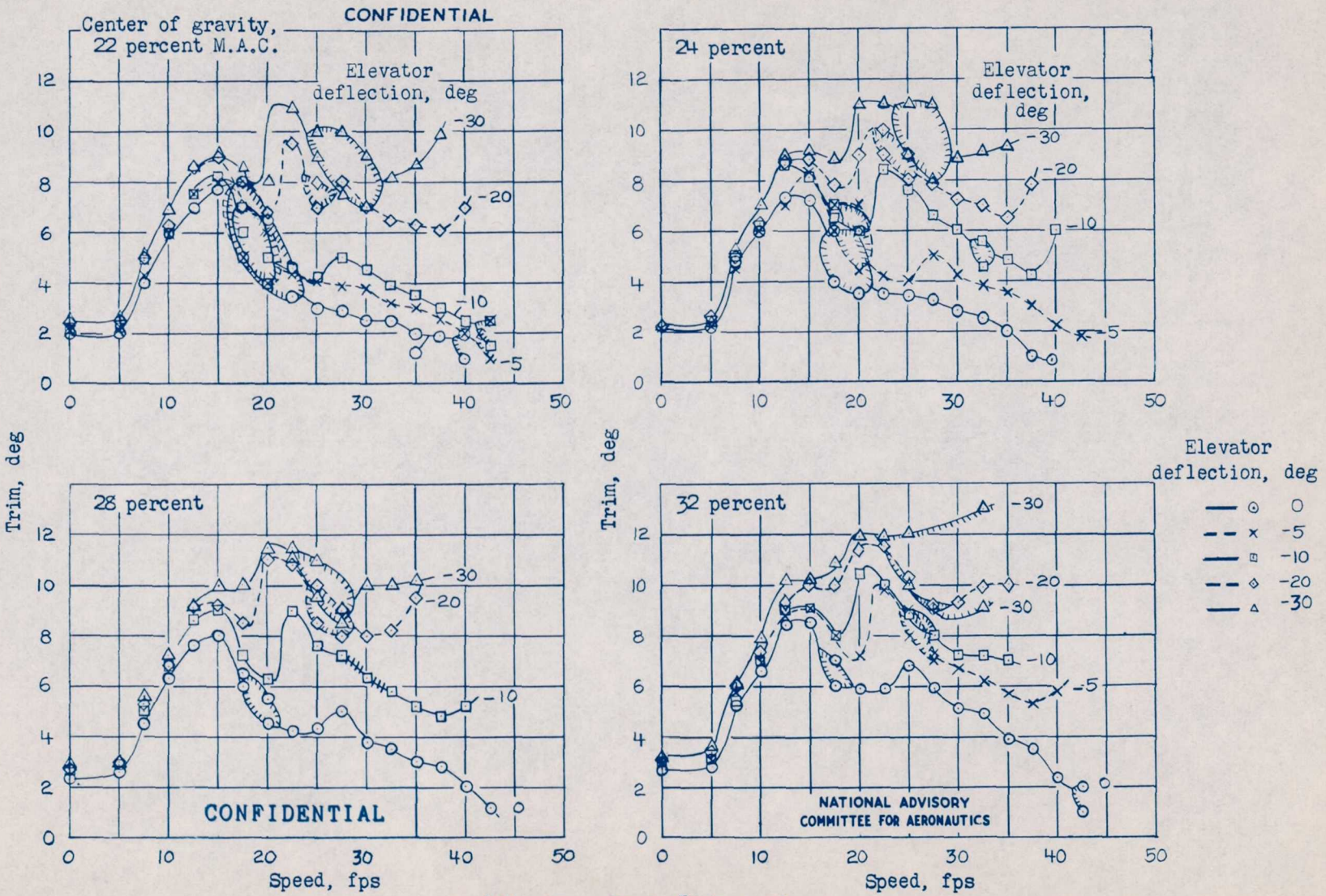

(a) Gross load, 60.5 pounds.

Figure 36.- Model 208. Variation of trim with speed. Takeoff power; flaps, 30°; stabilizer, -2°.

NACA RM No. L6I20

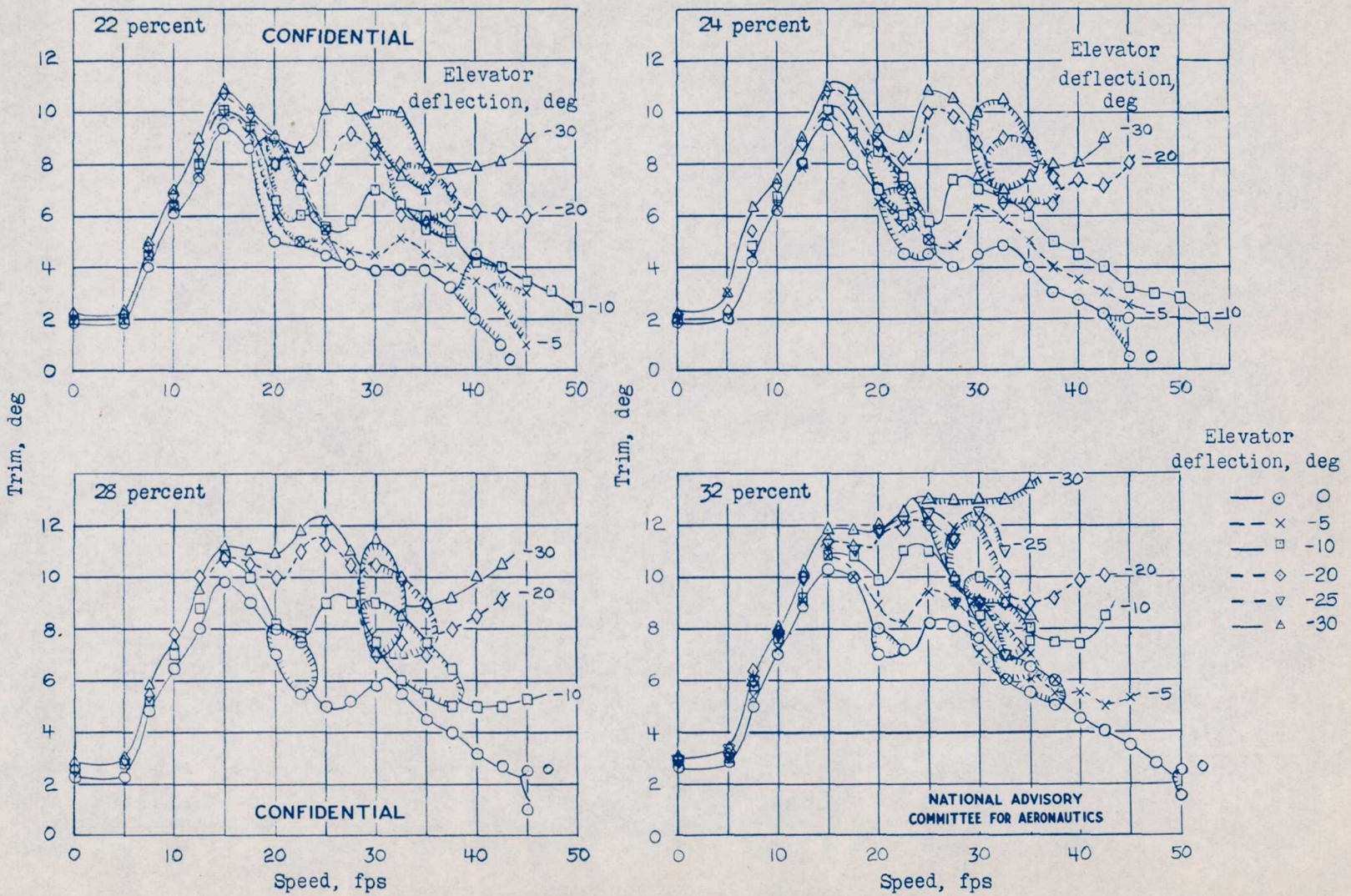

(b). Gross load, 77.4 pounds.

Figure 36.- Model 208.- Concluded.

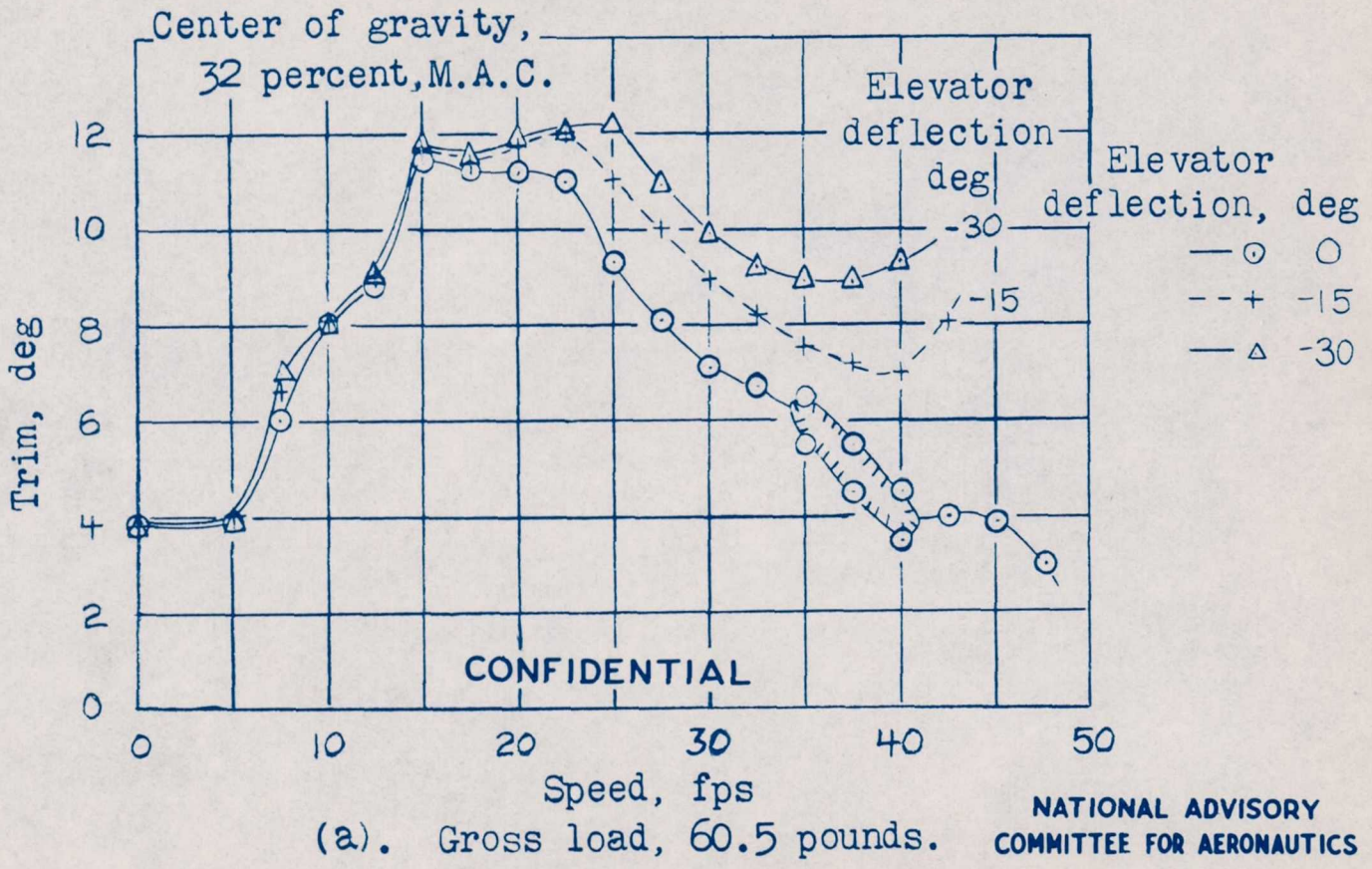

(a). Gross load, 60.5 pounds.

Figure 37.- Model 208. Variation of trim with speed. Without power; flaps, 30°; stabilizer, -2°.

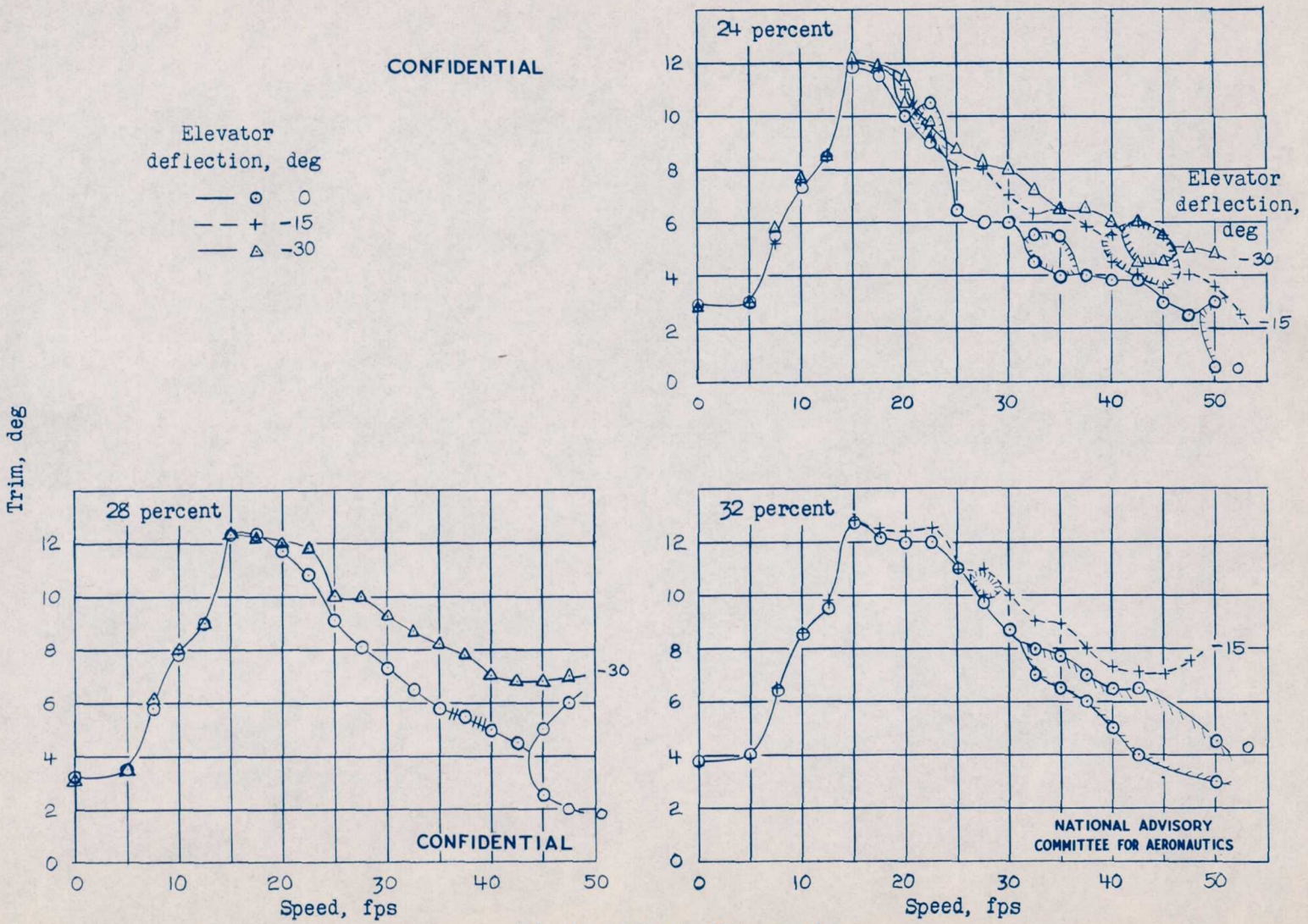

(b). Gross load, 77.4 pounds.

Figure 37.- Model 208.- Concluded.

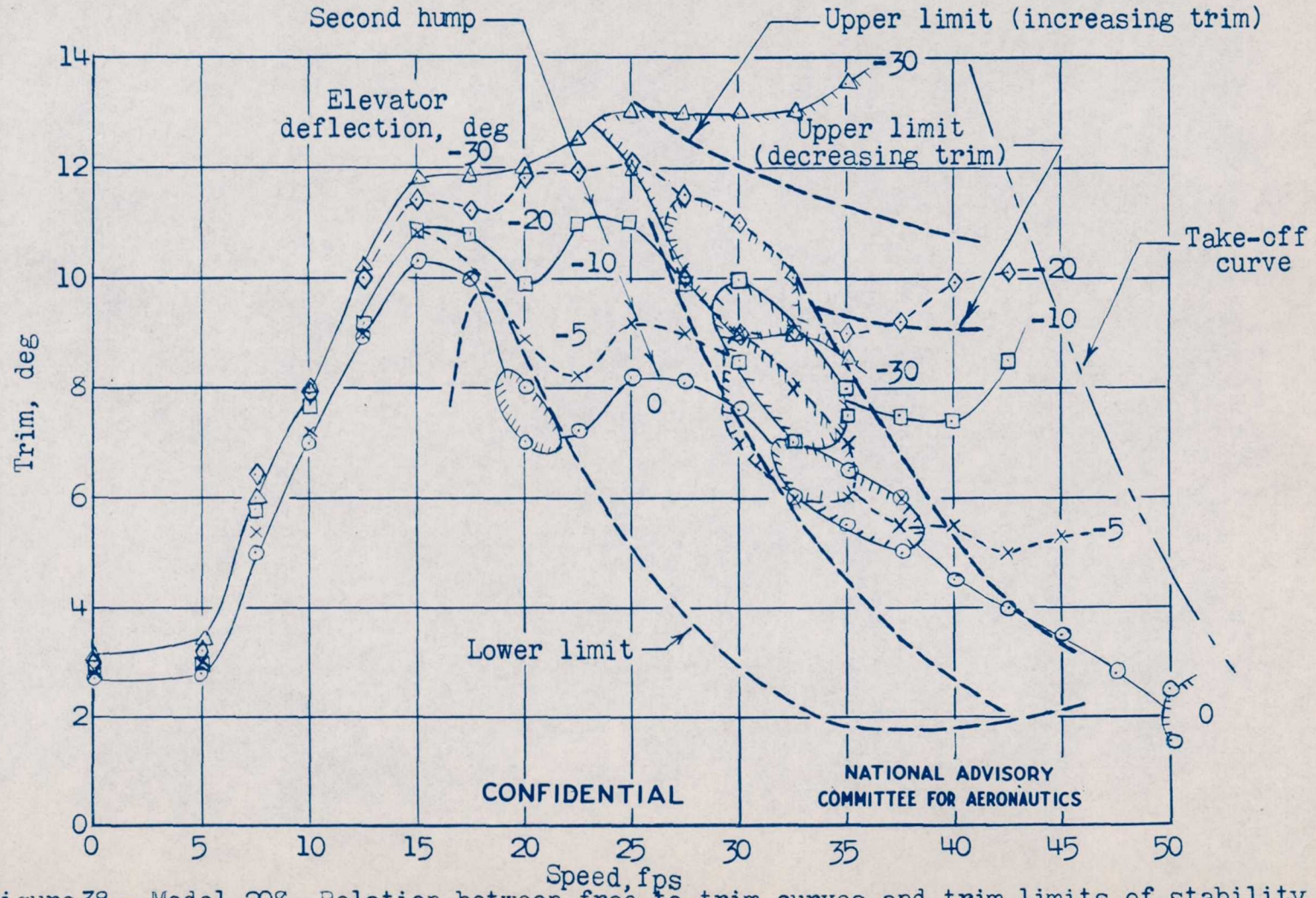

Figure 38.- Model 208. Relation between free-to-trim curves and trim limits of stability. C. G., 32 percent M.A.C.; take-off power; flaps, 30°; gross load, 77.4 pounds.

NACA RM No. L6I20

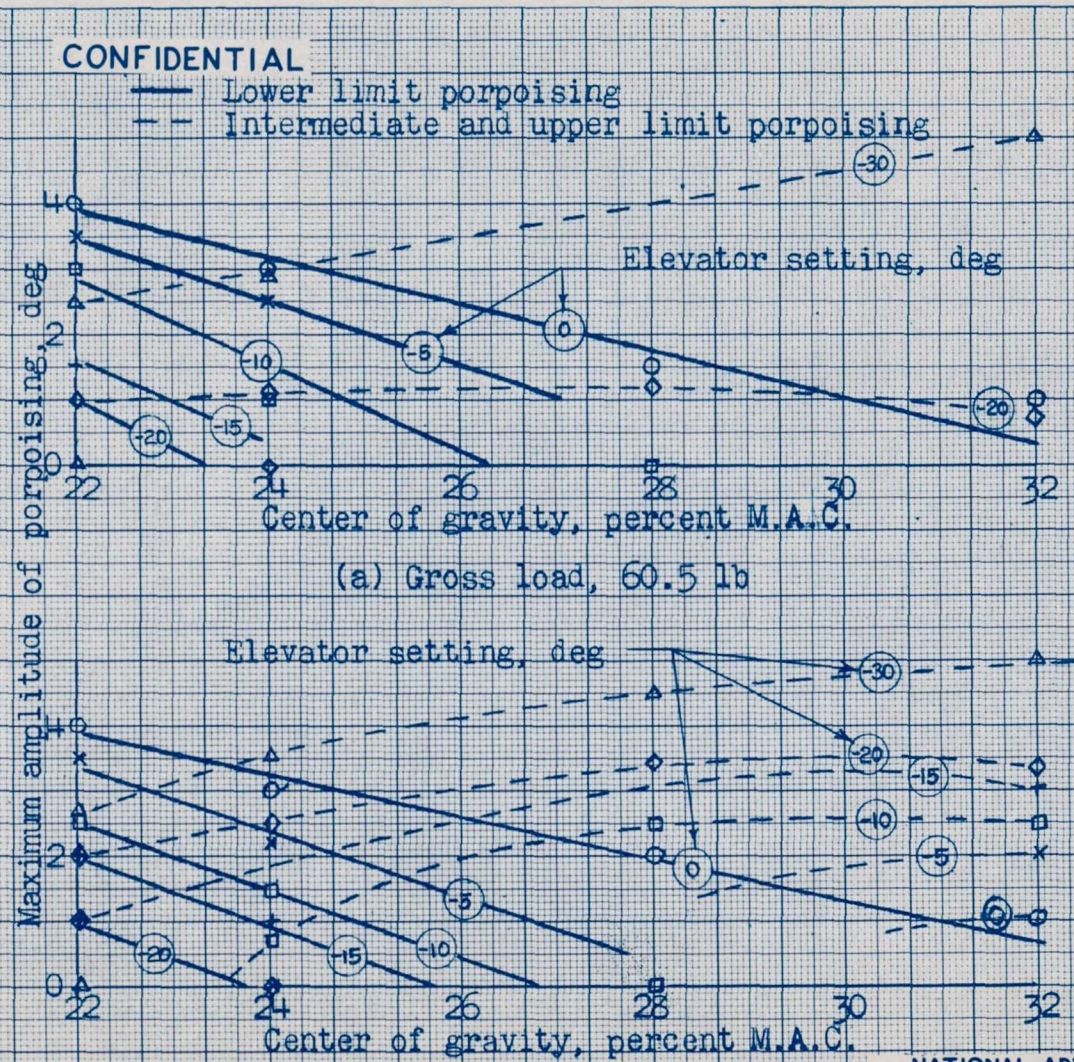

Figure 39.- Model 208. Variation of maximum amplitude of porpoising with position of center of gravity. Take-off power; flaps, 30°; stabilizer, -2°.

NACA RM No. L6I20

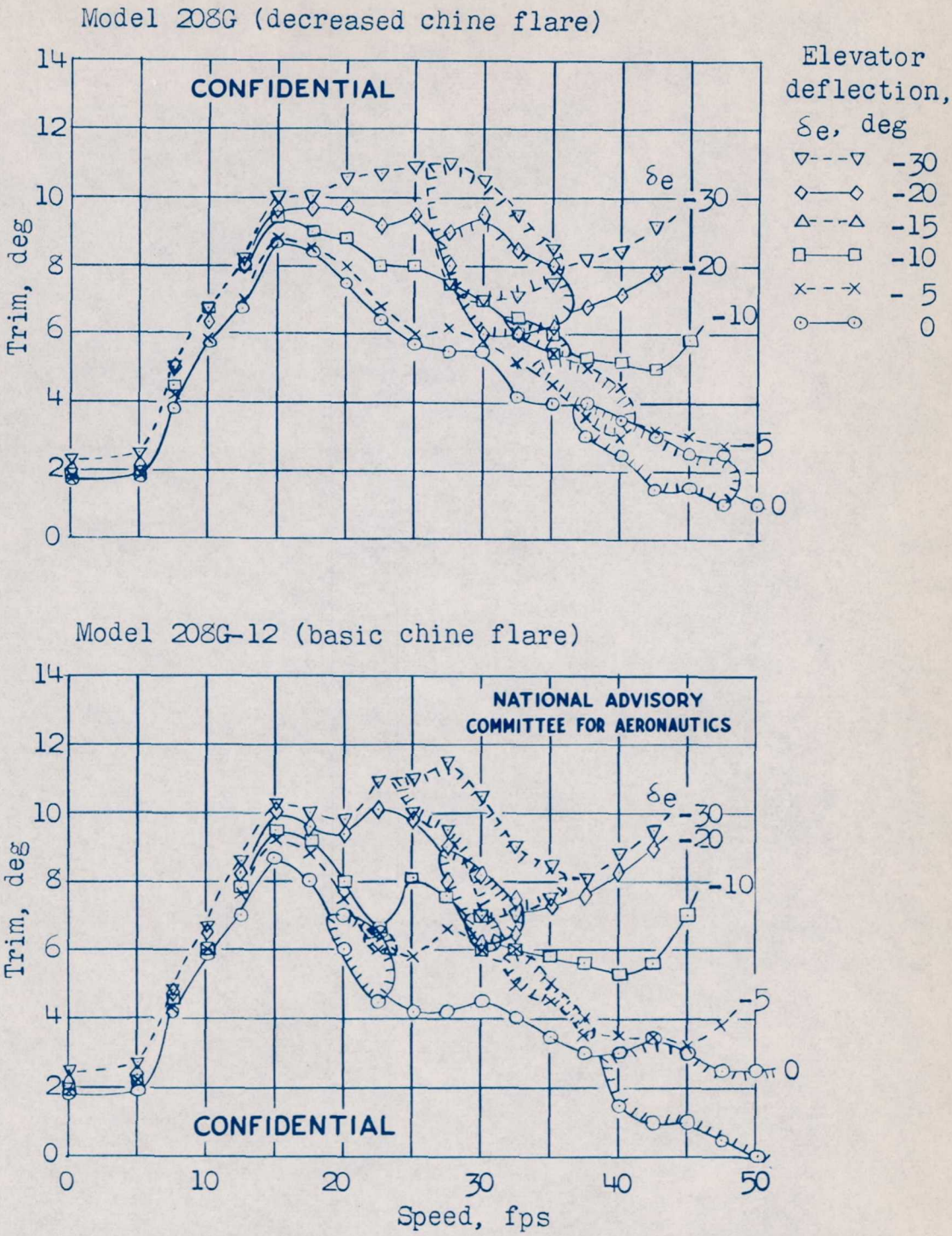

Figure 40.- Models 208G and 208G-12. Variation of trim with speed. Gross load, 77.4 pounds; take-off power; center of gravity, 28-percent mean aerodynamic chord; flaps, 30°; stabilizer, -2°.

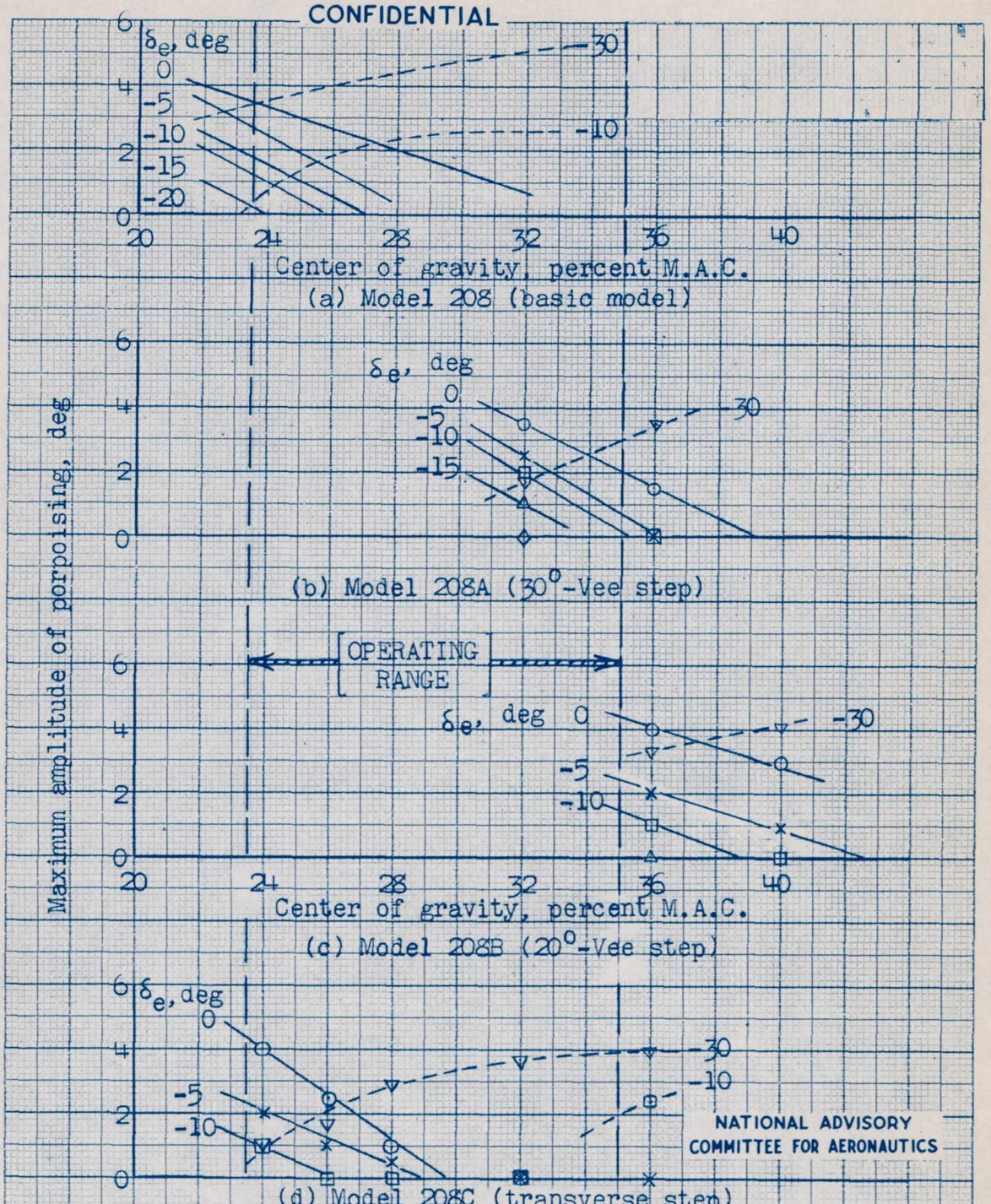

Figure 41.- Model 208. Variation of maximum amplitude of porpoising with position of center of gravity. Gross load, 77.4 lb; take-off power; flaps, 30°, stabilizer -2°.

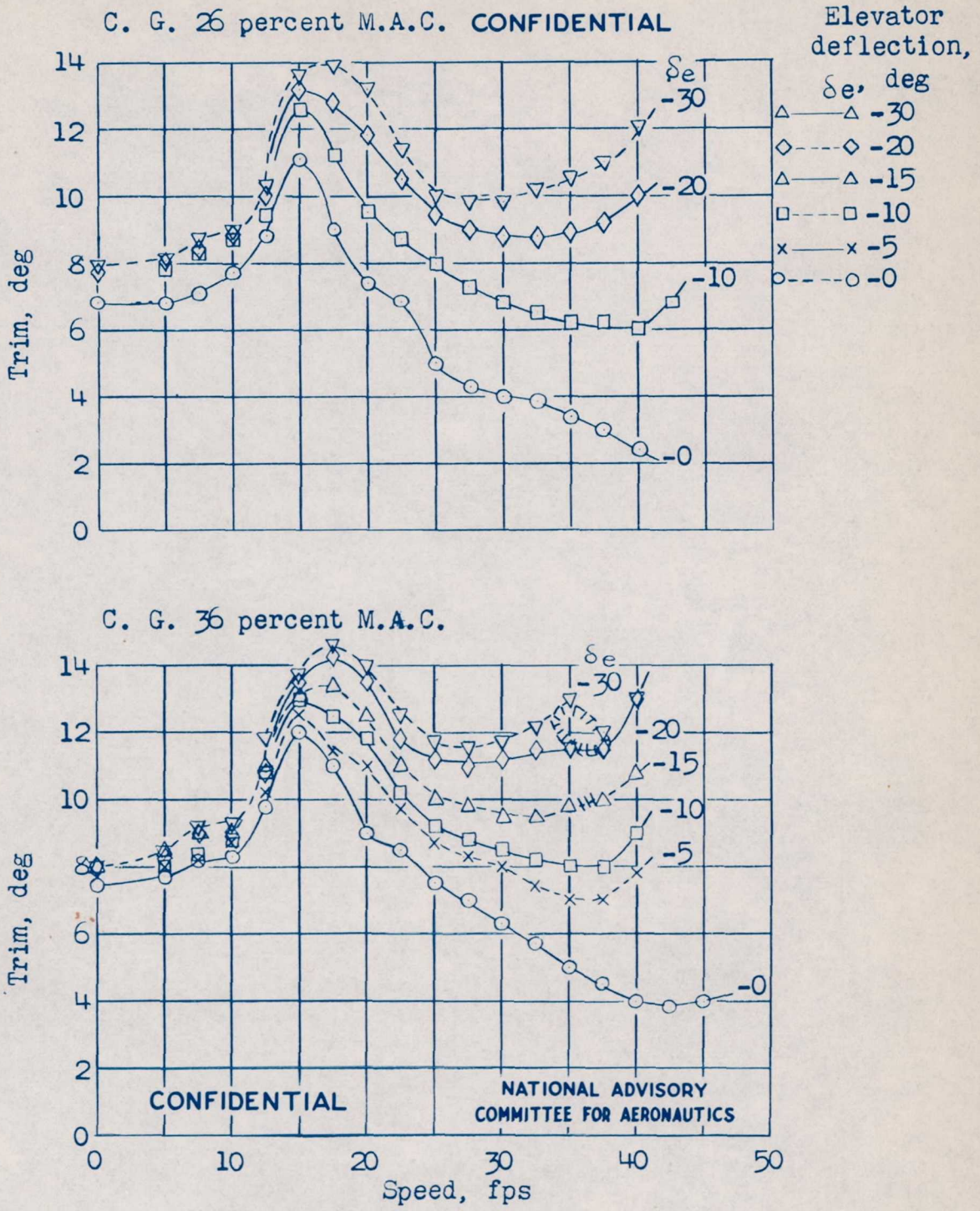

Figure 42.- Model 208D (Afterbody removed). Variation of trim with speed. Gross load, 77.4 lb; take-off power; flaps, 30°; stabilizer, -2°.

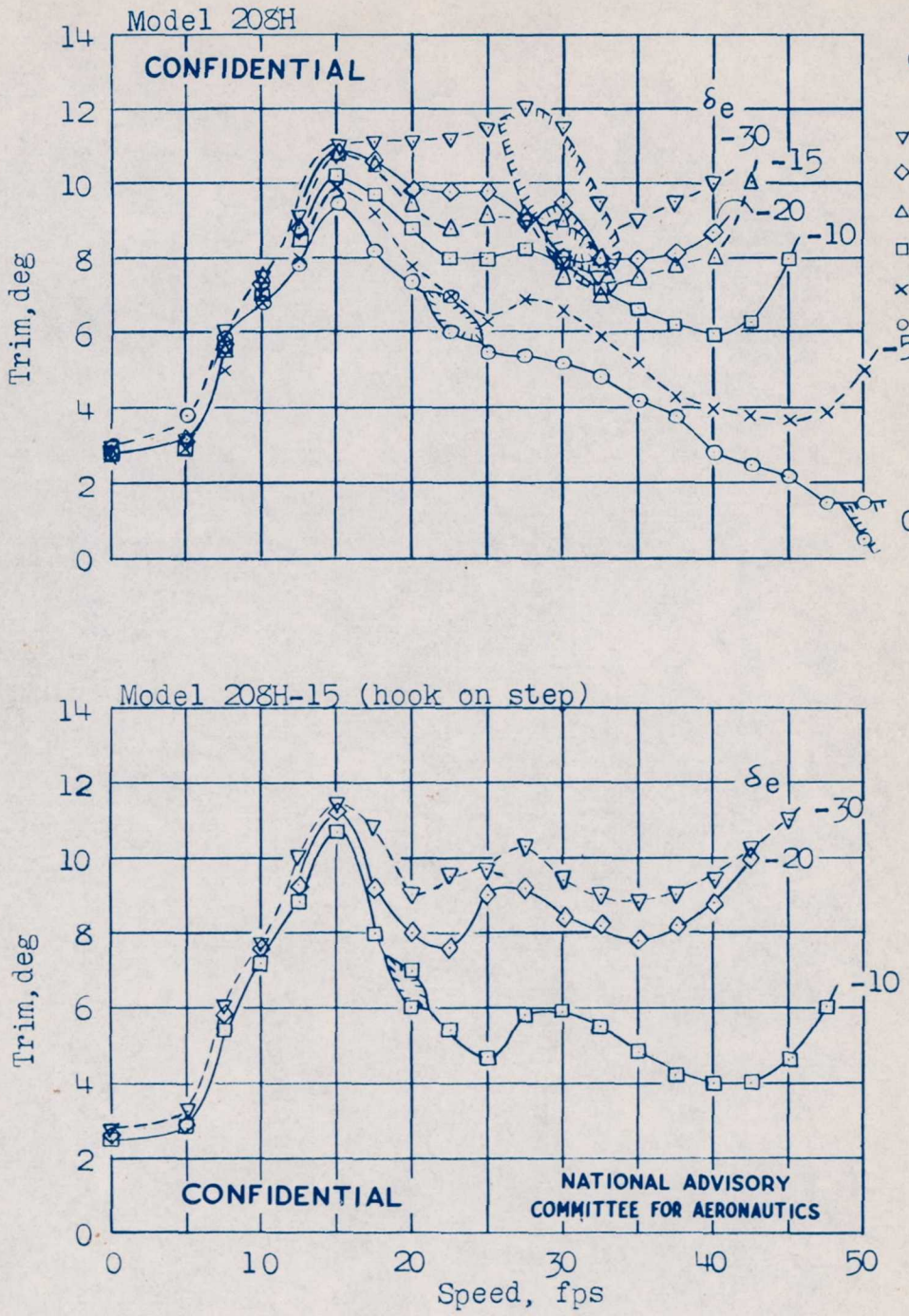

Figure 43.- Models 208H and 208H-15. Variation of trim with speed. Center of gravity, 28 percent M.A.C.; gross load 77.4 lb; take-off power; flaps 30°; stabilizer -2°.

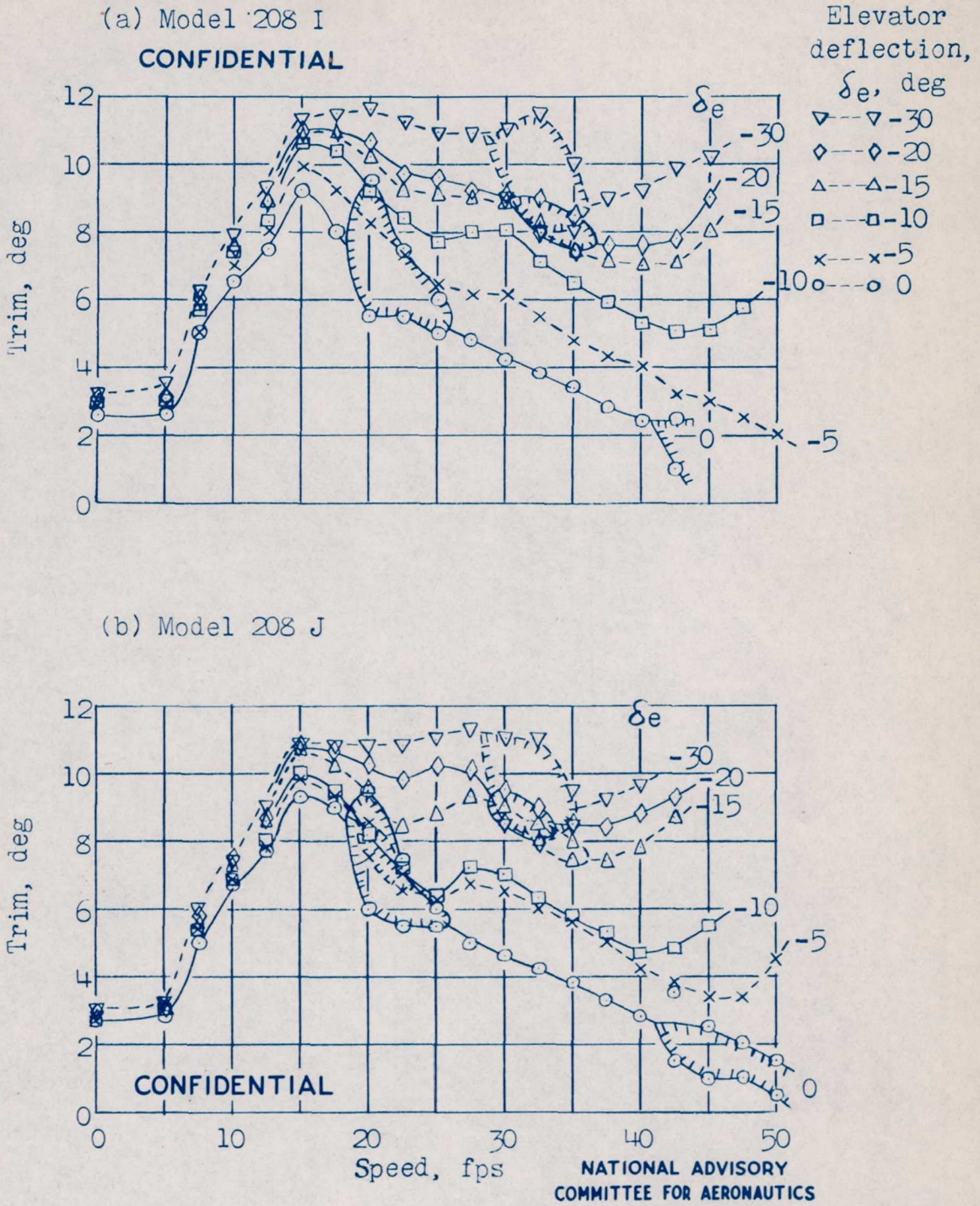

Figure 44.- Models 208 I and 208 J. Variation of trim with speed; Gross load, 77.4 lb; take-off power; center of gravity, 28 percent M.A .C.; flaps, 30°; stabilizer, -2°.

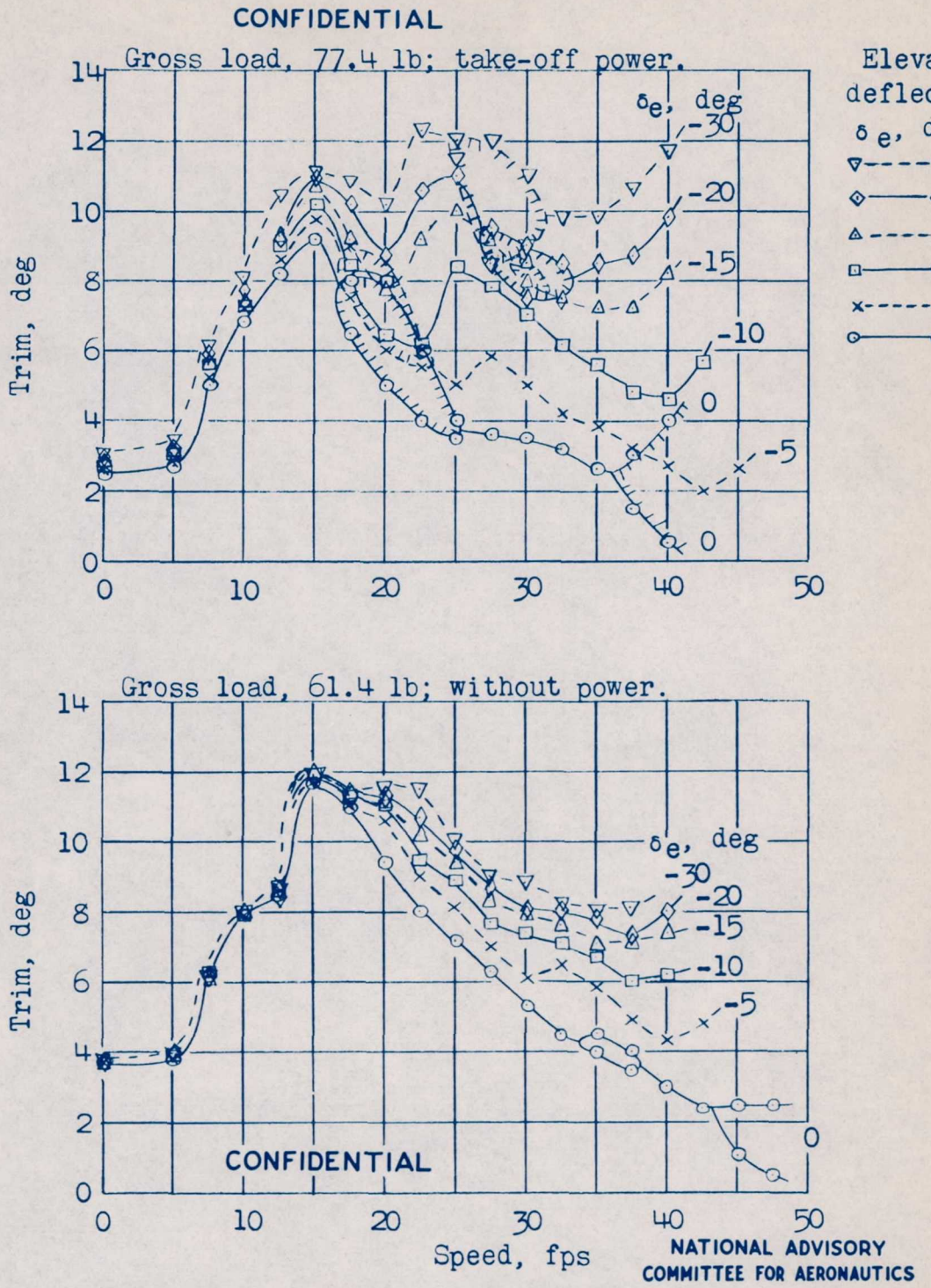

Figure 45.- Model 208M. Variation of trim with speed. Center of gravity, 28 percent M.A.C.; flaps 30°; stabilizer, -2°.

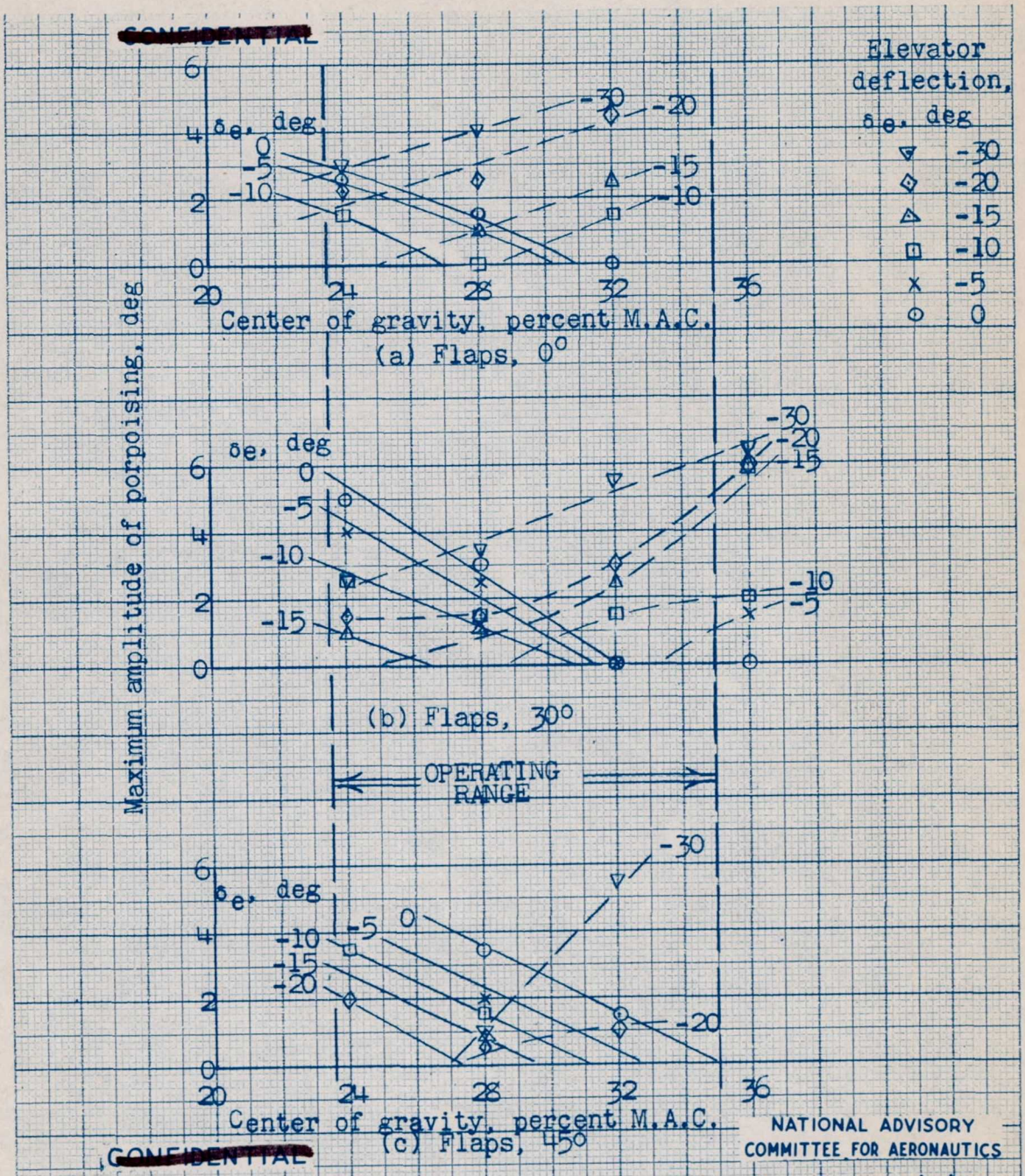

Figure 46.- Model 208M. Variation of maximum amplitude of porpoising with position of center of gravity. Gross load, 77.4 lb; take-off power; stabilizer, -2°.